

**High Resolution Facies Analysis and Sequence Stratigraphy of  
Mixed Clastic-Carbonate Deposits of Miocene Dam Formation  
Outcrops, Al Lidam Area, Eastern Province of Saudi Arabia**

BY

**Mazin Abdelgadir Abdelrazig Bashri**

A Thesis Presented to the  
DEANSHIP OF GRADUATE STUDIES

**KING FAHD UNIVERSITY OF PETROLEUM & MINERALS**

DHAHRAN, SAUDI ARABIA

In Partial Fulfillment of the  
Requirements for the Degree of

**MASTER OF SCIENCE**

In

**GEOLOGY**

April 2015

KING FAHD UNIVERSITY OF PETROLEUM & MINERALS

DHAHRAN- 31261, SAUDI ARABIA

**DEANSHIP OF GRADUATE STUDIES**

This thesis, written by **Mazin Abdelgadir Bashri** under the direction his thesis advisor and approved by his thesis committee, has been presented and accepted by the Dean of Graduate Studies, in partial fulfillment of the requirements for the degree of **MASTER OF SCIENCE IN GEOLOGY**.



Dr. Osman M. Abdullatif  
(Advisor)



Dr. Abdulaziz Al-Shaibani  
Department Chairman



Dr. Lamidi Babalola  
(Member)



Dr. Salam A. Zummo  
Dean of Graduate Studies



11/6/15

Date



Dr. Mike Kaminski  
(Member)

© Mazin Bashri

2015

## ***Dedication***

*It is with my deepest and warmest affection that I dedicate this work  
to Gaddora and Amona; the sole of my life, to Jalmood, flood,  
haramona, chinese, lilo and Kadees*



## ACKNOWLEDGMENTS

All praise is to Allah, the lord of the worlds, the most gracious and the most merciful till satisfaction, if satisfied and after satisfaction as befits his dignity.

I would like to express my deepest gratitude to my advisor Dr. Osman Abdullatif for his constant supervision, guidance, and valuable advices. I am also very grateful to my committee members Dr. Lamidi Babalola and Dr. Mike Kaminski for their patience and assistance during the whole work. Dr. Abdulaziz Al-Shaibani, head of the Earth Sciences Department at the King Fahd University of Petroleum & Minerals is, also, greatly thanked for his continuous cooperation and for opening his doors toward my problems. I'm obliged to the whole ESD faculty, staff and technician for their support through my MSc period in KFUPM. Thanks also extend to the Center of Petroleum and Minerals (CPM) represented by Dr. Khalid Alsultan for providing the lab facilities.

It has been my privilege to work closely with Dr. Hassan Eltoum, Dr. Fawwaz Alkhaldi, Dr. Aus Altawil, Dr. Khalid Alramadan, Dr. Dave Cantrell and Professor Stephen Hasiotis. I have enjoyed the opportunity to watch and learn from their knowledge and experience. Their frequent insights and patience with me are always appreciated. I am very proud of what we have achieved together, thank you all.

I would not have accomplished this MSc without the wise counsel of my friends and colleges Mutasim (Gissa), Moaz (Halfa), Ammar (Dabaiwa) & Ammar (Warag), Mohammed (Jungur) and all the Sudanese geologists who have been steady hands to steer me through postgraduate career at KFUPM. |

# **TABLE OF CONTENTS**

<b>ACKNOWLEDGMENTS .....</b>	<b>V</b>
<b>TABLE OF CONTENTS .....</b>	<b>VI</b>
<b>LIST OF TABLES.....</b>	<b>IX</b>
<b>LIST OF FIGURES.....</b>	<b>X</b>
<b>ABSTRACT .....</b>	<b>XIV</b>
<b>ملخص الرسالة .....</b>	<b>XV</b>
<b>1 CHAPTER 1 INTRODUCTION .....</b>	<b>1</b>
1.1 Introduction.....	1
1.2 Statement of Problem.....	3
1.3 Objective and Scope of Work .....	4
1.4 Study Area .....	5
<b>2 CHAPTER 2 LITERATURE REVIEW.....</b>	<b>9</b>
2.1 Introduction.....	9
2.2 Tectonic History Related to Study Area .....	9
2.3 Miocene Stratigraphy of Eastern Arabian Plate and Chronostratigraphically Correlated Formations in the Area .....	16
2.4 The Dam Formation .....	18
<b>3 CHAPTER 3 METHODOLOGY.....</b>	<b>24</b>
3.1 Introduction.....	24
3.2 Sedimentology, Facies and Sequence Stratigraphical Analysis .....	24

3.2.1	Field Work .....	24
3.2.2	Sampling Strategy.....	25
3.2.3	Laboratory Work .....	25
3.3	Outcrop Photomosaic .....	27
4	CHAPTER 4 LITHOFACIES ANALYSIS .....	29
4.1	Introduction.....	29
4.2	Facies Description and Interpretation .....	31
4.2.1	Interbedded Dolomudstone and Evaporite Facies (ME).....	31
4.2.2	Interbedded Cross-bedded Sandstone and Mudstone Facies (SM) .....	36
4.2.3	Channelized Medium Sandstone Facies (Sc) .....	43
4.2.4	Trough Cross-Bedded Sandstone (St).....	47
4.2.5	Interbedded Cross-bedded Coarse Limestone and Mudstone Facies (GM) .....	52
4.2.6	Intra-formational Limestone Conglomerate (Gmm).....	55
4.2.7	Stromatolites (BS) .....	58
4.2.8	Massive Quartz Skeletal Pelletal Wacke-Packstone (PWm) .....	62
4.2.9	Planar Cross-Bedded Skeletal Peloidal Grainstone (Gp).....	68
4.2.10	Herringbone Cross-Bedded Skeletal Oolitic Grainstone (Gh).....	69
4.2.11	Trough Cross-Bedded Aggregate Intraclastic Oolitic Grainstones (Gt) .....	75
4.2.12	Massive Peloidal Skeletal Packstone (Pm) .....	80
4.2.13	Channelized Planar Cross-Bedded Skeletal Oolitic Grainstone (Gcp) .....	83
4.2.14	Massive Skeletal Wackstone (Wm) .....	86
4.2.15	Dipping Planar-bedded Skeletal Oolitic Grainstone (Gl) .....	89
4.3	Discussion .....	95
4.3.1	Processes.....	95
4.3.2	Depositional Environments .....	96

4.3.3	Relative Abundance of Facies .....	101
4.3.4	Palaeocurrent Analysis .....	101
4.3.5	Dolomite in the XRD Analysis .....	104
5	CHAPTER 5 SEQUENCE STRATIGRAPHY.....	108
5.1	Introduction.....	108
5.2	Sequence Stratigraphic Units .....	108
5.3	Terrigenous Siliciclastics vs Carbonate Sequence Stratigraphy .....	110
5.4	The Dam Formation Sequence Stratigraphy Literature .....	111
5.5	The study Area Sequence Stratigraphic Interpretation.....	112
6	CHAPTER 6 CONCLUSIONS AND RECOMMENDATIONS.....	127
6.1	Conclusions .....	127
6.2	Recommendations .....	128
	REFERENCES.....	130
	VITAE .....	140

## **LIST OF TABLES**

Table 4.1: Summary of characteristics of lithofacies in the Dam Formation .....	97
Table 4.2: Summary of characteristics of lithofacies in the Dam Formation .....	98

# LIST OF FIGURES

Figure 1.1: Google map shows the location of study area in the eastern province of Saudi Arabia .....	6
Figure 1.2: Google map shows the studied outcrops in the study area.....	7
Figure 1.3: Geological map of the Arabian Peninsula showing the distribution of the lithological units, the Miocene Dam Formation outcrops are illustrated in yellow (Powers, 1968) .....	8
Figure 2.1: Cartoon explains the chronological stages of the Neo-Tethys creation and its relation to the Arabian Plate location (Stamp and Borel, 2002).....	13
Figure 2.2: The Miocene paleofacies map (Ziegler, 2001).....	14
Figure 2.3: Major basins and structural features of the Arabian Plate (study area is inferred to by the blue star) (Ziegler, 2001) .....	15
Figure 2.4: Type section of the Dam Formation (Steineke and Koch, 1935).....	20
Figure 2.5: The age and lithostratigraphic position of the Dam Formation in the Dammam dome (Weijermars, 1999) .....	21
Figure 3.1: Image of Outcrop 19 showing the talus covering most of the outcrop .....	26
Figure 3.2: Determining outcrops strikes before field work.....	28
Figure 4.1: Vertical stratigraphic sections and sedimentary facies of the studied outcrops	30
Figure 4.2: (A) Massive mudstone facies with distorted evaporite layers (arrows). (B) Dissolved and calcified chicken wire anhydrites (note the pattern of the vugs) .	33
Figure 4.3: (A) Horizontal lamination in the mudstone. (B) Desiccation cracks in the mudstone with sandstone fill .....	38
Figure 4.4: (A) Channel architecture of medium grained sandstone facies.....	44

Figure 4.5 (A) Trough cross-bedded sandstone facies with sharp erosional base and Ophiomorpha trace fossil; (B) Ophiomorpha burrow in the same facies found in outcrop 19 .....	49
Figure 4.6 Carbonate interbedding lithofacies: (A) Highly interbedded (arrow) with tepee structure (dashed curve). (B) Planar cross-bedded skeletal oolitic grainstone (upper zone) capping the interbedded facies.....	53
Figure 4.7 Carbonate conglomerate facies: (A) Light-colored rounded pebbles (arrow) of carbonate intra-formational para-conglomerate. (B) Dark green to gray angular pebbles (arrow) of carbonate intra-formational ortho-conglomerate .....	57
Figure 4.8: Stromatolite lithofacies morphologies in the Dam Formation following Logan et al; (A) Laterally linked hemispheroid (LLH). (B) Discrete spheroids (SS) .....	59
Figure 4.9: (A) Stratigraphic position of skeletal peloidal wackestone facies and zones of intraclasts (arrow). (B) Bioturbation in the same facies.....	63
Figure 4.10 (A) Planar cross bedding sets in grainstone facies and the associates facies. (B) Keystone vugs and tangential bottom sets in the cross bedding .....	70
Figure 4.11 Herringbone cross-bedded grainstone facies: (A) Herringbone cross bedding structure (B) Keystone vugs within the cross bedding (arrow) .....	72
Figure 4.12 (A) Trough cross bedding in grainstone facies. (B) Flaser bedding structure with fine mud seams within the troughs .....	77
Figure 4.13 (A) Stratigraphic position of skeletal packstones, the intensive bioturbation within it and the vugs (arrow). (B) Coral fragment within the massive bioturbated skeletal packstone facies (arrow).....	81



Figure 4.14: Channelized grainstone facies: (A) Channel architecture cutting through other facies. (B) Thin section showing ooids and skeletal grains with moderately well sorting and intergranular and intragranular porosities .....	84
Figure 4.15: (A) The domal shape of massive skeletal wackestone facies (dashed line follows the boundaries) and the associated facies .....	87
Figure 4.16 (A) Dipping layers of beach facies. (B) Changing from lamination to bedding upward .....	91
Figure 4.17: Schematic 3D diagram for depositional model of the Dam Formation in the study area .....	100
Figure 4.18: Lithology abundance percentage in the Dam Formation in the study area .	102
Figure 4.19: Relative abundance of facies in the study area.....	102
Figure 4.20: Rose diagram for the paleocurrent measurements .....	103
Figure 4.21: Diffractogram showing the dolomite as main mineral content in the mudstone when interbedded with evaporites.....	106
Figure 4.22: Small mud diapir in mudstone-sandstone facies .....	106
Figure 4.23 Ball and pillow structures in the sandstone-mudstone facies.....	107
Figure 4.24 Minor normal fault with dragging and fracturing in its hanging wall.....	107
Figure 5.1: Rhizolith (arrows) in the mud of mud-evaporite facies as indicator of exposure.....	114
Figure 5.2: Transgressive ravinement surface with mud intraclasts (A) and Stromatolites (B) (arrow);.....	116
Figure 5.3: Composite Stratigraphic Section of outcrop 8 showing fabric textures, structures and and sequence stratigraphic subdivisions.....	119

Figure 5.4: Composite stratigraphic section of outcrop 23 showing fabric textures, structures, lithology and sequence stratigraphic subdivisions .....	120
Figure 5.5: Composite stratigraphic section of outcrop 1 shwoing fabric textures, structures and sequence stratigraphic subdivisions .....	121
Figure 5.6: Compoite stratigraphic section of Outcrop 2 showing fabric textures, structures and sequence stratigraphic subdivisions .....	122
Figure 5.7: Cross section through studied outcrops showing the sequence stratigraphy of the Dam Formation in the study area.....	123
Figure 5.8: Facies and sequence stratigraphy interpretation of outcrop No. 23 .....	124
Figure 5.9: Facies and sequence stratigraphy interpretation of outcrop No. 1 .....	125
Figure 5.10: Facies and sequence stratigraphy interpretation of outcrop No. 2 .....	126

## ABSTRACT

Full Name : Mazin Abdelgadir Abdelrazig Bashri

Thesis Title : HIGH RESOLUTION FACIES ANALYSIS AND SEQUENCE  
STRATIGRAPHY OF MIXED CLASTIC-CARBONATE DEPOSITS  
OF MIOCENE DAM FORMATION OUTCROPS, AL LIDAM  
AREA, EASTERN PROVINCE OF SAUDI ARABIA

Major Field : Geology

Date of Degree : April, 2015

The Burdigalian mixed siliciclastic-carbonate deposits of the Dam Formation are well exposed in Al-Lidam area, within the eastern province of Saudi Arabia. The formation is correlatable to Miocene reservoirs in both Iran and Iraq. Therefore, studying its lithologic heterogeneity in small distance with high resolution could help in further work related to reservoir properties pattern prediction. The Miocene Epoch in the Arabian Plate was tectonically unstable. The opening of the Red Sea and the following eastward movement of the Arabian Plate and collision with Eurasia cause regional changes in the depositional system of the area. This complexity in the tectonics caused complexity in the stratigraphy and increased the heterogeneity.

A traverse composed of six outcrops was studied in detail to investigate the Dam Formation stratigraphy. Four of them were correlated laterally and the other two were included only in the analysis of facies. Facies parameters (lithology, sedimentary structures, main fossils, paleocurrents patterns and sedimentary bodies' geometries) were described and each bed was sampled.. The samples were slabbed, processed for thin section analyses and powdered for mineralogical phase determination using XRD.

Fifteen lithofacies were identified through the studied traverse. They are: (1) Channelized Medium Sandstone; (2) Interbedded Mudstone and Evaporites; (3) Stromatolites; (4)

Interbedded Cross-bedded Sandstone and Mudstone; (5) Interbedded Cross-bedded Coarse Limestone and Mudstone; (6) Intra-formational Limestone Conglomerate; (7) Trough Cross-Bedded Sandstone; (8) Planar Cross-Bedded Skeletal Peloidal Grainstone; (9) Herringbone Cross-Bedded Skeletal Oolitic Grainstone; (10) Trough Cross-Bedded Aggregate Intraclast Oolitic Grainstones; (11) Massive Peloidal Skeletal Packstone; (12) Channelized Planar Cross-Bedded Skeletal Oolitic Grainstone; (13) Massive Quartz Skeletal Peloidal Wacke-Packstone; (14) Massive Skeletal Wackstone and (15) Dipping Planar-bedded Skeletal Oolitic Grainstone. They were interpreted as subtidal shoreface, intertidal, foreshore, supratidal and estuarine deposits. These facies are stacked in shallowing upward parasequences and compose bigger three 4<sup>th</sup> order sequences. Two sequence boundaries characterized by subaerial exposure were delineated. The sabkha and intertidal siliciclastics represent the Lowstand Systems Tract (LST) whereas estuarine sandstone, tidal carbonate channels and the quartz skeletal peloidal wackestone represent the Transgressive Systems Tract (TST) and the shallowing upward wackestone to grainstone cycles represent the Highstand Systems Tract (HST). |

الاسم الكامل: مازن عبدالقادر عبدالرازق باشري

عنوان الرسالة: التحليل السحني عالي الدقة والتتابعية الطبقيّة للمتكشّفات الرسوبية الفتاتية الكربوناتيّة المختلطة لمتكون الدام الميوسيني، منطقة اللّدام، المنطقة الشرقيّة بالمملكة العربيّة السعوديّة

التخصص: جيولوجيا

تاريخ الدرجة العلميّة: أبريل ٢٠١٥ |

تتكشف صخور متكون الدام من العمر الميوسيني (بردياليان) الفتاتية الجيرية المختلطة بصورة جيدة في منطقة اللّدام بالمنطقة الشرقيّة من المملكة العربيّة السعوديّة. هذه الصخور تضاهي مكامن للنفط بكل من العراق وإيران. لذلك فالدراسة الدقيقة لعدم التجانس الصخري لمتكون الدام ربما تساعد في الدراسات اللاحقة عن التنبؤ بخصائص مكامن عصر الميوسين. العصر الميوسيني في الصفيحة العربيّة لم يكن مستقرا من الناحية التكتونية فانفتاح البحر الاحمر وما لحقه من حركة في الصفيحة العربيّة باتجاه الشرق والاصطدام بالصفيحة الايوراسية تسبب في تغير اقليمي بالنظام الترسيبي بالمنطقة. هذه التعقيدات التكتونية تسببت في تعقيد التسلسل الطبقي وزيادة عدم التجانس.

تمت دراسة مسار يتكون من ست متكشّفات بالتفصيل للتحقق من التسلسل الطبقي في متكون الدام. اربعة من هذه المتكشّفات تمت مضاهاتها جانبيا، اما المتكشّفين المتبقين فقد تم ضمهما في الوصف والتحليل السحني فقط. تم وصف المعاملات السحنية (التركيب الصخري، التراكيب الرسوبية، المستحاثات الاساسية، انماط التيارات القديمة واشكال الاجسام الرسوبية) لكل طبقة ، ولقد تم اخذ العينات ايضا لكل طبقة على حدة. تم تدوين الملاحظات على انماط تموضع الطبقات واسطح الحدود الطبقيّة تزامنا مع دراسة السحن الصخرية. اضافة الى ذلك تم اخذ الصور الفوتوغرافية الدقيقة ومن على البعد للمتكشّفات الصخرية وذلك لعمل الفسيفساء الصورية. تم تقطيع العينات الى شرائح وتم كذلك طحنها ودراستها بواسطة تقنية الاشعة السينية المتشتتة، كما تم تحضير الشرائح الرقيقة منها.

خلال المسار المدروس تم التعرف على خمسة عشر سحنة صخرية، وهي كما يلي: (١) قنوات الحجر الرملي المتوسط، (٢) صخور الطين والمتبخرات المتداخلة، (٣) البساط الطحلي الرسوبي المستحاث، (٤) صخور الحجر الطيني والرملي ذو التطبيق المتقاطع المتداخلة، (٥) صخور الحجر الطيني والحجر الجيري الخشن ذو التطبيق المتقاطع المتداخلة، (٦) صخور المتدملكات الجيرية ذات النشأة المحلية، (٧) الحجر الرملي ذو التطبيق المتقاطع الحوضي، (٨) الحجر الجيري الحبيبي البلويدي الهيكلي ذو التطبيق المتقاطع المستوي، (٩) الحجر الجيري الحبيبي

الاوليتي الهيكلية ذو التطبيق المتقاطع، (١٠) الحجر الجيري الحبيبي الاوليتي المتملك والمحتوي علي الشظايا محلية النشأة ذو التطبيق المتقاطع الحوضي، (١١) الحجر الجيري الدعامي الهيكلية البلويدي المصمت، (١٢) قنوات الحجر الجيري الحبيبي الاوليتي الهيكلية ذو التطبيق المتقاطع المستوي، (١٣) الحجر الجيري الدعامي الواكي البلويدي الهيكلية السلكي المصمت، (١٤) الحجر الجيري الواكي الهيكلية المصمت، (١٥) الحجر الجيري الاوليتي الهيكلية ذو التطبيق السطحي المائل. فسرت هذه السحن على انها ترسبت في بيئات تحت مديّة، مديّة، تحت شاطئية، شاطئية، فوق مديّة وبيئات انهار شاطئية.

تترتب هذه السحن في دورات ترسيبية تميل الى الضحالة الى الاعلى، وهي بدورها تكون اجمالاً ثلاثة تتابعات من الرتبة الرابعة. تم تحديد سطحين يمثلان عدم توافق رسوبي بين هذه التتابعات وهما يظهران دلائل التكشف تحت هوائي، تمثل الرسوبيات الفتاتية السلسية (عندما توجد) حزمة الصخور المتوضعة في حال الانخفاض بينما تمثل الكربونات حزم الصخور المتوضعة في الوضع البحري التقدمي و الوضع البحري العالي . بالاضافة الى ذلك فان صخور الطين الجيري المتداخلة مع المتبخرات تمثل الوضع البحري المنخفض المبكر.

# CHAPTER 1

## INTRODUCTION

### 1.1 Introduction

Outcrop analogs are used to improve the characterization of reservoir stratigraphy, to better understand of subsurface facies architecture and heterogeneity, and to overcome the limitations associated with large inter-well spacing within individual oil fields (Pringle et al., 2004, Girard et al., 2008). The escarpment in the Lidam area, eastern Saudi Arabia provides excellent exposure of mixed siliciclastic-carbonate rocks of the Dam Formation which were interpreted to have been deposited in a restricted embayment (Al-Khaldi et al., 2010). These outcrops are composed of rocks equivalent to prolific hydrocarbon bearing subsurface reservoirs and were deposited in similar depositional environments to most of giant reservoirs in the Arabian Plate. Better understanding of the facies distribution and depositional environments of the mixed siliciclastic-carbonates rocks of the Dam Formation at outcrops level allows for better prediction of the quality and heterogeneity within reservoir rocks in subsurface.

The shallow marine successions of mixed siliciclastic-carbonate deposits have many distinctive features. These successions are highly sensitive to sea level variations, sediments supply, climatic conditions and tectonics. However, mixed siliciclastic-carbonates successions received less attention from sedimentologists than the



siliciclastics and carbonates end members. Moreover, their sequences' development processes and controls are less studied and documented. Within tectonically active basins (such as foreland basins), the basin fill of these mixtures provides a very effective tool for studying the basin evolution, because different lithologies will respond differently to events of subsidence, uplifting and deformation (Saylor 2003). One of the challenges that face the interpretation of mixed siliciclastic-carbonates depositional environments is that the detrital siliciclastic influx toward the shallow marine changes the chemistry of the water and affects (reduces) the biogenic carbonates factory (Wright and Burchette, 1996).

In the Al-Lidam area, more than 40 outcrops of the Dam Formation are exposed as isolated mesas and benches. These outcrop extend NE of the Dammam-Riyadh highway for about 20 km where the Dam Formation is unconformably overlain by the Hofuf Formation. This suggest that up-dip and older strata are exposed near the Dammam-Riyadh highway while the down-dip younger strata of the Dam Formation are exposed near the contact with the Hofuf Formation. Al-Khalidi (2009) conducted detailed facies and stratigraphy analysis on one outcrop of the Dam Formation near the Dammam-Riyadh highway (older outcrop strata); in which, the facies are stacked into 17 cycles that are stacked, in turn, to form 4 cycle sets (High Frequency Sequence, HFS). They are arranged in 3 composite sequences to form the overall Dam Formation supersequence. Al-Khalidi (2010) studied 12 outcrops in the Al-Lidam area to refine their facies model and stratigraphy and to develop 2-D stratigraphic correlation of the Dam Formation using some of these outcrops. The unique exposure of the Dam Formation outcrops may point to a change of depositional patterns within Al-Lidam following the general dipping (SW-

NE) of strata in the Arabian Plate. Under this hypothesis, the following research questions are addressed in this study:

- 1- How the facies and sequence stratigraphic model of the Dam Formation in Al-Lidam area, which was conducted previously on selected outcrops, is related to other unstudied outcrops?
- 2- How can the sequence stratigraphic framework of the Dam Formation in Al-Lidam area improve our understanding of facies distribution when using outcrops lining in traverse perpendicular to the main layers strike through Al-Lidam area?
- 3- How can the sequence stratigraphic framework of the Dam Formation will help in sampling programs for further studies and their sampling strategy?

## **1.2 Statement of Problem**

Most of the Dam Formation correlative formations (chronostratigraphically) in other marginal locations of the Neo-Tethys are great hydrocarbon reservoirs. The regional tectonic setting caused some places to be uplifted, subsidized, isolated or submerged by marine water. This complex topography resulted in increased sediment sources in some locations, sediments starvation at other locations, hypersaline locations, and the great effect of marine transgression in others, respectively. Consequently, a great degree of facies lateral and vertical variations occurred. For that, using lithology as a the only correlation tool between Miocene formations in different areas has its limitation because of the high number of controllers on the sedimentation process, and their differences in

rates and types from one location to another. Instead, chronostratigraphy and sequence stratigraphy could play major roles in regional correlation. Also in addition to high resolution sequence stratigraphy, high resolution sedimentary facies analysis, could help in lithologic correlation, locally.

The goal of this thesis is to construct a depositional model for the Dam Formation supported by stacking patterns and sequence stratigraphic framework at outcrop scale using facies analysis (petrography, sedimentary structures analysis, architectural elements of sediments, grain size analysis, paleocurrents and ichnofacies analysis). The outcome of the study will serve as the base for any subsequent subsurface exploration attempts that target the Miocene Dam Formation in Saudi Arabia. The more detailed the resulted depositional model would be, the more it would be useful in vertical and horizontal lithofacies prediction. The depositional setting of the Dam Formation during the Miocene (Burdigalian), which shows high degree of variability and substitution between the coarse and fine sediments of both carbonates and siliciclastic origins, requires more deliberateness in creating the model because of the high complexity.

### **1.3 Objective and Scope of Work**

The main objectives of this thesis could be summarized as follows:

- 1) To identify the different lithofacies of unstudied outcrops of the Dam Formation in its type locality, and investigate their vertical and lateral variations.

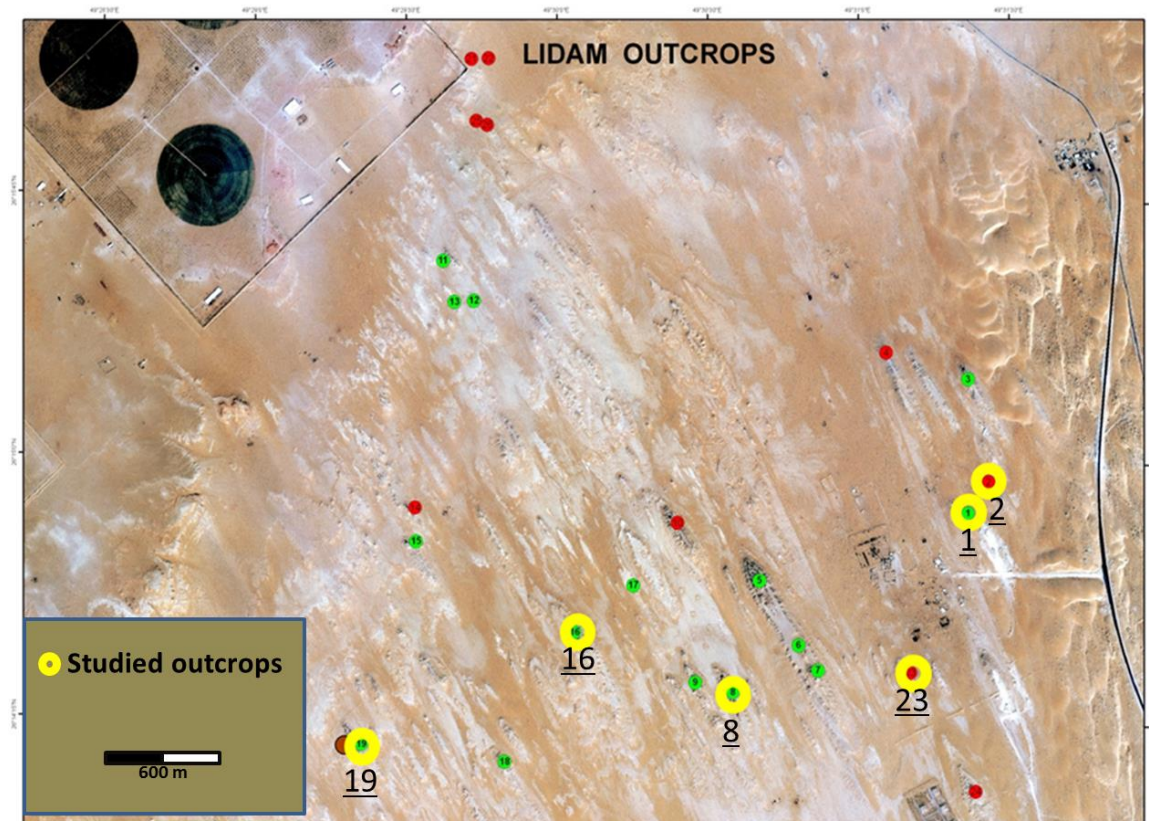
- 2) To interpret the paleodepositional environments of the lithofacies in studied sections; including the main dominant processes and current strengths.
- 3) Establish a sequence stratigraphic model of the Dam Formation in Al-Lidam area to understand the big picture of facies distribution in the study area for future higher-resolution interwell and field scale studies.
- 4) Develop strategic plan for outcrops sampling in the study area based on the sequence stratigraphic framework. This will help in integrating facies and sequence stratigraphy with biostratigraphical, petrophysical, geochemical, geomechanical, and geostatistical data. |

## **1.4 Study Area**

The Al Lidam area lies about 80 km west of Dhahran city in the eastern province of Saudi Arabia (Figure 1.1). It's located between  $49^{\circ} 28' 30''$  &  $49^{\circ} 31' 30''$  E and  $26^{\circ} 15' 45''$  &  $26^{\circ} 14' 15''$  N coordinates (Figure 1.2). The elevation of the area ranges between 87 m and 132 m above sea level. The Al Lidam area has a mixture of topographic features, shifting from desert sand dunes that extend eastwards and reach the Arabian Gulf in some localities. The outcrops in the study area are surrounded by featureless lands with a cover of those desert sands. The Miocene Burdigalian outcrops are greatly distributed in the eastern province of Saudi Arabia (Figure 1.3). In the study area, the outcrops of this formation occur as small continuous platforms or mesas with a general NNW-SSE trend, and also as irregular isolated inselbergs with heights ranging from 10-20 m..

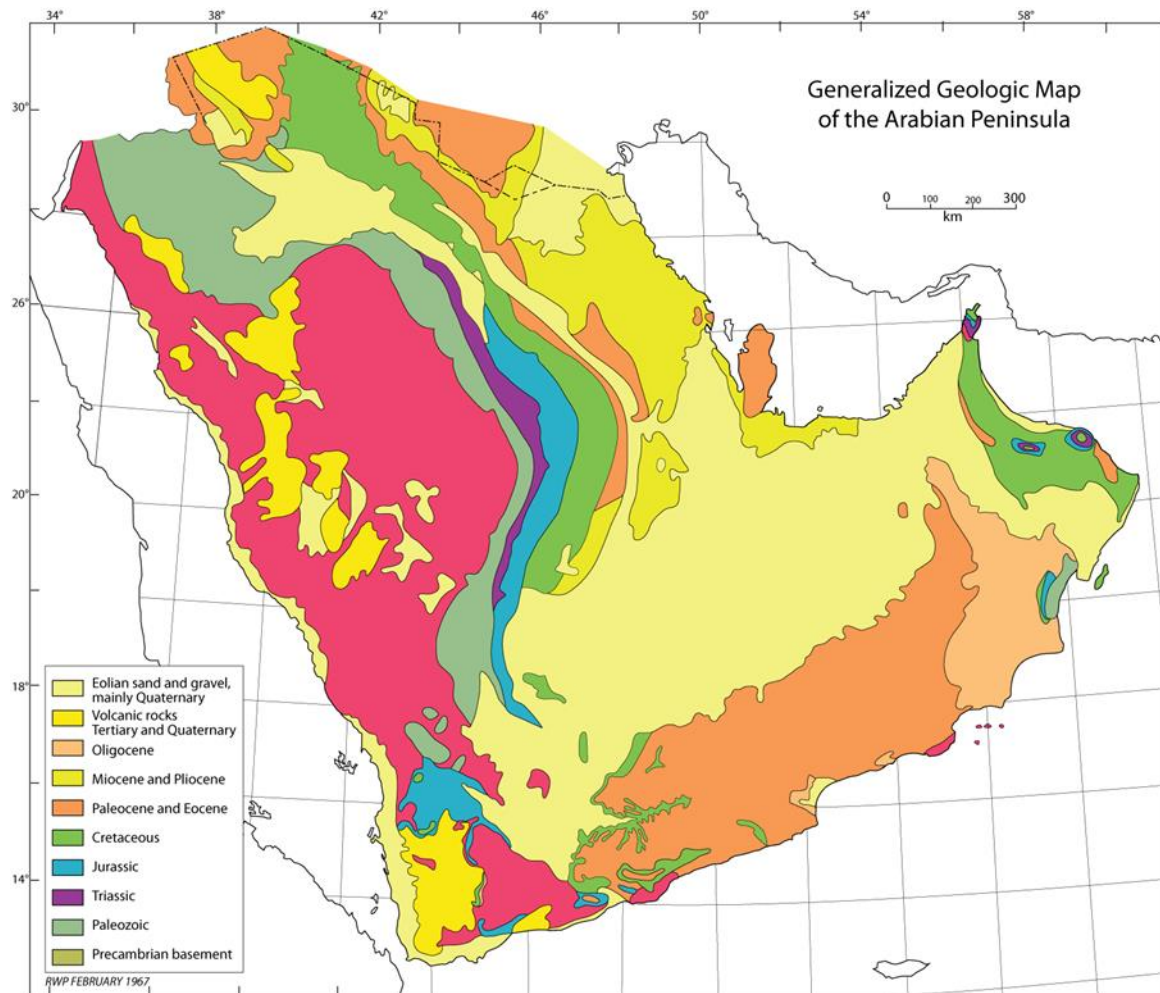


**Figure 1.1: Google map shows the location of study area in the eastern province of Saudi Arabia**



**Figure 1.2: Google map shows the studied outcrops in the study area**





**Figure 1.3: Geological map of the Arabian Peninsula showing the distribution of the lithological units, the Miocene Dam Formation outcrops are illustrated in yellow (Powers, 1968)**



## **CHAPTER 2**

### **LITERATURE REVIEW**

#### **2.1 Introduction**

The Dam Formation has been studied by many authors. It represents the focus of attention for those studying the tectonostratigraphic evolution of the Arabian Plate, because of the dramatic changes in the tectonic setting during the Cenozoic Era.

#### **2.2 Tectonic History Related to Study Area**

Before 640-620 My, the Precambrian Amar collision occurred by the movement of the Ar Rayn microplate westward to collide with the Arabian shield. This collision took place along the Amar suture in a N-S direction. It resulted in the formation of giant anticlines that are bounded by the Abu Jifan (NW trend) and Wadi Batin (NE trend) faults (Al-Husseini, 2000). The Amar collision was followed by extensional events caused by A-type granitic intrusions that resulted in crustal thinning (Blasband et al., 2000). The Najd rifting system was formed during the last stages of the extension, causing the whole Arabian Shield to be shifted laterally in a left-hand side movement to about 300 km in NW trend. This caused many rift basins with a NE trend to be formed in the Arabian Gulf, Oman, Zagros Mountains and Pakistan. The giant anticlines remained high and formed horsts between normal faults with grabens between them. The grabens were filled by clastics, carbonates and wide sedimentation of salt. Subsequently, these basement horsts and folds, in addition to the salt that diapirized, formed the major structures that

trapped the oil in the area, such as in the Ghawar Field, the Qatar Arch and the Khurais-Burgan anticline (Al-Husseini, 2000). Along the Oman-Zagros suture, The Neo-Tethys was created in the late Permian due to increasing in the extensional stresses that enlarged the accommodation space for sediments. This resulted in the formation of the new ocean over the split-up unconformity (pre-Khuff Unconformity) (Al-Jallal, 2010).

Stamp and Borel (2002) developed a plate tectonic model trying to describe the tectonic setting of the Paleozoic and Mesozoic. They used the plate buoyancy, plate boundaries locations, distribution and geochemistry of magmatic bodies and mid oceanic ridges spreading rates to analyze the ancient tectonism. The proposed timing of the Neo-Tethys rifting initiation, according to their results, is in the Late Carboniferous to Late Early Permian. The new opening caused the Cimmerian plate to be separated from Pangea and, also, the closure of the Paleo-Tethys to start (Figure 2.1). Muttoni et al., (2009) used paleomagnetism and stratigraphy of Permian lateritic soil profiles in Iran and Pakistan to study the opening of the Neo-Tethys; their results were similar to the Stamp model.

After the opening of the Neo-Tethys, highly variable (spatially and temporally) paleo facies were deposited in the Arabian Plate basins. There was interchange between shallow marine carbonates and evaporites dominance periods and siliciclastics' in the foreland areas, with dominance of the deep marine facies in the northern and eastern foredeep parts of the Neo-Tethys margin (Ziegler, 2001).

The Red Sea region started rifting by small depressions caused by magmatism and mantle plumes. Many hypothesis have been made on the timing of the beginning of the Red Sea tectonism (Ghebreab, 1998). Shallow subtidal to intertidal carbonates and evaporites in addition to lacustrine deposits that are interbedded locally with basaltic layers were

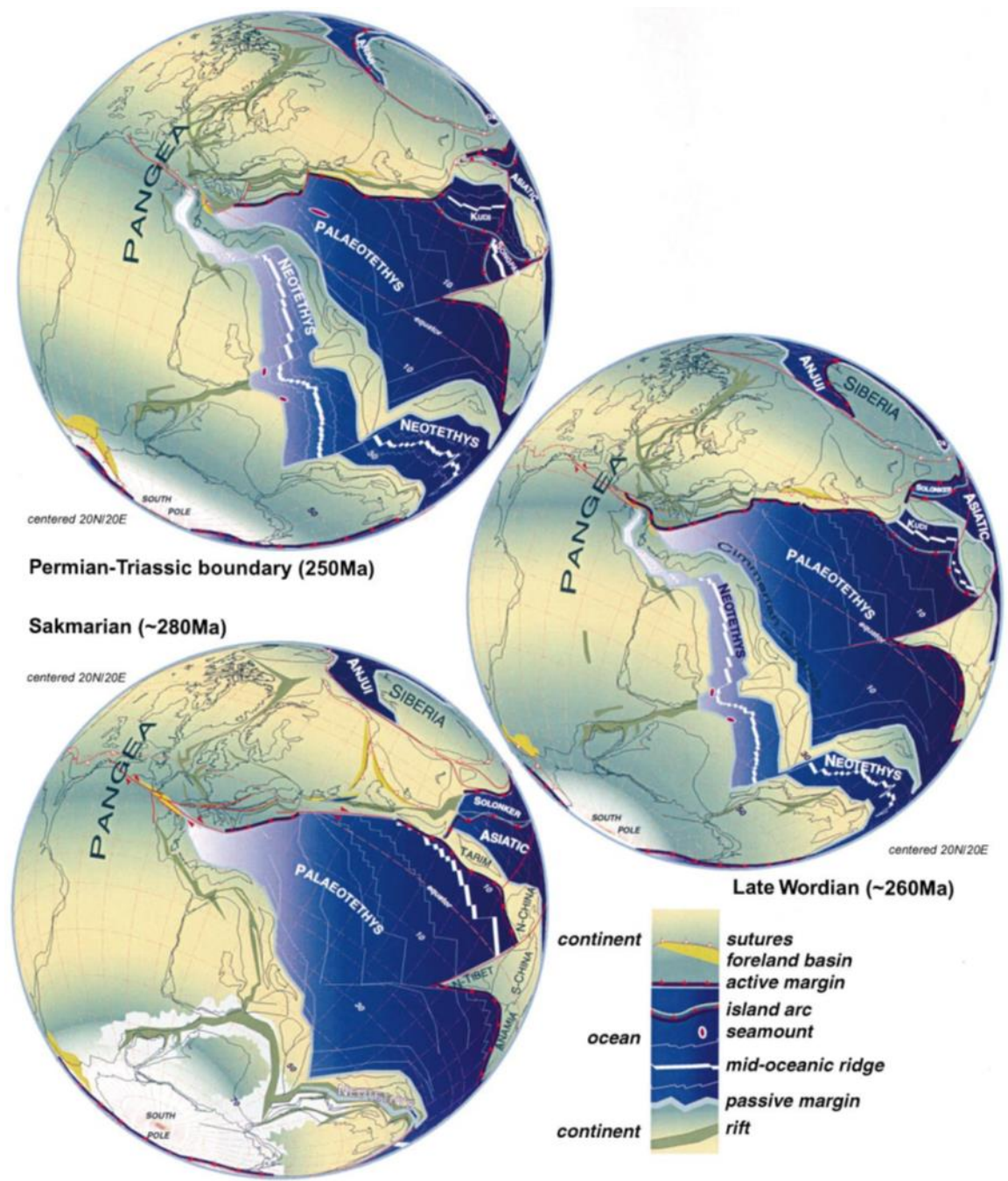
deposited in the northern part of present-day Red Sea during the Late Cretaceous to Early Paleocene. The new accommodation space, was filled by sediments brought in by a southward transgression of the Neo-Tethys. Contemporaneously during this period, obducted ophiolite bodies were formed in eastern Oman (Ziegler, 2001).

During the Miocene, the Red Sea rifting was started and the Arabian Plate began to separate from African Plate and to collide with Eurasia in an eastward anti-clockwise movement. Consequently, the whole succession deposited in the newly formed basins (including Dam Formation) was compressed. These tectonic activities were associated with complex strike-slip deformation in the Dead Sea area that extended to the Syria Arc (Figure 2.2) (Brew et al., 1999; de Ruiter, 1995).

The Arabian Plate has three main fault trends:

- 1) North trend with regular inter-fault spacing (Al-Husseini, 2000)
- 2) Northwest oriented set of faults; they follow the Najd fault system and are clear in the Arabian Shield. These faults bound the Arabian Plate along the Zagros Suture line in the east.
- 3) Fault sets with northeast major trend which correspond and control the distribution and alignment of most salt basins in the Arabian Gulf area (Figure 2.3) (Al-Husseini, 2000; Hussein and Hussein 1990; Loosveld, Bell, and Terken 1996). Those faults were interpreted to follow the Proterozoic basement architecture and formed during the Amar Collision before 640-620 My, when the Rayn Plate moved westward and collided with the Arabian-Nubian Shield.

The study area (Al-Lidam), which is the type locality of the Dam Formation, lies in the Arabian Basin which contains faults that follow the N-S trend. This basin contains the famous Ghawar Field which is the largest oil field worldwide.



**Figure 2.1: Cartoon explains the chronological stages of the Neo-Tethys creation and its relation to the Arabian Plate location (Stamp and Borel, 2002)**

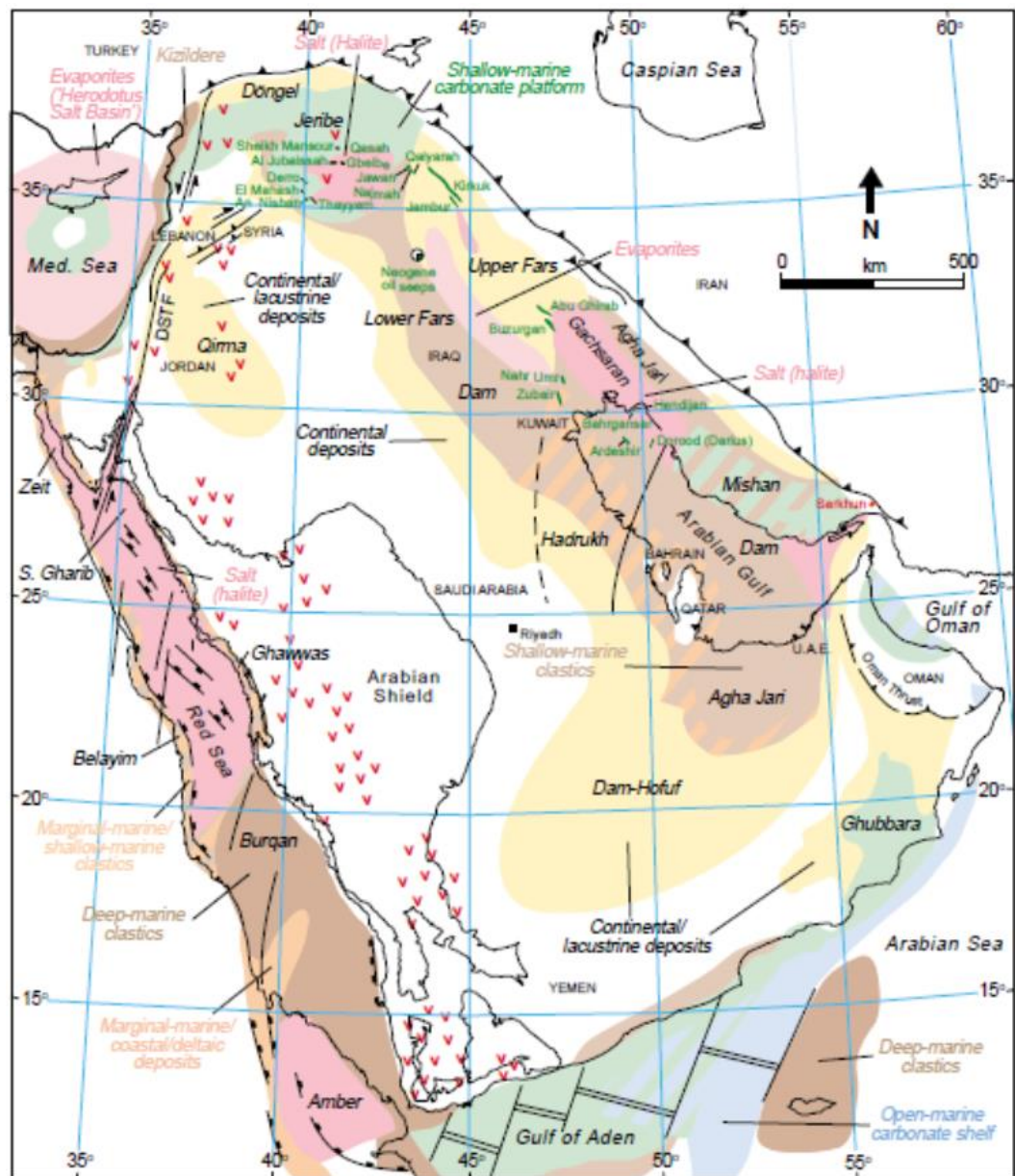


Figure 2.2: The Miocene paleofacies map (Ziegler, 2001)



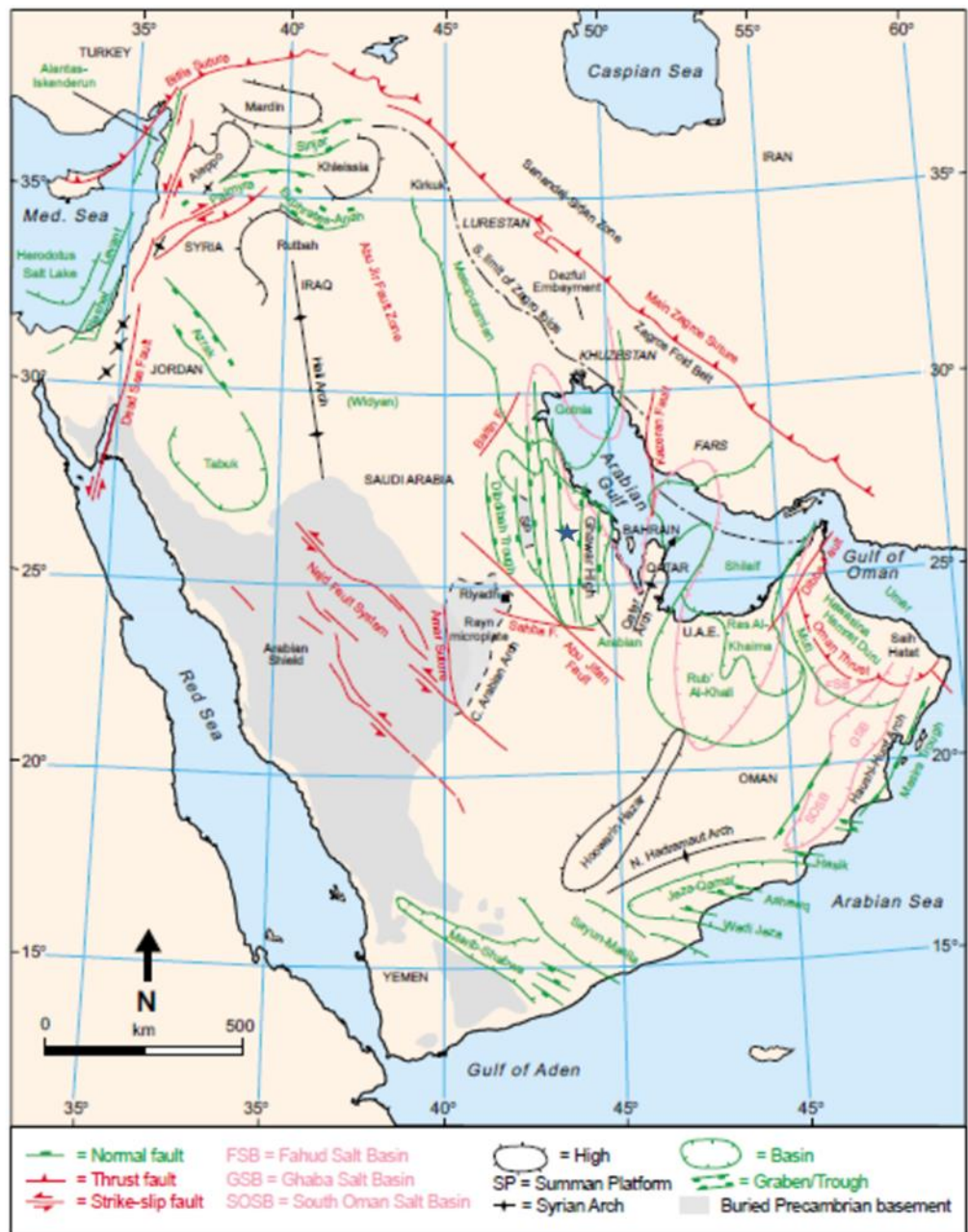


Figure 2.3: Major basins and structural features of the Arabian Plate (study area is inferred to be by the blue star) (Ziegler, 2001)



### **2.3 Miocene Stratigraphy of Eastern Arabian Plate and Chronostratigraphically Correlated Formations in the Area**

Powers et al. (1966) mentioned the existence of a belt of Miocene strata that extends from southern Qatar to the northeast and north of Saudi Arabia. The sediments are mainly of non-marine sandstones with some sandy limestones, calcareous sandstones and clays. Similar aged strata exist in Rub' Al khali depression. Powers et al. assigned them in stratigraphic position that overlies the Eocene and older rocks (with the absence of Oligocene layers) unconformably. The upper boundary with Pliocene and Quaternary sands and gravels is regarded as an unconformity.

The initiation of the independent Arabian Plate by the Red Sea rifting and the collision with Eurasia closed a large part of the Neo-Tethys, and changed it to a small relict sea. Since then, continental sedimentation dominated the area with the exception of intermittent marine flooding in the middle Miocene time. These shallow marine coastal conditions were in Saudi Arabia interbedding with fluvial and lacustrine facies from the west, and flanking the deepest part of the new subsidence in Iran and Iraq, where evaporites dominated.

With increasing tectonism and deformation in the eastern Zagros Mountains belt during the Late Miocene, Iraq and Iran had more sources of sand and gravel-size siliciclastic deposits. In some localities, these siliclastic sdeiments reached in a thickness of 4000 m.

The Lower Fars Formation (or the Fatha Formation) in Iraq and Iran is a Burdigalian mixed siliciclastic-limestone-evaporite succession, and it's strongly correlatable lithologically, with exception of evaporites, to the Dam Formation. Because of the hydrocarbon resources contained in it, the Lower Fars Formation has been widely

studied. The outcrops of Lower Fars Formation in Iraq have the same general NW-SE trend as those of the Dam Formation outcrops in the Eastern Province. Due to the deformation and rising of the Zagros Mountain belt, the terrestrial siliciclastic sediments had the greatest effect in the succession between the whole Miocene Formations in the adjacent areas. Another distinctive feature, which was caused by tectonic collision and the resulting deep basin evolution, is the existence of evaporites between other lithologies. The general arrangement of lithologies, westwards of the Zagros Mountain belt, is comprised of coarse siliciclastics, fine siliciclastics, carbonates and finally evaporites. These lithologies are arranged in cycles starting with red clastic clays at the base, sandstones, carbonates and capped by evaporites at the top (Bakhtiar, 2006).

In Egypt, the Mamura Formation represents the Burdigalian part of the Miocene record (with exception to the Miocene Nile Delta record). The formation is comprised of green limestone and shale of shallow marine origin. Their depositional environments and age were studied using planktonic Foraminifera. This formation also shows gradual changes from shallow marine to fluvial-marine setting (Hassan, 2013).

The Miocene stratigraphy in Libya contains white fine crystalline, thickly bedded carbonates (skeletal wackestone, packstone and grainstone) rock units of the Benghazi Formation that are chronostratigraphic and biostratigraphic correlatable to the Burdigalian Dam Formation of Saudi Arabia. . The skeletal grains in the formation are mainly large benthic foraminifera. The presence of the early Miocene benthic foraminiferal index species *Borelis melo melo* was used to date the formation (Abdulsamad and Bu-Argoub, 2006). The carbonates of the Benghazi Formation show shallowing upward trend which appears in the decrease of micrite

contents and the dominance of high energy grainstone facies. This fact goes parallel with the presence of fresh water ostracodes in some layers, associated with terrigenous quartz grains. These observations ensure the effect of freshwater in the Benghazi Formation sedimentation processes, (Abdulsamad et al. 2009).

## **2.4 The Dam Formation**

The Dam Formation was named in 1935 by Steineke and Koch as a phase and then as a formation representing a part of Miocene and Pliocene coastal succession (Figure 2.4). The name was formally published by Steineke et al. (1958). Its type locality is located in Jebel Al Lidam, which is this thesis study area. Powers et al. (1966) mentioned that only the lower part of Dam Formation crops out in its type locality. Dam Formation in its initial description by Powers et al. is composed of red to pink marl layers interbedded with olive green clay layers, sandstones, chalky limestones, skeletal grainstones and packstones (coquina). The basal layers of the formation that are in contact with the Hadrukh Formation contain a high abundance of echinoids represented by *Echinocyamus* sp. and the benthic foraminifera *Archaias* sp.

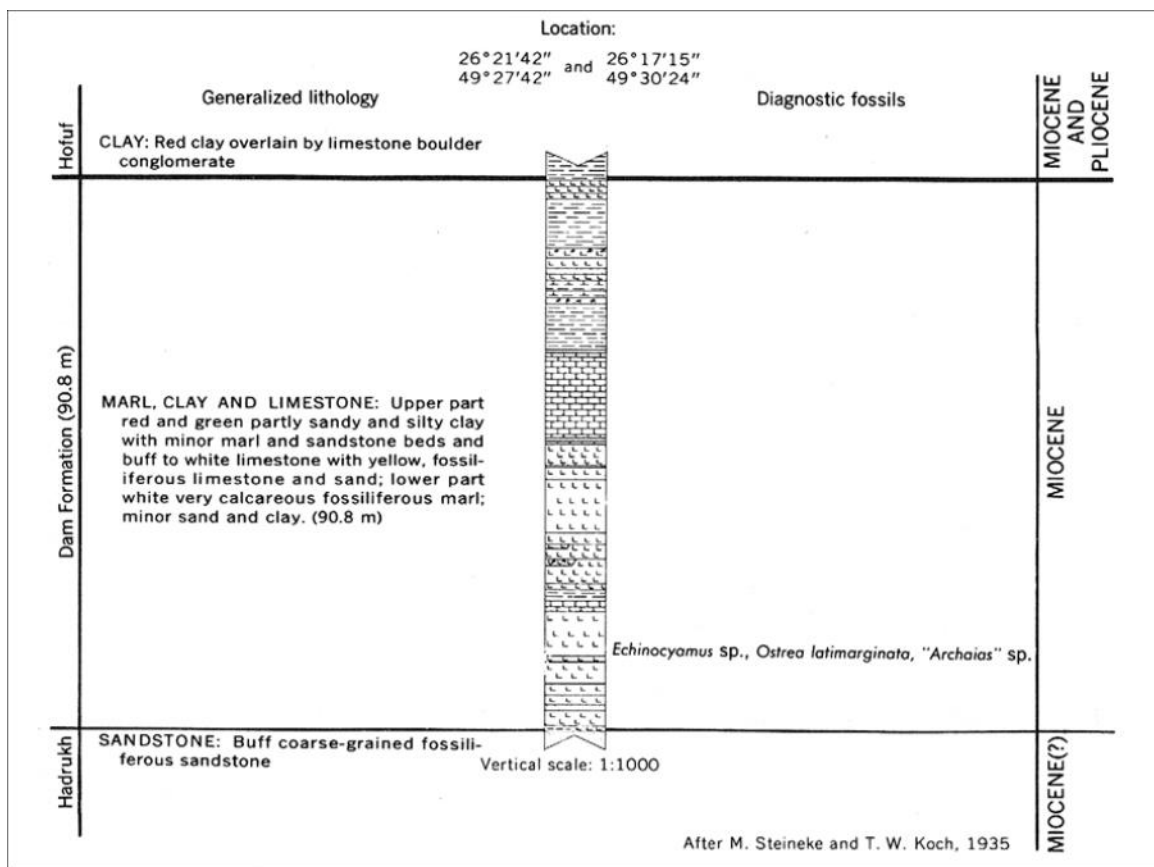
Irtem (1987) studied the stromatolites found in the Dam Formation in the Al Lidam area. He described their existence at the top of three deepening upward cycles. The cycles start by a gypsiferous claystone of supratidal origin, that grades into intertidal sandstone, lower intertidal to subtidal oolitic grainstone and finally the stromatolites at the top of the grainstones. The stromatolites are of columnar type occurring in closely spaced

distribution, and with 0.5 m to 0.8 m thickness. They have also found in the oolitic grainstones as intraformational clasts. This close relationship between stromatolites and oolitic grainstones allowed Irtem to suggest them as they were deposited within the same depositional setting.

Weijermars (1999) included the Dam Formation in his study of the structures of the Dammam Dome and its lithostratigraphy (Figure 2.5). He studied the Dam outcrops in Jebels of Al Rus, Midra Al-Shamali and Midra Al-Janoubi in the Eastern Province. In the Dammam Peninsula, the Dam Formation thickness reaches more than 75 m of basal colored intraformational conglomerates, with boulders of Lower Khobar limestone in the sand and fine grained carbonaceous matrix. A stromatolitic zone overlies the basal conglomerates and is followed by a succession of interbedded clastic and microcrystalline limestone with geodes. Finally, Weijermars included the ancient karst layers overlain by massive reefal facies into the Dam Formation lithologies.

Al-Saad and Ibrahim (2002) studied the benthic foraminiferal assemblages of the Miocene Dam Formation outcrops in the South of Qatar. These authors described 38 species distributed in shallowing upward sequences, and used the species "*Borelis melo melo*" as indicator of the Early Miocene, Burdigalian Age. The authors were successful in subdividing the formation lithostratigraphically into two members; the Al-Kharrara Member at the base and the Al-Nakhash Member at the top. The Al-Kharrara Member is composed of limestone, marl and claystone, whereas the Al-Nakhash Member is composed of limestones associated with evaporites and microbial heads (stromatolites). They proposed shallow clear marine water as the site of the deposition of the Al-Kharrara

Member, and oscillating, warm and hypersaline shallow marine water for the Al-Nakhash Member that allowed the deposition of stromatolites and evaporites.



**Figure 2.4: Type section of the Dam Formation (Steineke and Koch, 1935)**

PERIOD		EPOCH	AGE	Ma	DEPOSITION
Quaternary		HOLOCENE		0.01	Sabkha Eolian Sand
		PLEISTOCENE		1.8	
NEOGENE	PLIOCENE		Piacenzian	3.4	Hofuf Formation
			Zancian	5.3	
			Messinian	6.5	
	MIOCENE		Tortonian	11.2	
			Serravallian	15.1	
			Langhian	16.6	
			Burdigalian		
			Aquitania	21.8	
				23.7	
		NE	Chattian		Pre-Neogene Unconformity

Figure 2.5: The age and lithostratigraphic position of the Dam Formation in the Dammam dome (Weijermars, 1999)

More detailed lithostratigraphic studies been carried by Dill et al. (2005). They mapped the Dam outcrops in southwestern Qatar. Thin sections, X-Ray Diffraction (XRD), X-Ray Florescence (XRF) and C and S isotope analyses were used to carry out the petrographic and minerlogical analyses of the rock facies in the outcrops that they investigated. These authors re-subdivided the Dam Formation into seven members: the Lower, Middle and the Upper Salwa, Lower, Middle and the Upper Al Nakhsh and Abu Samrah Members. The Salwa Members, at the base, are composed, mainly, of calcareous siliciclastics deposited in microtidal settings. On the other hand, the Al Nakhsh Members are of microbial mats, gypsum and celestites. They were deposited in macrotidal settings containing subtidal, intertidal and supratidal signatures. The authors observed a parallel relationship between stromatolites and gypsum precipitation. The Abu Samrah Member which is the topmost member at the outcrops is mainly composed of marine carbonaceous sediments that were deposited in microtidal wave-dominated settings.

Dill and Henjes-Kunst (2007) integrated  $^{87}\text{Sr}/^{86}\text{Sr}$  ratios,  $^{44}\text{Ca}/^{40}\text{Ca}$  and  $^{44}\text{Ca}/^{42}\text{Ca}$  and integrated them with previously measured  $^{13}\text{C}/^{12}\text{C}$  &  $^{18}\text{O}/^{16}\text{O}$  from the Dam Formation samples in Qatar. That was a try to utilize them as stratigraphic correlation and depositional environments interpretation tools. They observed an oscillating nature in the Sr, C and O isotopes' curves, instead of a uniform character. This observation was their bases for proposing a wave-dominated regime for the Dam Formation deposition instead of a tidal-influenced one. The authors also used the Sr isotope and proved more enrichment of Sr from the hinterland and date the age of the Dam Formation in Qatar as Late Aquitanian to Early Burdigalian.

Alkhaldi (2009) studied the lithofacies and sequence stratigraphy of the Dam Formation in the Al Lidam area. He subdivided the formation into three composite sequences; each one is comprised of a number of cycles. Alkhaldi proposed that the cross-bedded sandstone facies (estuarine fill) and microbial banks were deposited during the transgressive system tract (TST) and the skeletal grainstone banks as products of the highstand system tract (HST).



## **CHAPTER 3**

### **METHODOLOGY**

#### **3.1 Introduction**

The basic field sedimentology and sequence stratigraphy notes has been recorded and vertical sections has been drawn for each studied outcrop. Lateral facies changes have been traced through the outcrops. These changes have been illustrated on the outcrops photomosaic.

#### **3.2 Sedimentology, Facies and Sequence Stratigraphical Analysis**

##### **3.2.1 Field Work**

In the study area, six outcrops were sedimentologically logged and studied (Figure 1.2). Four of the outcrops (1, 2, 8 and, 23) were studied, logged and correlated. The remaining two outcrops (16 and 19) are highly covered by recent talus (Figure 3.1) and were therefore only included in the description, facies analysis, and the sequence stratigraphy interpretation but not in the correlation. Each outcrop included two to four vertical sedimentary logs depending on its width. The field work observations were the main investigation tool in this thesis. These sedimentological logs are detailed in description, bed by bed, to ensure that the high resolution objective is reached. They included description of composition, textures, sedimentary structures, bed thicknesses, paleocurrent measurements (where possible), trace and macrofossil content, and bioturbation. The paleocurrents were estimated and measured using grain and intraclast

imbrication and dipping direction. Paleocurrent data were also obtained by the measuring the planar cross-bedded layers dips where a 3-D view is available.

Standard geological tools were used during the field investigation. The position of the logged sections and the elevations of their bottoms and tops were determined using a Global Positioning System tool (GPS). A Silva-type compass was utilized to measure the dip and strike of beds (attitudes) and of sedimentary structures (e.g. cross bedding). Topographic map (Figure 1.2) was used as the base map (the targeted outcrops are plotted on this map).

### **3.2.2 Sampling Strategy**

For each of the six outcrops, sampling method was based on bed thickness. Thin beds range between 10 to 40 cm while thick beds range between 70 to 100 cm. For thin beds, one representative sample was collected whereas thick beds were sampled at every 30cm.

### **3.2.3 Laboratory Work**

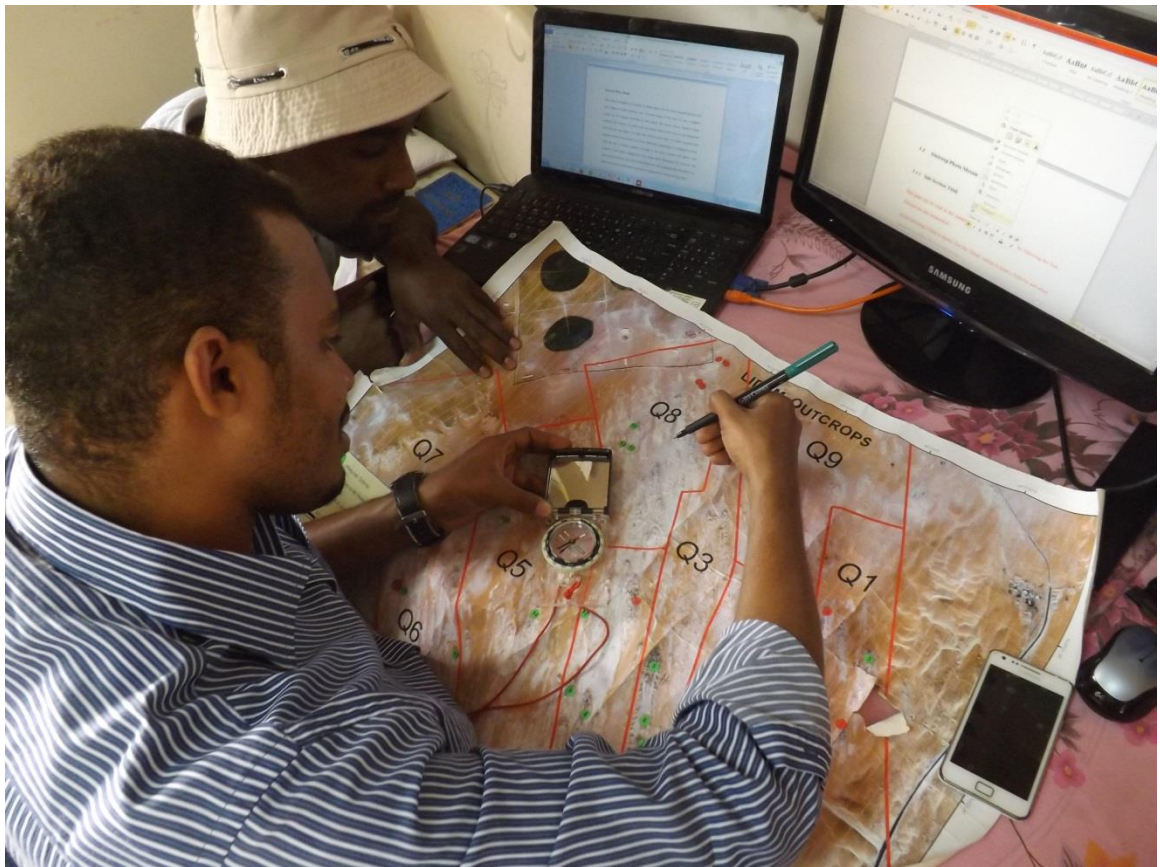
Collected samples were slabbed in the laboratory; imaged, re-described and thin sections were made out of them for more detailed investigation. Thin section investigation was carried out using polarizing microscope, and this instrument was used to characterize different parameters including mineralogy, grain types and percentages, textures, visual porosity, porosity types, and major fossil groups. Carbonate thin sections were stained by Alizarin Red to help in differentiating carbonate minerals and they were classified following the Dunham classification (Dunham, 1962). For muddy samples, X-Ray Diffraction technique (XRD) and Scanning Electron Microscope (SEM) were applied to determine their mineralogical content of them.



**Figure 3.1: Image of Outcrop 19 showing the talus covering most of the outcrop**

### **3.3 Outcrop Photomosaic**

This method integrates a low number of distant photos for the whole targeted outcrop with a high number of high resolution ones. The main target of this step is to obtain a complete mosaic for the outcrop describing its fine details. The distant photos should be lined parallel to the outcrop. To achieve this, the general strike of the outcrop was determined from the base map (Figure 3.2), and a line with the same strike was made on the ground and imaging stations were located on it. Every photo had a percentage of overlap with the following one, to ensure complete coverage to the whole outcrop. The photos were merged to form a single composite image; using Adobe Photoshop CS5 software. The high resolution photos were used as describing tools. The sedimentological description was plotted and drawn on the photos and, later, transcribed onto the big outcrop photo.



**Figure 3.2: Determining outcrops strikes before field work**

## **CHAPTER 4**

### **LITHOFACIES ANALYSIS**

#### **4.1 Introduction**

Sedimentary facies are sedimentary rock masses that have their own distinctive features in term of lithology, sedimentary structures, paleocurrent patterns, fossils and geometry that can be used to distinguish them from other adjacent facies (Selley, 1970). They may be composed of one layer or a set of associated layers. They are of great importance in interpreting depositional environments; using their characteristics and the stratigraphic relationships between them (Boggs, 2006). Facies in the study area have been investigated using previously mentioned parameters, initially, in a purely descriptive way. Then, they were used as key for interpreting the ancient depositional environment of the Dam Formation in the study area by combining their internal characteristics with their spatial relations and adjacent facies.

The high resolution investigation of the studied outcrops has revealed fifteen carbonate and siliciclastic lithofacies. The following part of this chapter presents the description and the interpretation of the various lithofacies in the study area.

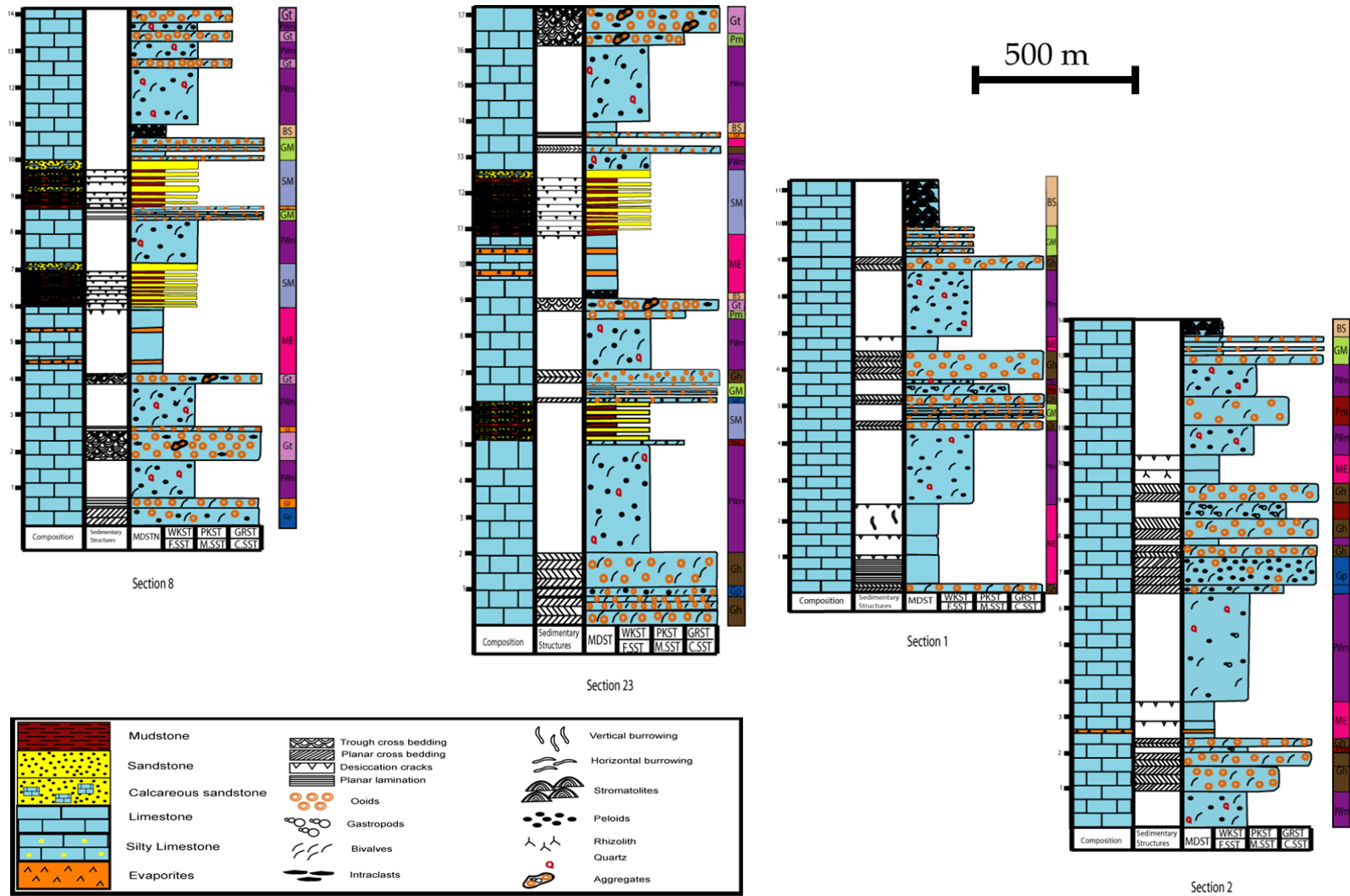


Figure 4.1: Vertical stratigraphic sections and sedimentary facies of the studied outcrops

## **4.2 Facies Description and Interpretation**

### **4.2.1 Interbedded Dolomudstone and Evaporite Facies (ME)**

*Description:* This facies shows a considerable abundance in the study area. It was found in different forms and at different stratigraphic levels in almost all the studied sections with a thickness ranging from 0.5 m to 1 m. Sediments are composed of carbonate mudstone interbedded with evaporites (Figure 4.2 (A)). The mainly massive mud occasionally shows some desiccation cracks and it is mainly massive. It also sometimes shows fine horizontal laminations with alternate light silty and dark finer laminae. The evaporites seem to be entirely dissolved, which causes the facies layers to be somehow distorted. By looking carefully into the samples from the dissolved evaporite layers, they show calcite crystal growth into a bee cell-shaped spots (Figure 4.2 (B)), which seems to be preserved traces of dissolved chicken wire anhydrite nodules.

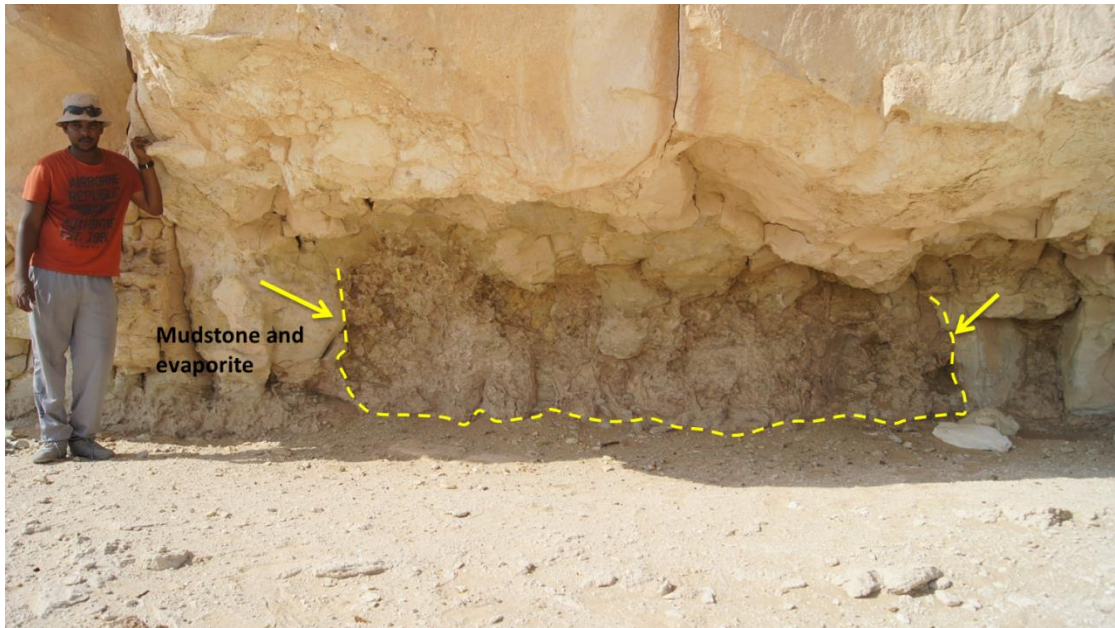
This facies shows more than one color ranging from green to red; especially when found near siliciclastic sand-dominated zones, probably due to oxidation or the existence of hematite (Tucker, 2001). It sometimes contains fine sand and mica grains. This facies is occasionally interrupted by U-shaped bodies occupied by fissile glauconitic mud (Figure 4.2 (C & D)). They are found in both outcrops 2 and 8. The mud here is highly fractured, and the fractures are filled with salt (Halite) and satin spar gypsum that sometimes show interbedding with the mud. Stratigraphically, this facies is always bottomed by cross bedded grainstones and capped by interbedded sandstone-mudstone facies except in outcrops 2 and 1 where siliciclastic facies are approximately absent. The XRD analysis of this mudstone shows complete dolomite composition (about 97.8 %) (Figure 4.2 (E)).



***Interpretation:*** The fine texture of this facies suggests a low energy environment and mainly deposition out of suspension. The existence of mud cracks and the red to brown color in some sections indicates deposition in low energy oxidizing conditions in a partially subaerial environment. The interbedding with evaporites points to saline to hypersaline environmental conditions. The associated facies, in addition to all previous evidence leads to the interpretation that this facies represents sabkha deposits on a supratidal flat. The U – shaped tongues with sharp boundaries, filled with fissile mud, with fractures filled with evaporites that lie in the middle of supratidal flat thick mud could be interpreted as small supratidal abandoned creeks.



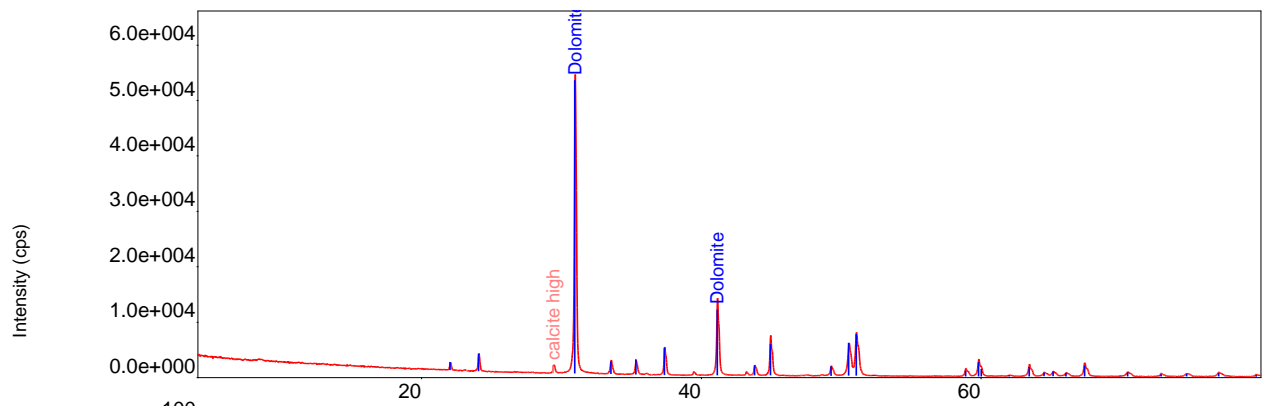
**Figure 4.2: (A) Massive mudstone facies with distorted evaporite layers (arrows). (B) Dissolved and calcified chicken wire anhydrites (note the pattern of the vugs)**



**Figure 4.2 (continued): (C) U-shaped body within the massive mudstone facies with semi vertical boundaries (arrows) in outcrop 2**



**Figure 4.2 (continued): (D) Evaporites (Halite and satin spar Gypsum) filling the U-shaped body in (C); Note the sharp boundaries**



**Figure 4.2 (continued): (E) The XRD analysis of mudstone samples showing the majority of dolomite**

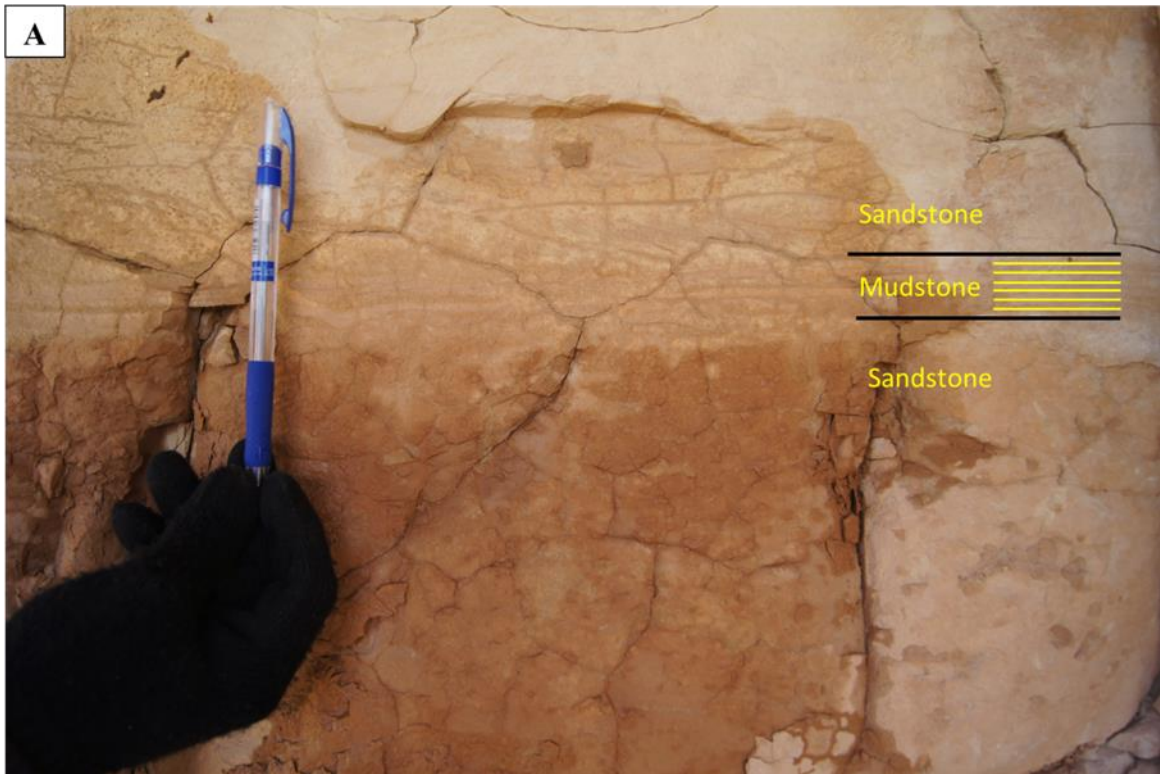
#### **4.2.2 Interbedded Cross-bedded Sandstone and Mudstone Facies (SM)**

**Description:** This facies is encountered in outcrops 23, 8 and 16. The lithofacies is absent in both outcrops 1 and 2 suggesting that it was not deposited in the eastern part of the study area. Its thickness reaches about 3.5 m. Stratigraphically, it overlies the thick brown cracked massive mudstone-evaporites facies in outcrop 23 and 16 and it is capped by a stromatolite facies of the combination type. It is also cut by medium to fine sandstone channels in outcrop 23. In outcrop 8, it overlies interbedded fine-grained oolitic grainstone and skeletal grainstone (Coquina). The thickness of both interbedding members varies vertically through the facies, alternating between thickening and thinning upward. The lithology of these members is fine calcareous sandstone and mudstone. The mudstone is mainly massive, but sometimes it shows horizontal lamination in addition to desiccation cracks (Figure 4.3 (A, B)). It is also characterized by bioturbation in the form of vertical burrows in places. The burrows are filled by the overlying calcareous sandstone (Figure 4.3 (C)). The color of the mudstone varies from the light brown to grey and light green. It contains trace fossils of rootlets (Rhizoliths) with a maximum length of 3 cm (Figure 4.3 (D)). On the other hand, the fine calcareous sandstone has creamy to yellow and sometimes gray color, composed mainly of quartz grains with rare skeletal grains and cemented mainly by calcite. It shows range of sedimentary structures; wavy bedding, mud drapes, tidal bundles, climbing ripples, herringbone cross lamination and lenticular bedding (Figure 4.3 (E, F, G & H)). XRD analysis of this facies samples show the dominance of quartz and calcite (Figure 4.3 (I)).

**Interpretation:** The high amount of interbedding between the fine sandstone and the mudstone in this facies could be interpreted as rapid fluctuation between the processes

that deposited them. This fluctuation is shown in the tidal bundles and the mud drapes that indicate a slack period during deposition. The fine grain size of the sand with the laminations indicate lower flow depositional regime. It was deposited by currents that were relatively stronger than those of the associated mud, but still generally moderate to weak. Moreover, the herringbone cross stratification indicates a bidirectional transporting current. The rhizoliths and desiccation cracks in the mud suggest intermittent subaerial exposure. The wavy bedding indicates shallow marine conditions (wavy ripples). All previous evidence, as well as associated facies, is characteristic of a shallow intertidal setting. Tide and ebb currents deposited the sand subaqueously in sand tidal flats during their active intervals, whereas the mud was most probably deposited out of suspension in mud tidal flats (Davis, 2012).



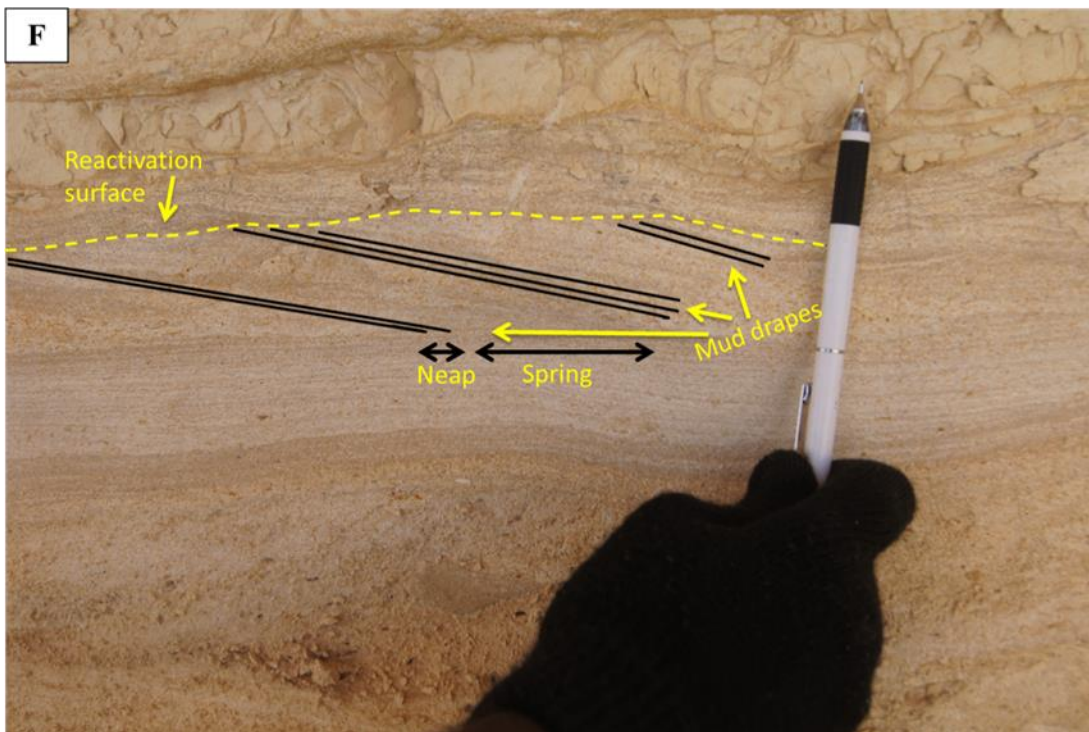
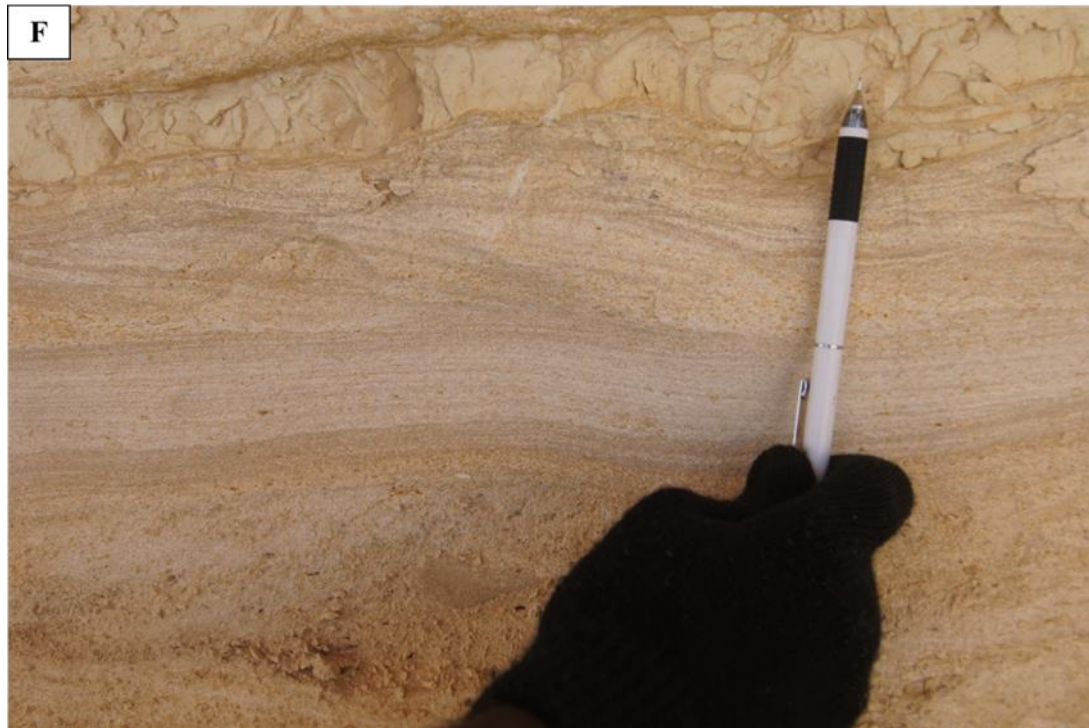


**Figure 4.3: (A) Horizontal lamination in the mudstone. (B) Desiccation cracks in the mudstone with sandstone fill**



**Figure 4.3: (continued): (C) Bioturbation in the mudstone. (D) Preserved rootlets (Rhizoliths) in the mudstone. (E) Wavy bedding in fine sandstones**

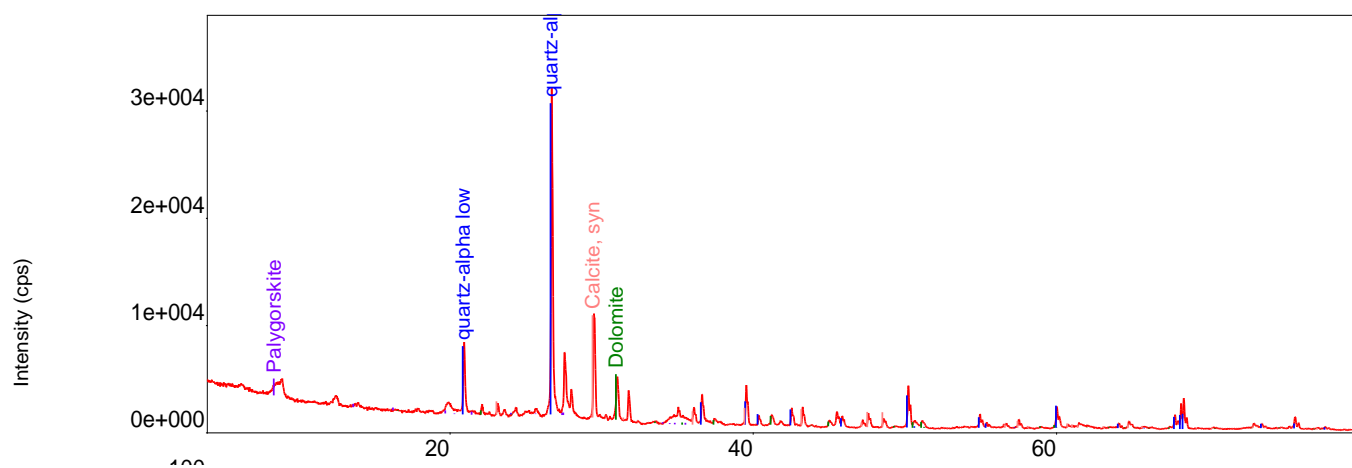




**Figure 4.3 (continued): (F) Reactivation surface between ripples in addition to tidal bundles**



**Figure 4.3 (continued): (G) Herringbone cross stratification in sandstone. (H) Cross-laminated thick connected lenticular bedded sandstone (arrow)**



**Figure 4.3 (continued): (I) XRD analysis of sandstone samples showing the dominance of quartz with minor amount of calcite**

### 4.2.3 Channelized Medium Sandstone Facies (Sc)

**Description:** This lithofacies was encountered in outcrop No 23 as a lens of medium-grained sandstone with 1-2 m thickness and 8 – 10 m width, in a north-south direction and based by a sharp erosional surface (Figure 4.4 (A)). The channel cuts through the interbedding sandstone-mudstone facies and is filled with calcite-cemented loose sandstone with medium grain size. The sandstone is intensively bioturbated which partially obscures its multi/bidirectional cross bedding (Figure 4.4 (B and C)). The bioturbation is mainly exemplified by a single ichnofacies (low diversity). The whole sequence shows a general fining upward grain size pattern. X-Ray Diffraction (XRD) analysis revealed predominance of quartz mineral with dolomite (Figure 4.4 (D)).

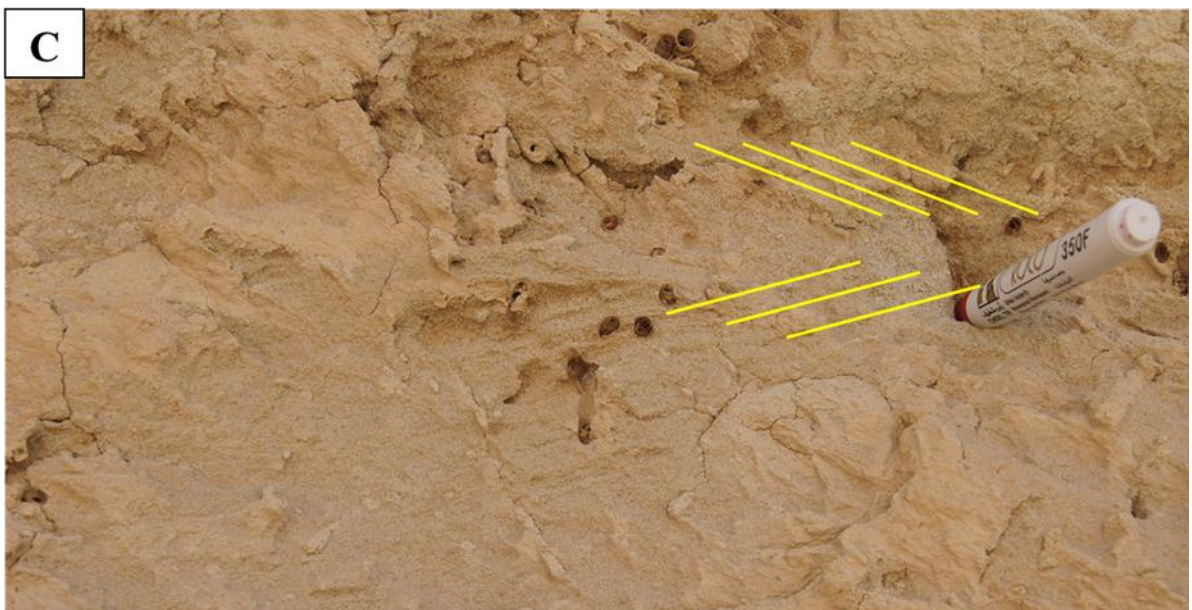
**Interpretation:** This lithofacies was deposited in a subaqueous flow with energy enough to cut across adjacent facies, and that the flow was through a channel. The partially covered bidirectional to multidirectional cross bedding indicates migration of straight to sinuous subaqueous dunes, respectively. The channel architecture with the erosive base cutting through interbedded sandstone-mudstone with desiccation cracks and the adjacent shallow marine carbonate facies makes it possible to interpret these sandstones as an estuarine channel fill. The bidirectional paleocurrent indicates the influence of tidal currents. The low diversity trace fossils suggests brackish water conditions. Moreover, the intensive bioturbation (Ichnofabric Index 4-5) by mono ichnospecies could be attributed, at least, to one of two reasons: First, the water was affected by a marine tide (which is proved by the existence of bidirectional currents) that brought food into a relatively lower energy environment and made it abundant in and on the sediment.



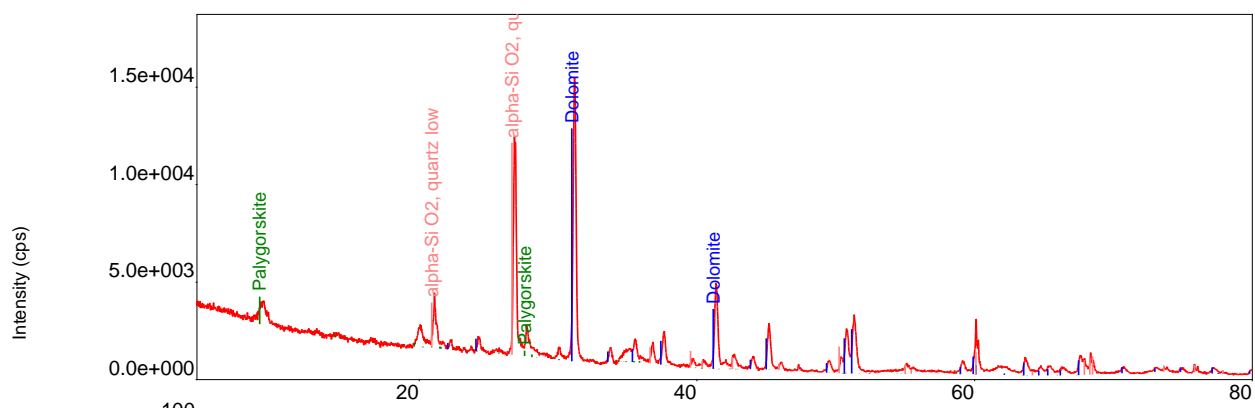


**Figure 4.4: (A) Channel architecture of medium grained sandstone facies**





**Figure 4.4 (continued): (B) Intensive bioturbation by very small vertical and horizontal burrows of approximately mono ichnospecies. (C) Traces of bidirectional cross bedding**



**Figure 4.4 (continued): (D) XRD analysis of estuarine calcareous sandstone samples showing the dominance of quartz mineral with dolomite**

Secondly, intensive competitions for food resources in brackish water led to the dominance and then flourishing of one species that dominates over the others (Pemberton et al., 1982). In addition, the very small size of the trace fossils could be considered as a brackish water indicator (Gingras et al. 2012).

#### **4.2.4 Trough Cross-Bedded Sandstone (St)**

**Description:** This facies is composed of white - green to gray trough cross-bedded fine sandstone, with erosive base (Figure 4.5 (A)). Its thickness ranges from 40 cm in outcrop 16 to 280 cm in outcrop 19; the only outcrops that show this facies. Generally, it contains no body fossils, but it shows scattered vertical burrows of *Skolithos* and *Ophiomorpha* trace fossils (Figure 4.5 (A) & (B)). The physical and biogenic structures are more obvious and noticeable in outcrops 16 than in outcrop 19. This facies overlies heterolithic facies and contains calcite geoids structures (Figure 4.5 (C)). The XRD analysis revealed the dominance of quartz mineral (Figure 4.5 (D)). Thin sections of this facies' samples show moderate sorting and intergranular porosity (Figure 4.5 (E)).

**Interpretation:** The trough cross bedding structure preserved in the facies indicates that it was deposited by the action of relatively high energy 3D dunes (Tucker, 2001). The interbedding between brown and green to gray colored beds in this facies suggest an oscillation between oxidizing and reducing conditions. These observations indicate that this facies is most probably an upper shoreface deposits (Thom et al., 1986; Roy et al., 1980).

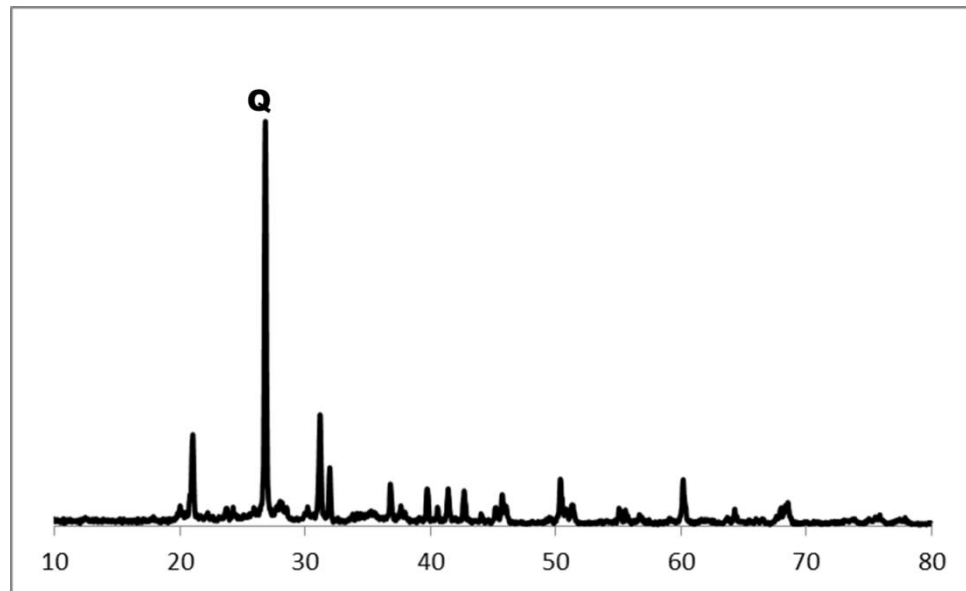
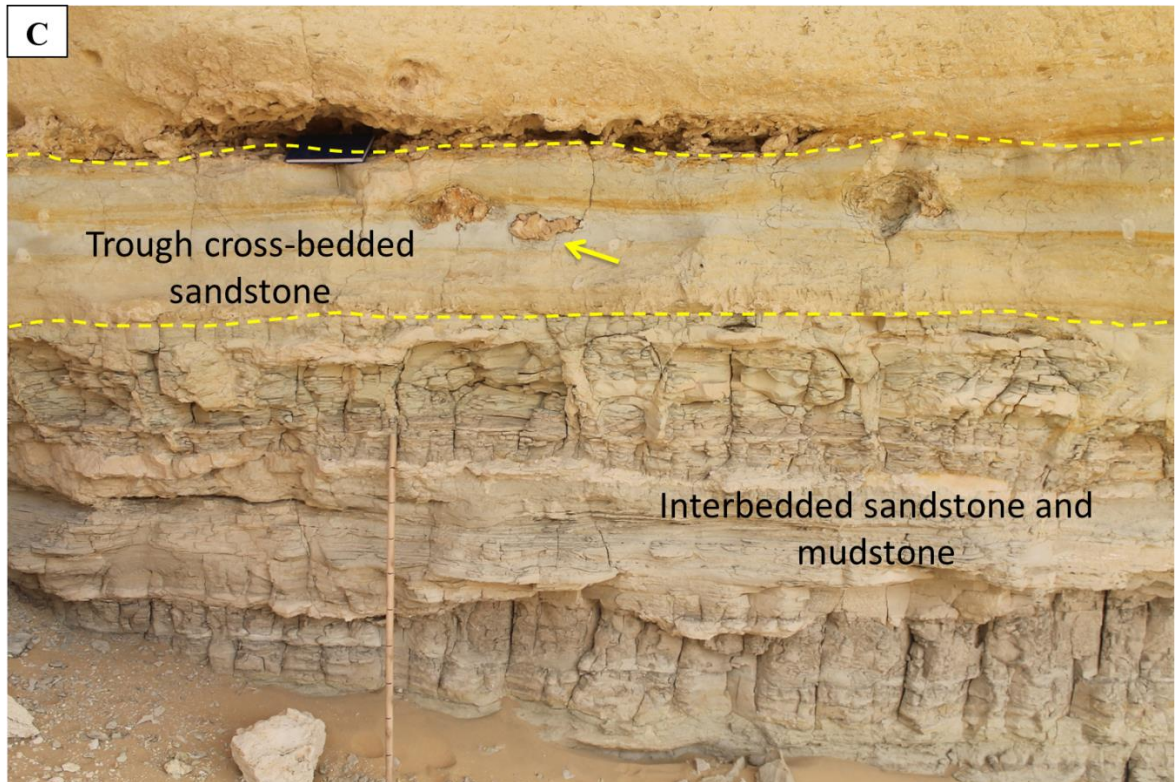
The high energy and continuous 3D subaqueous dune migration process is consistent with the observed scarcity in fossils and their poor preservation in the facies (Howard,



J.D. 1975). The existence of Ophiomorpha vertical burrows shows that, with this high energy conditions, only filter feeding, deep penetrating organisms could survive, which confirms the upper shoreface depositional environment interpretation (Pemberton et al. 2012).

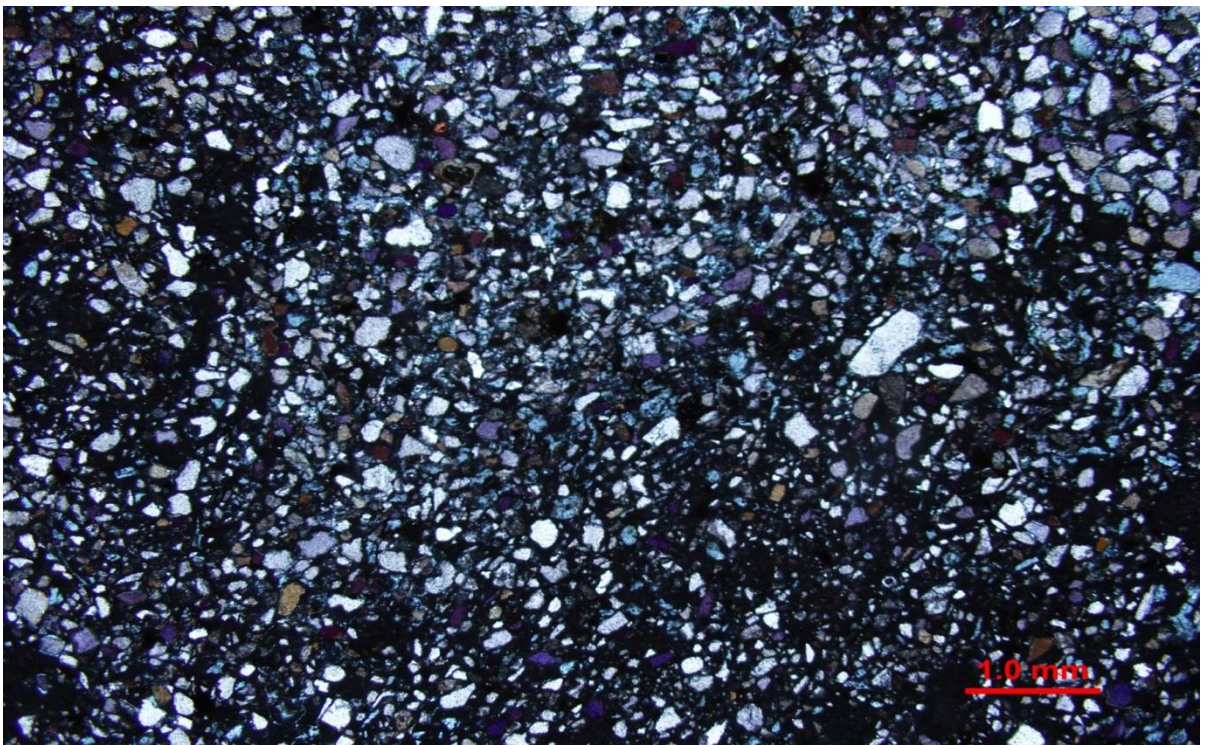


**Figure 4.5 (A) Trough cross-bedded sandstone facies with sharp erosional base and Ophiomorpha trace fossil; (B) Ophiomorpha burrow in the same facies found in outcrop 19**



**Figure 4.5 (continued): (C) Stratigraphic location of trough cross-bedded sandstone and their content of calcite geode structure (arrow). (D) The XRD analysis of trough cross-bedded sandstone facies which shows the dominance of quartz mineral.**





**Figure 4.5 (continued): (E) Trough cross-bedded sandstone facies thin section showing the intergranular porosity and the moderate sorting of rounded to subrounded quartz grains**

#### **4.2.5 Interbedded Cross-bedded Coarse Limestone and Mudstone Facies (GM)**

**Description:** This lithofacies is to some extent, similar to the siliciclastic heterolithites facies, except it is composed entirely of carbonate members. It is less represented and has maximum thickness of 60 cm. It is found in outcrops 1 and 2 situated in the eastern part of the study area. This facies is capped by adjacent stromatolite facies in the upper part of outcrop 2 with tepee structures (Figure 4.6 (A)). In the middle of section 1 it is capped by planar cross-bedded skeletal oolitic grainstone (Figure 4.6 (B)). The mudstone is mainly massive with some desiccation cracks. Otherwise, the other member is variable; planar cross-bedded skeletal packstone and fine-grained oolitic grainstone that contain quartz grains and rain drops at its top surface (Figure 4.6 (C)). The XRD analysis shows the dominance of dolomite and relatively high percentage of quartz (Figure 4.6 (D)).

**Interpretation:** The same depositional conditions of siliciclastic heterolithites facies are represented here with the absence of a major siliciclastic role. This rhythmic lithofacies was most probably deposited in an intertidal zone. The skeletal oolitic and oolitic packstone and grainstone, respectively, were deposited during the high energy periods of either tide or ebb currents whereas the fine muddy member was deposited during the current slack period. The V-shaped tepee structure denotes the peritidal depositional system (Kendall and Warren, 1987). The mud cracks and rain drop impressions indicate an intermittent subaerial exposure, while the presence of quartz grains suggests proximity to land.

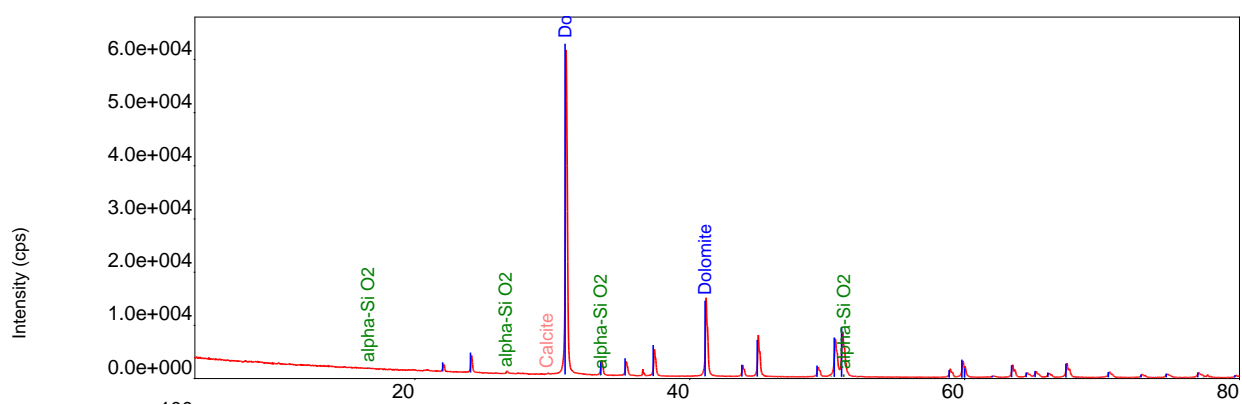


**Figure 4.6 Carbonate interbedding lithofacies: (A) Highly interbedded (arrow) with tepee structure (dashed curve). (B) Planar cross-bedded skeletal oolitic grainstone (upper zone) capping the interbedded facies**





**Figure 4.5 (continued): (C) Rain drop impressions on the top of the coarse interbedding member.**



**Figure 4.6 (continued): (D) XRD analysis shows the dominance of dolomite in coarse-fine limestone interbedded facies samples with high percentage of quartz**

#### **4.2.6 Intra-formational Limestone Conglomerate (Gmm)**

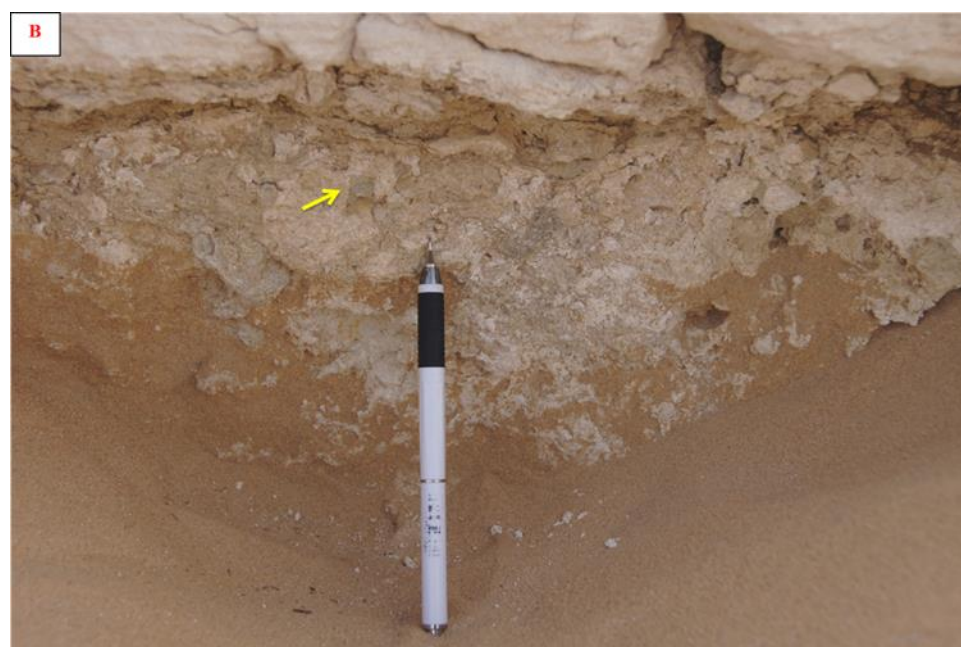
**Description:** The thickness of this facies ranges from 10 cm to 120 cm. It is mainly composed of intra-formational grain-supported (ortho) and matrix-supported (para) limestone conglomerates with rounded, sub-rounded to angular and few flat muddy pebbles (Figure 4.7 (A) & (B)). The high degree of roundness of the pebbles is mainly associated with light colored muddy pebbles, whereas the less rounded pebbles are mainly dark green to gray in color. This facies is found in all studied outcrops with distinctive appearance in both outcrops 23 and 8. They are mainly bottomed by erosional surfaces. The intra-formational pebbles, generally, show a fining upward grain size pattern. In outcrop 23, (Figure 4.7 (A)), this facies is represented by chaotic layer composed of muddy limestone intra-formational pebbles with normal graded bedding within a muddy matrix (para-conglomerate). The muddy pebbles are light brown in color and show some preserved fissility. They are rounded to sub rounded and rarely show flake shape. Few of the intraformational pebbles are of skeletal oolitic grainstones and fine sandstone. In outcrop 8 (Figure 4.7 (B)), the intra-formational conglomerate has gray to dark green muddy pebbles with overall thickness of 120 cm. The pebbles are, generally, angular to sub rounded in shape and support each other (ortho-conglomerate).

**Interpretation:** The sudden appearance of this facies through studied sections with erosional bases, the lateral continuous bedding in addition to the intraclasts and their fining upward pattern indicate an erosion followed by re-deposition mainly by storm events (tempestites) (Aigner, 1985, Lasemi et al., 2012). Carbonate tempestite layers in studied sections are found in different stratigraphic levels, with different facies associations and slightly different internal characteristics; that are interpreted as different



depositional settings. The intraclasts are mainly produced by ripping up mud clasts, transporting them by transgressive currents and then depositing them along the fine matrix in the depositional center (Lasemi et al., 2012).

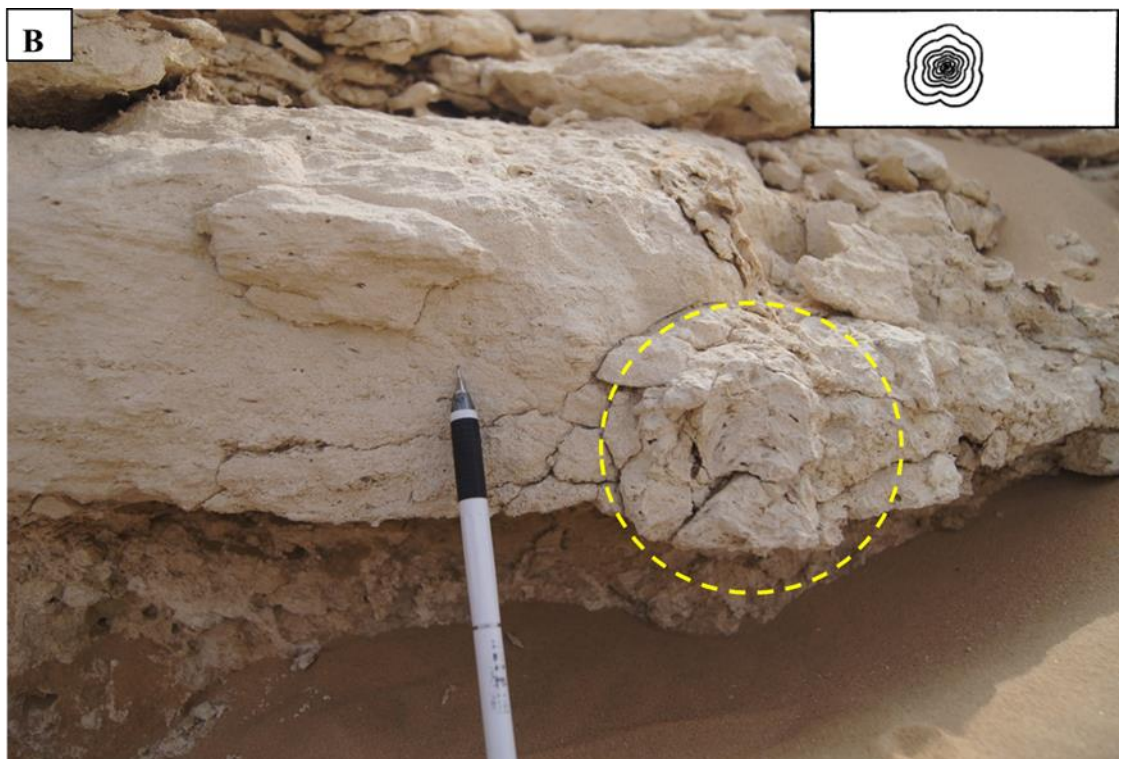
In outcrop 23, carbonate tempestites are interlayered with interbedded sandstone and mudstone rhythmites. Then, the association is overlain by combination type of stromatolites and cut by estuarine channels. According to its stratigraphic position and its light brown muddy intraclasts that are similar to the underlying muddy layers, tempestites in outcrop 23 are interpreted as supratidal to intertidal (Friedman, 1993). On the other hand, in outcrop 8, the intraclasts are dominantly of dark green to gray massive lime mud, which indicates relatively deeper source. It is overlain by trough cross bedded oolitic grainstone which contains spherical type of stromatolite and would be interpreted to be deposited most probably over the fair weather wave base in the upper shore face zone. Consequently, tempestites, here, are mainly proximal; been deposited below fair weather wave base, and above storm weather wave base (lower shoreface) (Friedman 1993). Finally, where tempestites are found within the thick massive to horizontally laminated carbonate wackestone, they are found as zones. The intraclasts are relatively finer in size but still could show general normal grading. The tempestites zones are thin (10 cm as maximum) and show fewer amounts of intraclasts and wider spaces between them. Additionally, they are entirely of muddy carbonates. All these characteristics indicate relatively deeper conditions below storm weather wave base, and tempestites, here, could be interpreted as distal tempestites (Friedman, 1993).



**Figure 4.7 Carbonate conglomerate facies: (A) Light-colored rounded pebbles (arrow) of carbonate intra-formational para-conglomerate. (B) Dark green to gray angular pebbles (arrow) of carbonate intra-formational ortho-conglomerate**

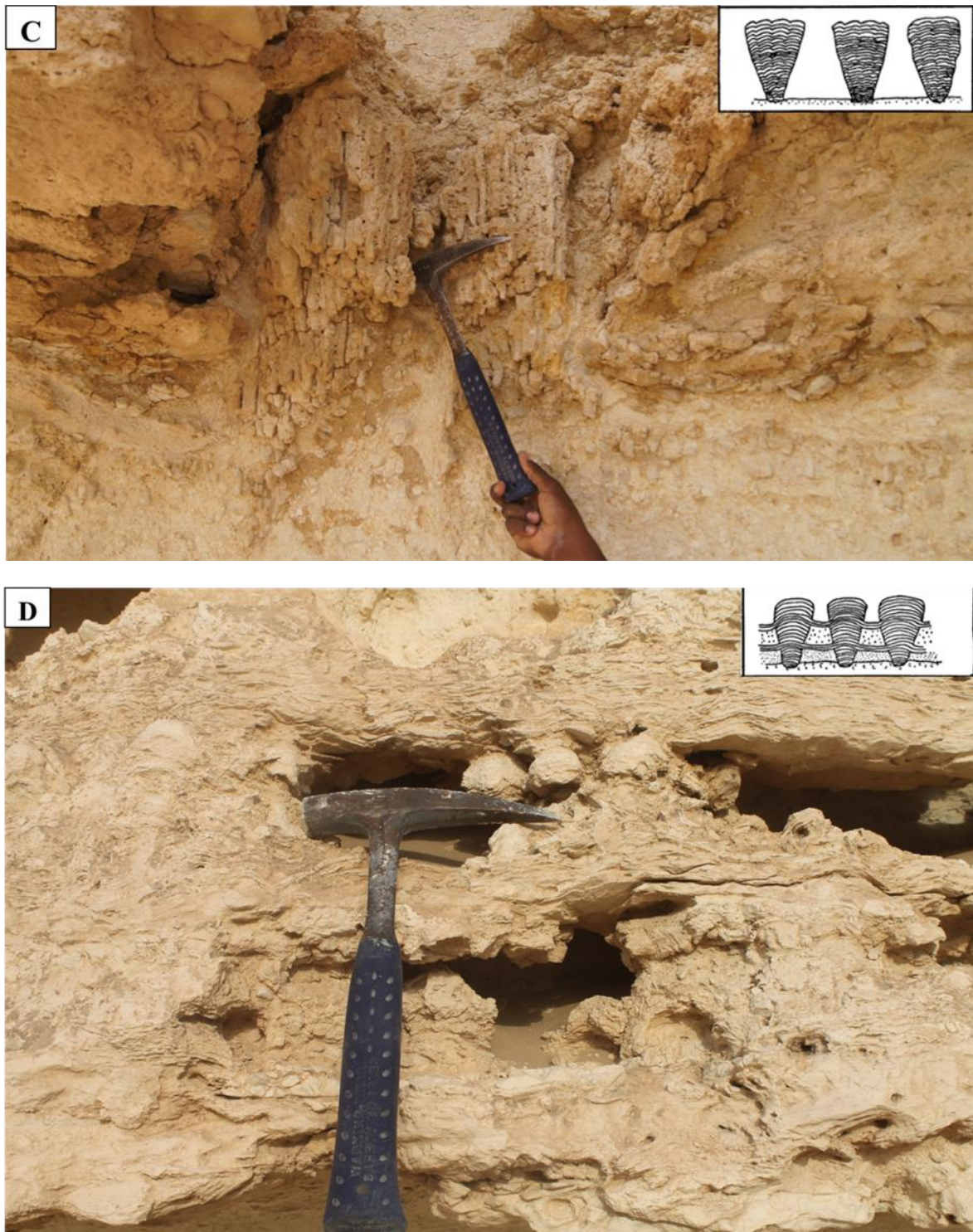
#### 4.2.7 Stromatolites (BS)

**Description:** Stromatolites is an organo-sedimentary laminated structure composed of alternation between fine-grained sediments and fine organic laminae. This facies is observed in all the studied outcrops with different thicknesses. Its thickness ranges from a few centimeters to 0.5 m. Following the Logan et al. (1964) classification scheme, the stromatolite lithofacies in the Dam Formation could be morphologically classified into: (1) laterally linked hemispheroid (LLH), (2) discrete spheroids (SS), (3) discrete vertical spheroids (SH) and (4) combination forms. The LLH type is found in the form of small-linked domes with a diameter that can reach up to 0.5 m. Since the space between the domes is less than the dome diameters themselves, they are classified as closed-linked hemispheroids (LLH-C) (Figure 4.8 (A)). The SS type shows smooth concentric lamination (SS-C) with a diameter of about 6 cm (Figure 4.8 (B)). The third type consists of discrete vertical spheroids (Figure 4.8 (C)). It has a maximum length of 40 cm and is concentrated in one stratigraphic horizon. The last type of stromatolite facies is a compound form which is an alteration between the LLH and the discrete vertically-stacked hemispheroidal type (SH). They alternate in a design of LLH-SH in three upward repetitive cycles (Figure 4.8 (D)). Both the LLH and the combination types are found, stratgraphically, capping the heterolithic facies of both siliciclastics and carbonates, whereas the SS-C type is found within trough cross-bedded oolitic grainstone layers. Important sedimentary structures are associated to this facies include: tepee structures which appear as psuedoanticlines, mud cracks that are found in between the LLH, and laminoid fenestral vugs that follow concentric laminae in SS-C type.



**Figure 4.8: Stromatolite lithofacies morphologies in the Dam Formation following Logan et al; (A) Laterally linked hemispheroid (LLH). (B) Discrete spheroids (SS)**





**Figure 4.8 (continued) (C) Discrete vertical spheroids (SH). (D) The combination form**

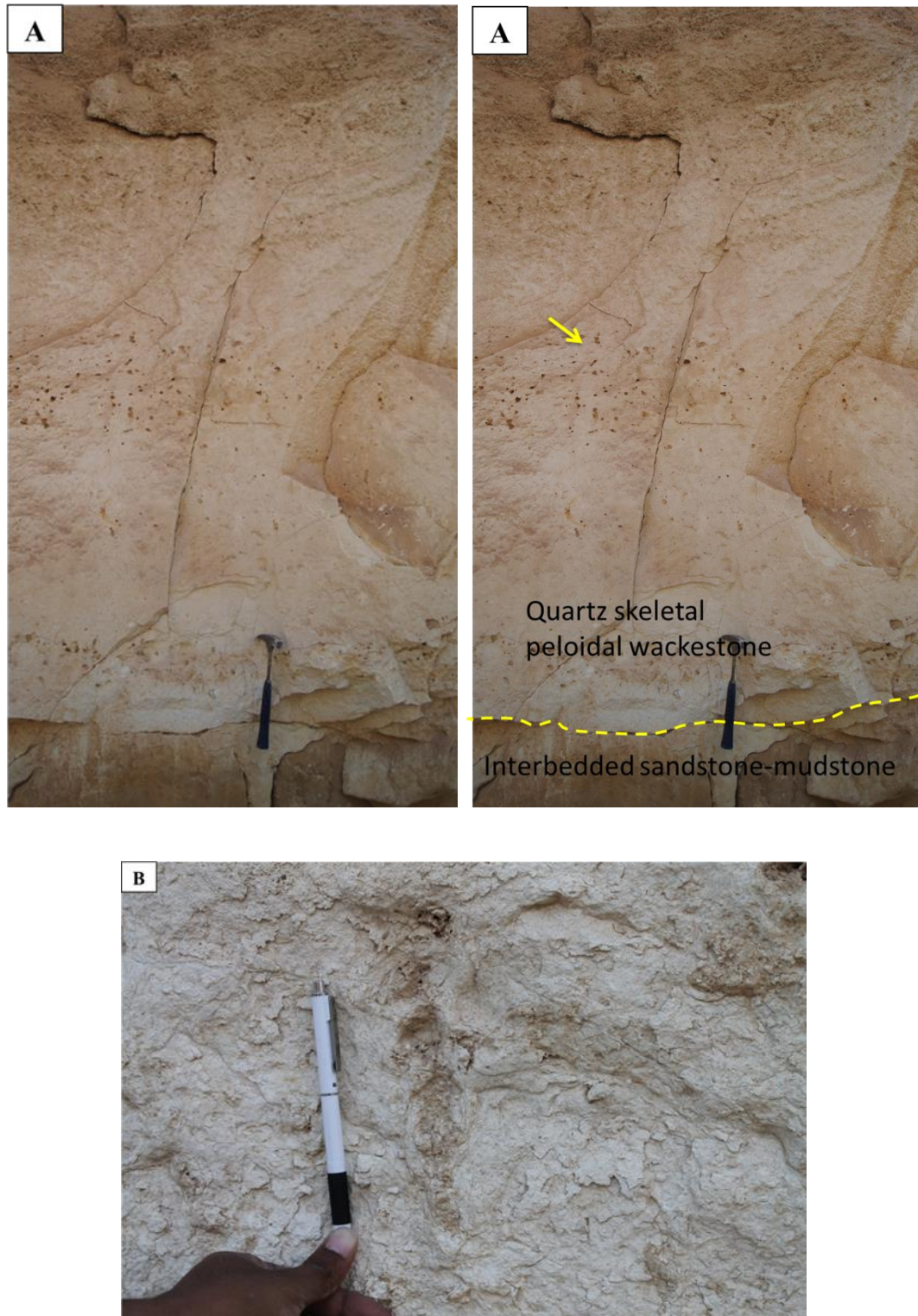
***Interpretation:*** Stromatolites is formed by a process of binding and trapping of fine sediments in mud matrix by bacteria followed by early cementation (calcification) and precipitation of new organic lamina. Stromatolites have been observed and described in modern and ancient subtidal and tidal flat environments (Dupraz et al. 2009). The shape of the stromatolites is a function of the dominant processes during precipitation (Boggs, 2006). The LLH type mainly indicates low energy conditions, and with the association of mud cracks between the domes. It was most probably deposited in an upper intertidal to supratidal environment. The SS-C type with laminated fenestrae, discrete vertical spheroids, and the surrounding trough cross-bedded oolitic grainstone show evidence of relatively higher energy, but still shallow water environmental conditions; mainly in the lower intertidal to upper shoreface zone. The combination form with repetitive LLH-SH signature and the adjacent heterolithic facies suggest a periodic alternation between high and low tide current energy in the intertidal zone.

#### 4.2.8 Massive Quartz Skeletal Peletal Wacke-Packstone (PWm)

**Description:** This facies is one of the most dominant and the thickest facies in the study area. It is found in outcrops 1, 2, 8 and 23 in the eastern part of the studied traverse. The thickness of the lithofacies ranges from 110 cm to 350 cm. It is characterized by relative westwards thinning pattern (towards outcrop 8). This facies is completely absent in outcrops 16 and 19. It always, stratigraphically overlies the mud cracked facies with sharp surface between them (Figure 4.9 (A)). The layers are intensively bioturbated by mud-filled vertical and horizontal burrows, which results in structure-less layers (Figure 4.9 (B)). This facies, in some locations, has sugar-like texture, white to creamy color and contains zones of well-rounded muddy intraformational pebbles with maximum diameter of 3-5 cm (Figure 4.9 (A) & (C)). In some layers, pebbles are randomly distributed and are relatively very fine (1 cm as diameter).

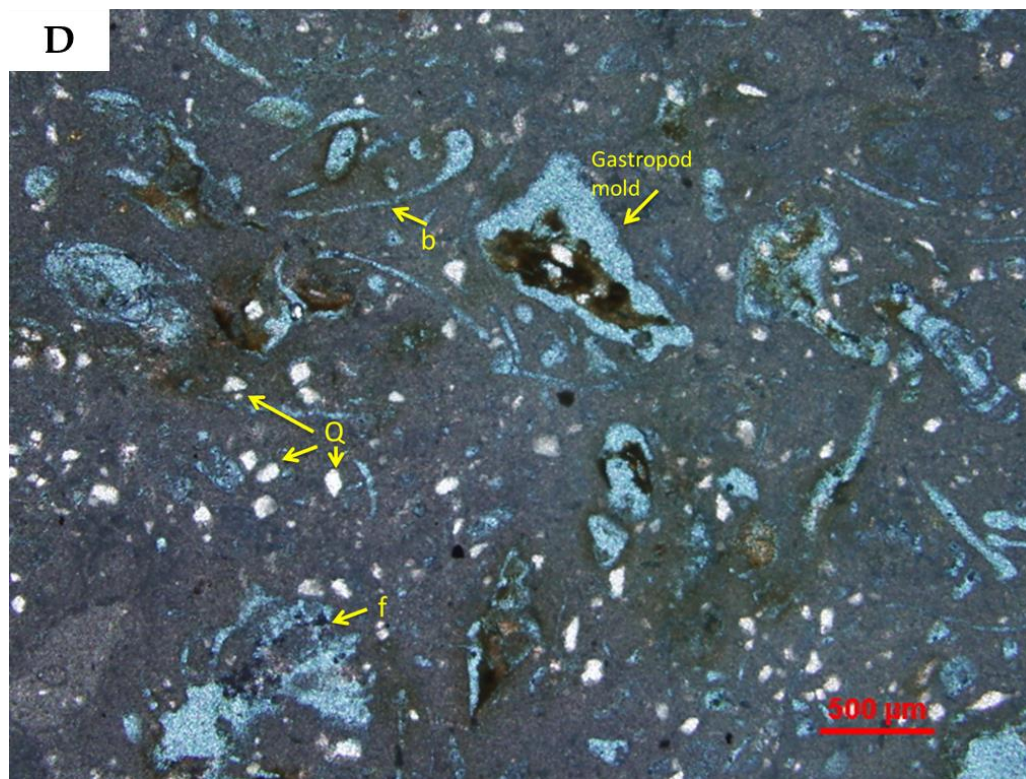
Thin sections of this facies samples show wackestone to packstone texture. Peloids are the main grain type in term of abundance. Skeletal grains mainly by foraminifera and bivalves are also present (Figure 4.9 (D)). Fossils in this facies have distinctive pattern of distribution upward; starting by bivalves dominance in the lower parts of the layers, and then alternates upward through the layers to foraminifera. Thin sections show the existence of *Alveolina* whereas SEM images show the existence of *Globigerina* and Miliolids (Figure 4.9 (E)). Fine quartz grains are also present in all the analyzed samples. They, generally, get coarser westward, and are sub-rounded to angular in shape.



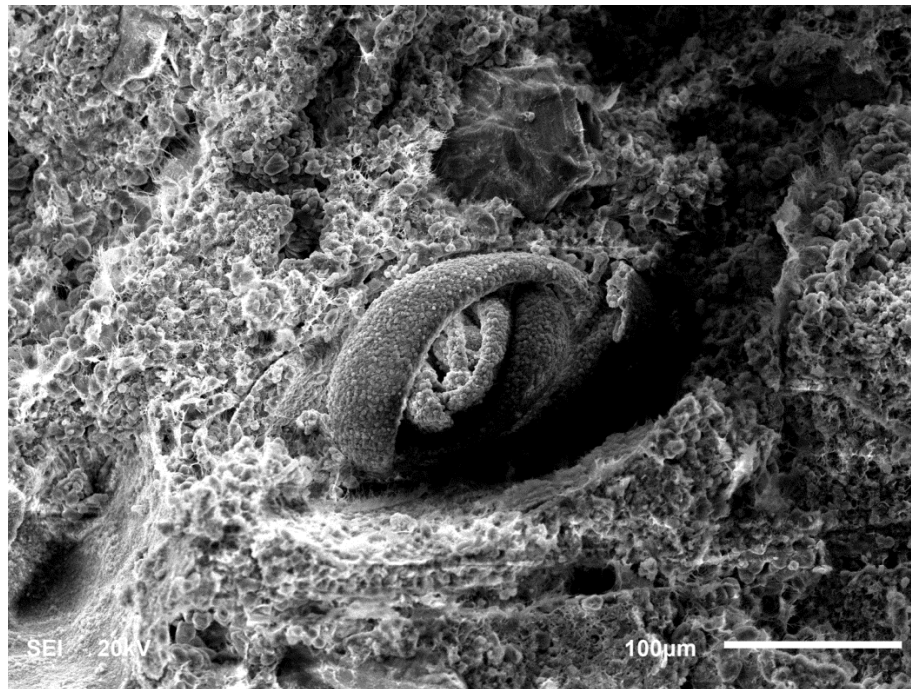
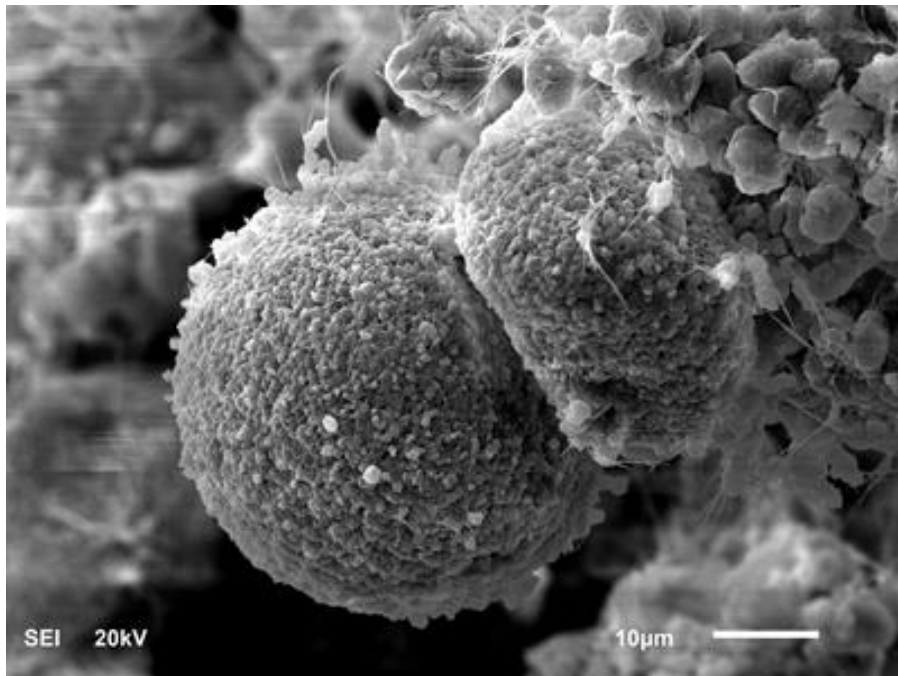


**Figure 4.9: (A) Stratigraphic position of skeletal peloidal wackestone facies and zones of intraclasts (arrow). (B) Bioturbation in the same facies**

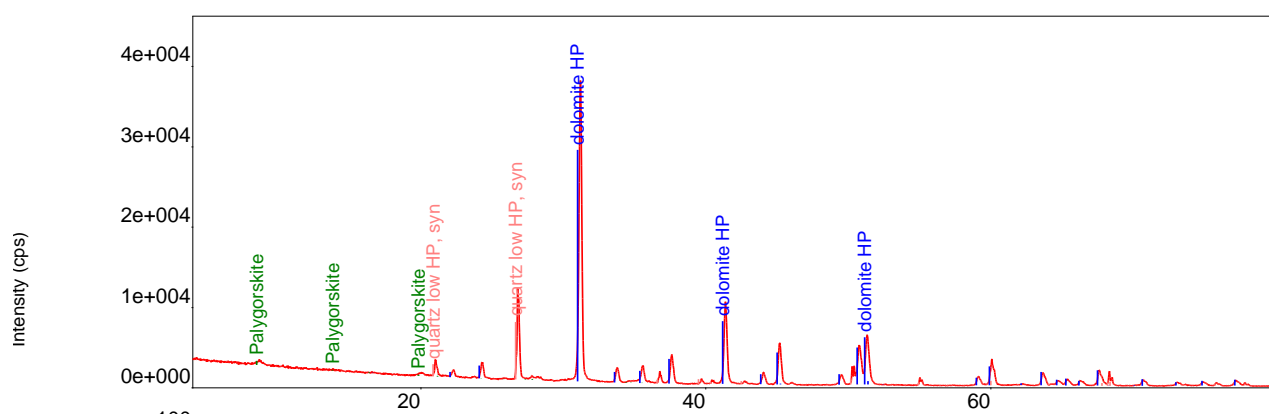




**Figure 4.9 (continued): (C) Magnified image of (A) for the dissolved intraclasts zones; note the fining upward pattern. (D) Foraminifera, bivalves and quartz grains in thin section with dominance of moldic and vuggy porosity**



**Figure 4.9 (continued): (E) SEM images show the planktonic foraminifera (*Globigerina*) and benthic Miliolids**



**Figure 4.9 (continued): (F) The XRD analysis of the massive quartz skeletal peloidal wackestone facies with the dominance of dolomite and minor amount of quartz**

The dolomite represents the dominance mineralogy whereas quartz is a minor mineral (Figure 4.9 (F)).

**Interpretation:** The fine textures of this facies, as well as its massive layers with the absence of physical current structures suggest a general low energy environment that sediments could settle out of suspension. The structure-less appearance could be, also, attributed to the intensive bioturbation. In addition, the dominance of peloids is common in low energy shallow intertidal to subtidal carbonate systems (Flügel, 2010). This facies, with the absence of exposure indications, was probably deposited below fair-weather wave base in the outer ramp zone.

The intraformational pebbles zones have sudden appearance through the layers, and they gradually disappear upwards where the pebbles get finer in normal graded bedding (Figure 4.9 (C)). These pebbles with previous characteristics and their existence in the middle of massive fine wacke-packstones are likely to be storm deposits. The storms, here, were short-lived depositional events, resulted in these thin and relatively fine intraclasts zones.

The skeletal dominance alternation through this facies could be linked to the difference in the environment conditions, varying from calm subtidal to storm agitated conditions.

With the existence of sandstone depositional systems, nearby, the fine-grained quartz grains in this facies could be attributed to suspended fine sand/silt grains clouds that were transported far away basinwards from a nearshore zone, and then settled out.

#### **4.2.9 Planar Cross-Bedded Skeletal Peloidal Grainstone (Gp)**

**Description:** This facies has white to beige color and variable thickness throughout the studied outcrops, ranging from 25 cm to 75 cm. It is observed in more than one stratigraphic position, in outcrops 1, 2 & 19. It is characterized by high angle planar cross bedding sets (dip 25°) (Figure 4.10 (A)). In some locations, it shows mud drapes on the cross bedding surfaces, keystone vugs and tangential bottom sets (Figure 4.10 (B)). Stratigraphically, it is adjacent to more than one facies: cracked mudstones, fine-coarse carbonate interbedding and massive skeletal packstone facies (Figure 4.10 (A)).

Petrographically, this facies is mainly composed of well-sorted fine peloids (mean grain size ( $\phi$ ) = 2.3) (Figure 4.10 (C)) with few skeletal grains (dominated by foraminifera and bivalves) (Figure 4.10 (D)). Scattered ooids are found with different percentages in this facies. They are superficial ooids with one to two preserved laminae in their cortices. Samples of this facies are visually porous (about 15 %) containing intergranular porosity as the main porosity type. Intragranular and moldic porosities through foraminiferal tests are also present.

**Interpretation:** The planar cross bedding sets indicate a subaqueous deposition by 2-D straight-crested bedforms migration by unidirectional currents (Boggs, 2006). The existence of mud drapes on the cross bedding indicates a deposition slack period (Tucker, 2001).

These observations in addition to the fine grain size and the superficial scattered ooids could be translated to a medium strength of the sediments transporting current. The association of interbedded carbonate heterolithic facies, herringbone grainstone facies

and the overlying cracked mud facies shows that this facies is most probably deposited in the lower intertidal zone (Lasemi et al., 2012).

#### **4.2.10 Herringbone Cross-Bedded Skeletal Oolitic Grainstone (Gh)**

**Description:** This facies is common throughout the study area. It was encountered in outcrops 2, 16, 19 and 23. It is a neighbor for many other facies including the trough cross-bedded grainstone, planar cross-bedded grainstone, carbonate heterolithites and cracked mudstone. The thickness of this facies varies from 10 cm to 60 cm. It contains distinct herringbone cross bedding structure (Figure 4.11 (A)), keystone vugs (Figure 4.11 (B)) and mud drapes (Figure 4.11 (C)). In some locations, it shows planar cross bedding sets with reactivation surfaces between them (Figure 4.11 (D)).

The petrography of this facies' samples shows grainstones composed mainly of moderately well-sorted medium grained size ooids with very thin cortices (superficial ooids) (Figure 4.11 (E)). In addition to quartz grains, the ooids commonly have foraminifera and bivalves as nuclei. The facies contains peloids in the form of micritized grains beside few scattered aggregates (Figure 4.11 (F)).

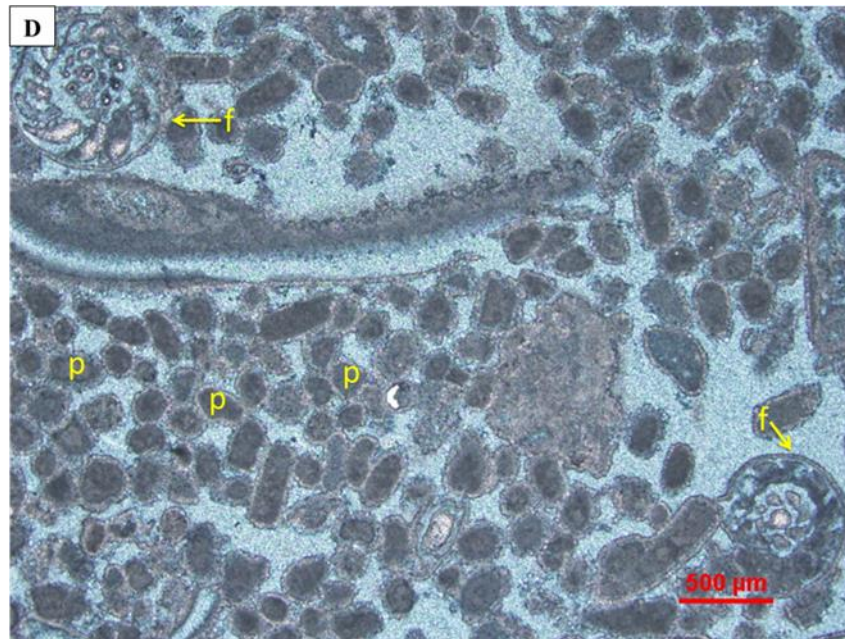
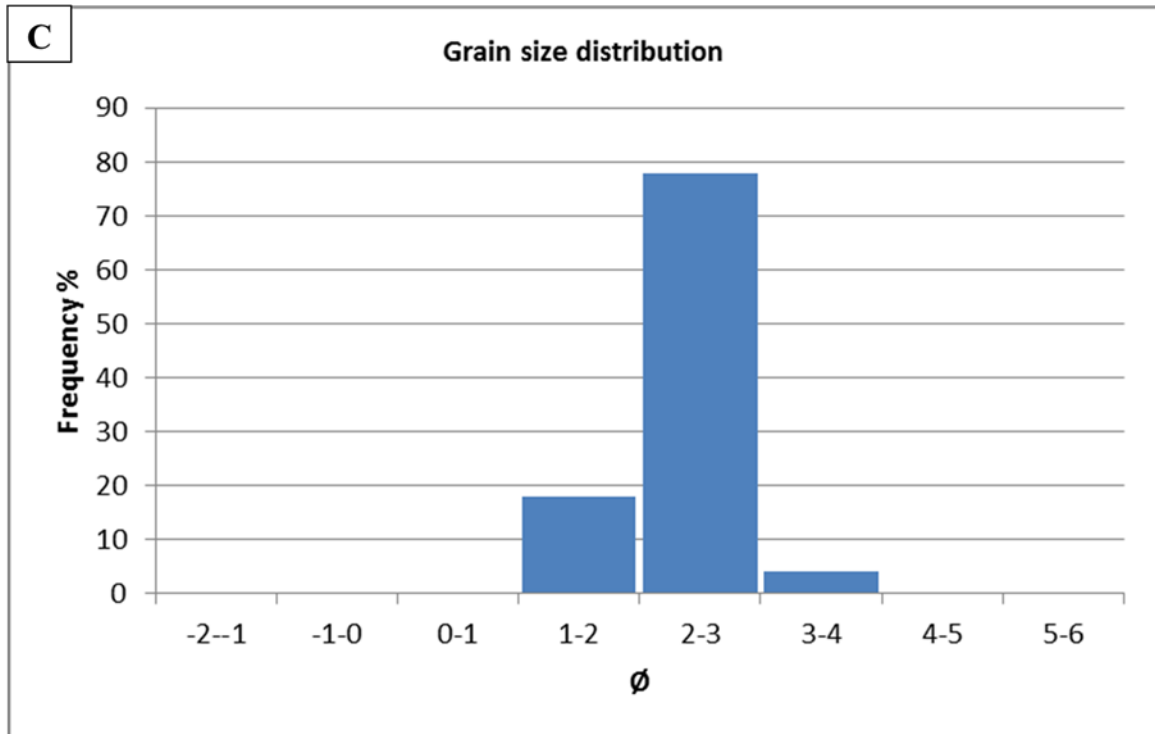
**Interpretation:** The observed associated physical sedimentary structures in this facies are distinctive features of the action of tidal currents. The mud drapes on the cross bedding surfaces, the reactivation surfaces and the clear herringbone cross bedding are tidal deposits diagnostic features (Eriksson and Simpson, 2004).





**Figure 4.10 (A) Planar cross bedding sets in grainstone facies and the associates facies. (B) Keystone vugs and tangential bottom sets in the cross bedding**



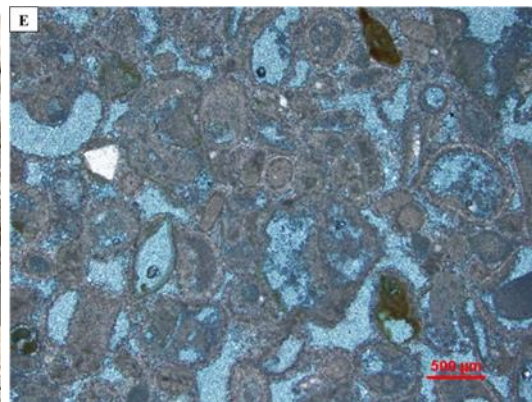


**Figure 4.10 (continued): (C) Histogram showing grain size distribution of planar cross bedded grainstones. (D) Thin section of planar cross-bedded grainstone facies showing peloids (p) and foraminifera (f) with intergranular and intragranular porosity types.**

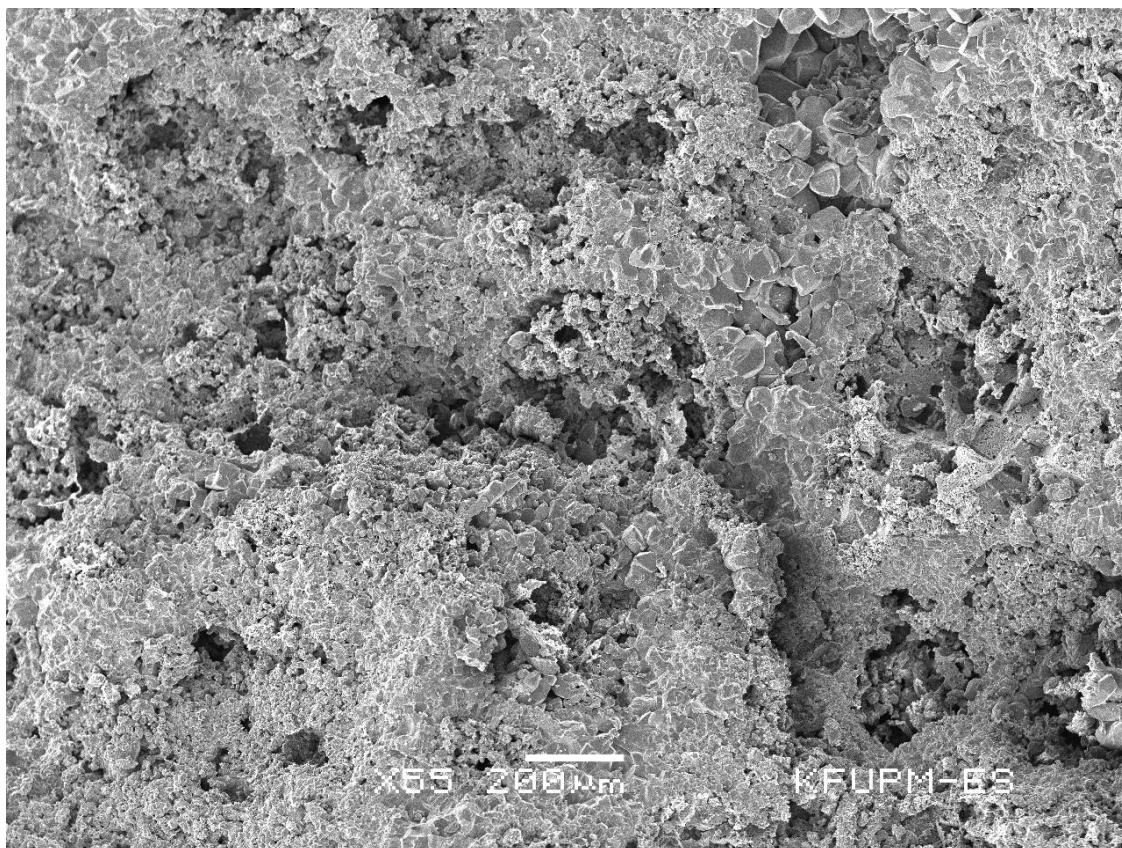


**Figure 4.11 Herringbone cross-bedded grainstone facies: (A) Herringbone cross bedding structure (B) Keystone vugs within the cross bedding (arrow)**





**Figure 4.11 (continued): (C) Mud drapes (circle) within the herringbone cross bedding. (D) Reactivation surfaces (RS) between cross bedding sets. (E) Thin section showing the superficial ooids, the intergranular and bivalves moldic porosities**



**Figure 4.11 (continued): (F) SEM image showing the high degree of micritization of the ooids grains in the herringbone cross-bedded grainstone facies**

The mud drapes indicate a relatively low current velocity, and slack deposition periods (Tucker, 2001). The herringbone cross bedding indicates a bidirectional transporting currents, generated mainly by succession of flood tide and ebb tide, whereas the reactivation surfaces indicate unequal strengths of flood and ebb which causes erosion of created bedforms (Boggs, 2006; Tucker, 2001).

Previous observations in addition to the associated facies indicate a deposition by 2-D bedforms, in shallow subaqueous conditions, guided by flood and ebb tide currents in the intertidal zone.

#### **4.2.11 Trough Cross-Bedded Aggregate Intraclastic Oolitic Grainstones (Gt)**

**Description:** This facies is found in outcrops 2, 8, 16 and 19. Stratigraphically, it is observed mainly in association with planar and herringbone cross-bedded grainstone facies, carbonates conglomerates, and massive skeletal wackestone facies. When it is associated with the conglomerates and wackestone facies, it mainly overlies them with erosive base.

This lithofacies is characterized by trough cross bedding structure (Figure 4.12 (A)), with some flaser beddings (Figure 4.12 (B)). In outcrop 8, it contains spherical stromatolites (Figure 4.12 (B)), whereas in outcrop 19, it shows discrete, vertically stacked hemispheroid stromatolites type (Figure 4.12 (C)). Thin sections of this facies samples (Figure 4.12 (C)) show grainstones mainly composed of ooids with partial micritization, grapestones as well as peloidal packstone intraclasts with few quartz grains within them. The peloids within the intraclasts seem to be micritized ooids, originally. Grapestones are

more preserved in this facies than in the others, and are composed of bounded ooids. Few quartz and skeletal grains (bivalves) exist in this facies. The main porosity types in this facies are intergranular, moldic and intragranular (Figure 4.12 (D)).

***Interpretation:*** The dominance of grain-supported rock fabric, pay in addition the presence of ooids, peloidal packstone intraclasts, and grapestones infer to relatively high energy shallow marine depositional settings (Palma et al., 2007). The trough cross bedding, basically, is a result of 3-D multidirectional bedforms migration, with sinuous crests (Lee and Chough, 2006).

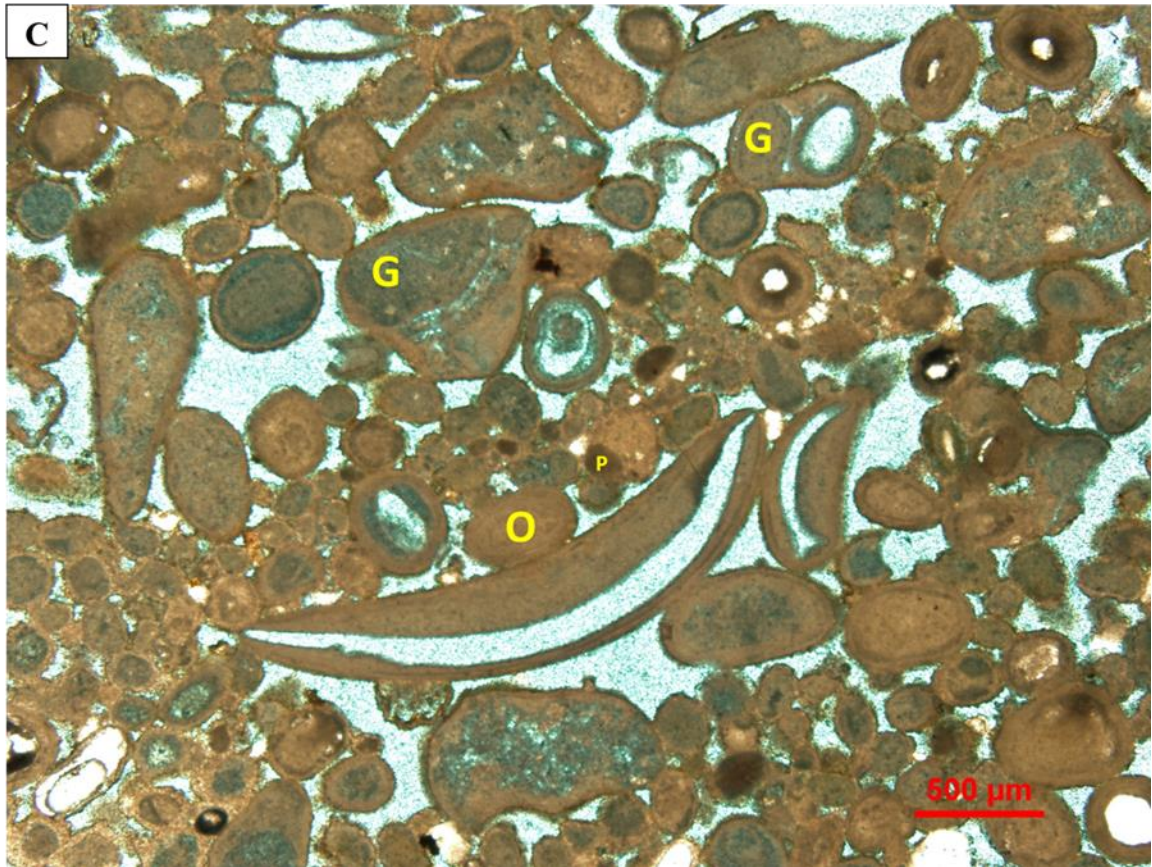
The discrete vertically stacked stromatolites, also, suggest high energy setting, whereas existence of spherical stromatolites type could be interpreted as higher energy conditions, that the cyanobacteria can't build long vertical colonies.

The neighborhood of lower shoreface carbonate conglomerates, subtidal skeletal wackestone and intertidal planar and herringbone cross bedded grainstones, in addition to previous observations, lead to the interpretation that this facies mainly represents subaqueous carbonate sand waves in upper shoreface zone. The very thin mud streaks in the troughs of the cross bedding sets (flaser bedding) indicate short periods of energy waning during deposition.



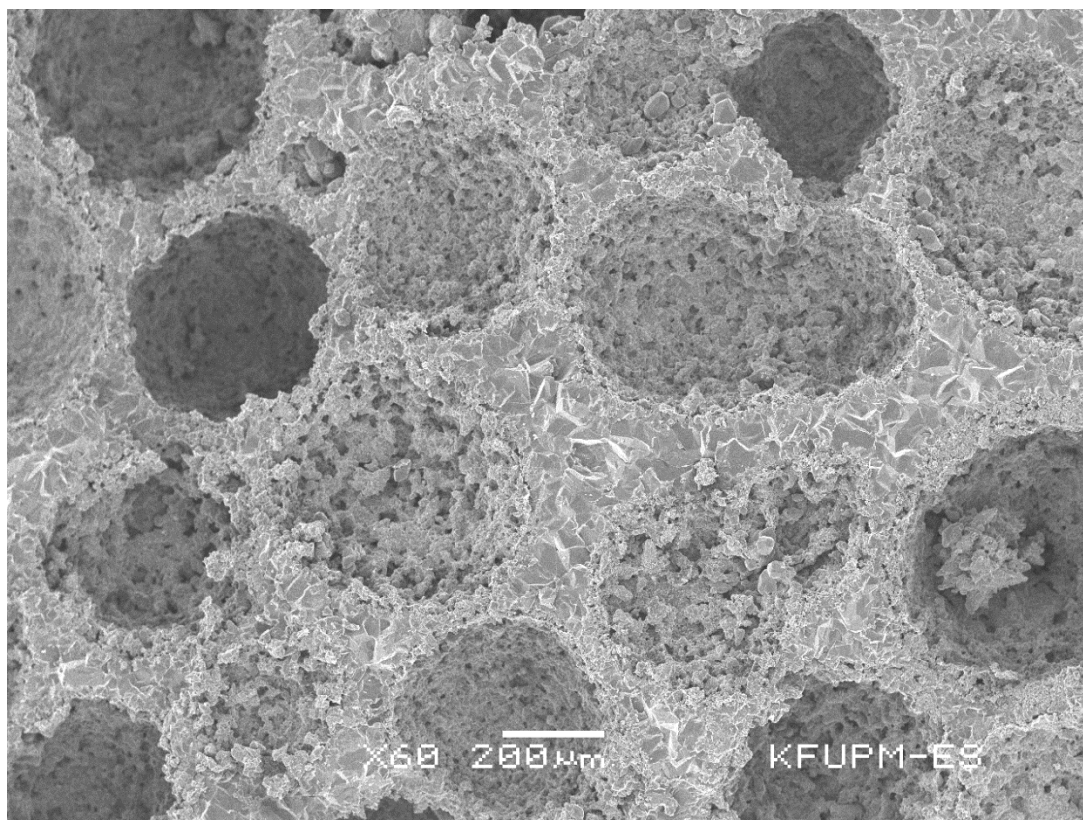


**Figure 4.12 (A) Trough cross bedding in grainstone facies. (B) Flaser bedding structure with fine mud seams within the troughs**



**Figure 4.12 (continued): (C) Thin section of trough cross bedded grainstone facies showing dominance of superficial ooids (O) and aggregates (G). Note the high percentage of intergranular, intragranular and moldic porosity.**



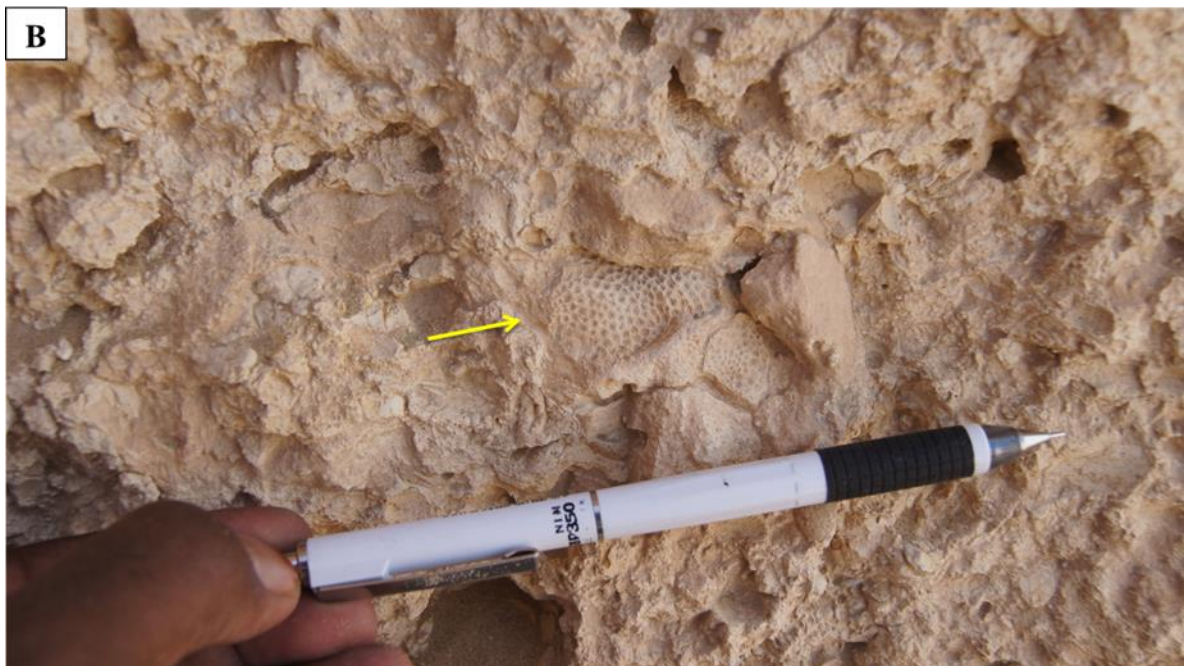


**Figure 4.12 (continued): (D) SEM image of trough cross-bedded oolitic grainstone facies showing the great existence of moldic porosity (within dissolved ooids).**

#### **4.2.12 Massive Peloidal Skeletal Packstone (Pm)**

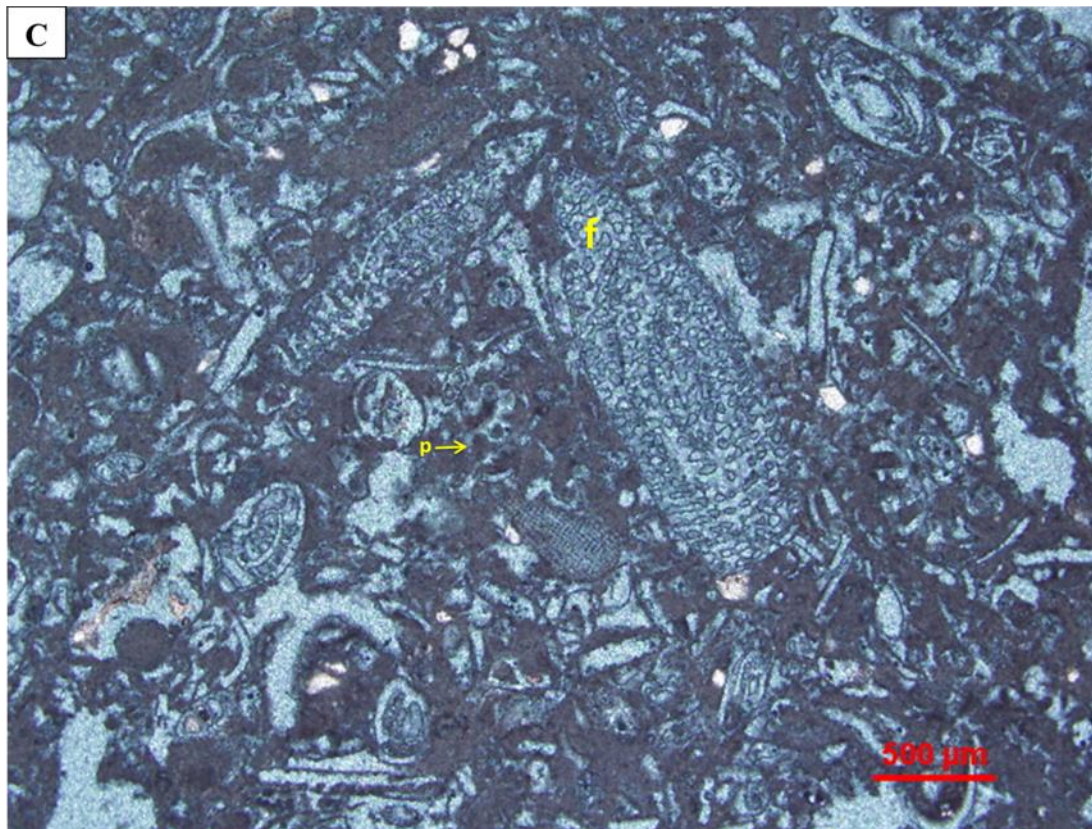
**Description:** With thickness of 40 cm, this facies was encountered only in outcrops 1 and 2. It is white to beige in color and contains vugs (Figure 4.13 (A)). This facies overlies the planar cross-bedded grainstone facies. Macrofossils in this facies are mainly gastropods and bivalves in the form of internal molds. Distinction of this facies is in the hexagonal coral head fragments that it contains (Figure 4.13 (B)). This facies is intensively bioturbated by vertical and horizontal burrows. Thin sections show peloids and to a great existence the presence of foraminifera and bivalves. Most of the microfossils are either completely dissolved (forming moldic porosity) or partially dissolved (forming intraparticle porosity) (Figure 4.13 (C)).

**Interpretation:** The high abundance of macro- and microfossils in this facies, beside the apparent absence of major physical current sedimentary structures give misleading criteria for subaqueous skeletal banks (biostrome). However, the abundance of broken gastropods and bivalve fragments, as well as coral fragments indicate that this facies components are allochthonous rather than autochthonous. The adjacent planar cross-bedded grainstone (lower intertidal) in addition to the intensive bioturbation, which mainly had destroyed all previously existed current structures, both point to middle intertidal depositional environment (Rankey, 2012).



**Figure 4.13 (A) Stratigraphic position of skeletal packstones, the intensive bioturbation within it and the vugs (arrow). (B) Coral fragment within the massive bioturbated skeletal packstone facies (arrow)**





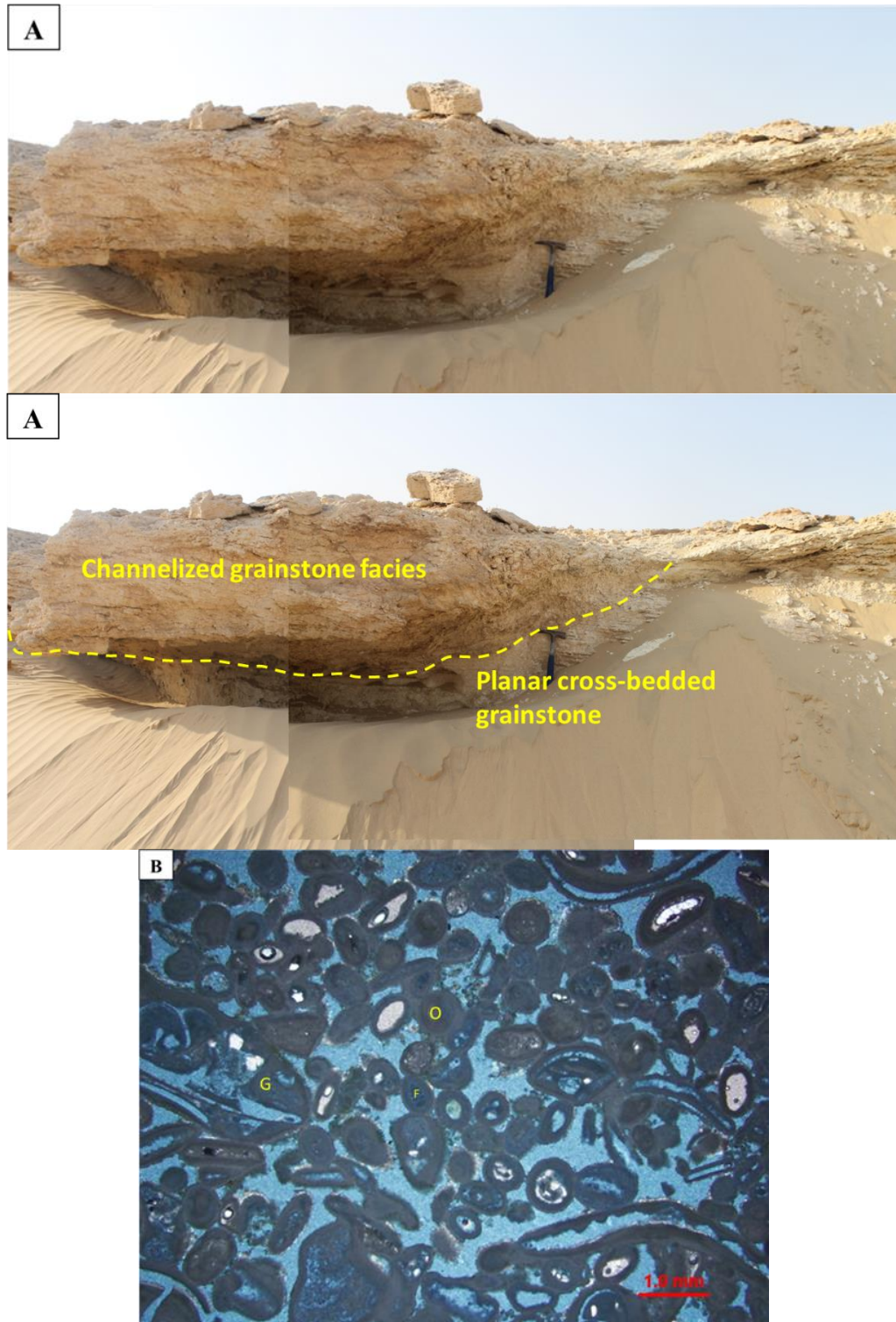
**Figure 4.13 (continued): (C) Thin section of peloidal skeletal packstone facies showing the dominance of skeletal grains; foraminifera (f) and peloids (p). Note the high porosity percentage between the grains (intergranular) and within the skeletal grains (intragranular and moldic types).**



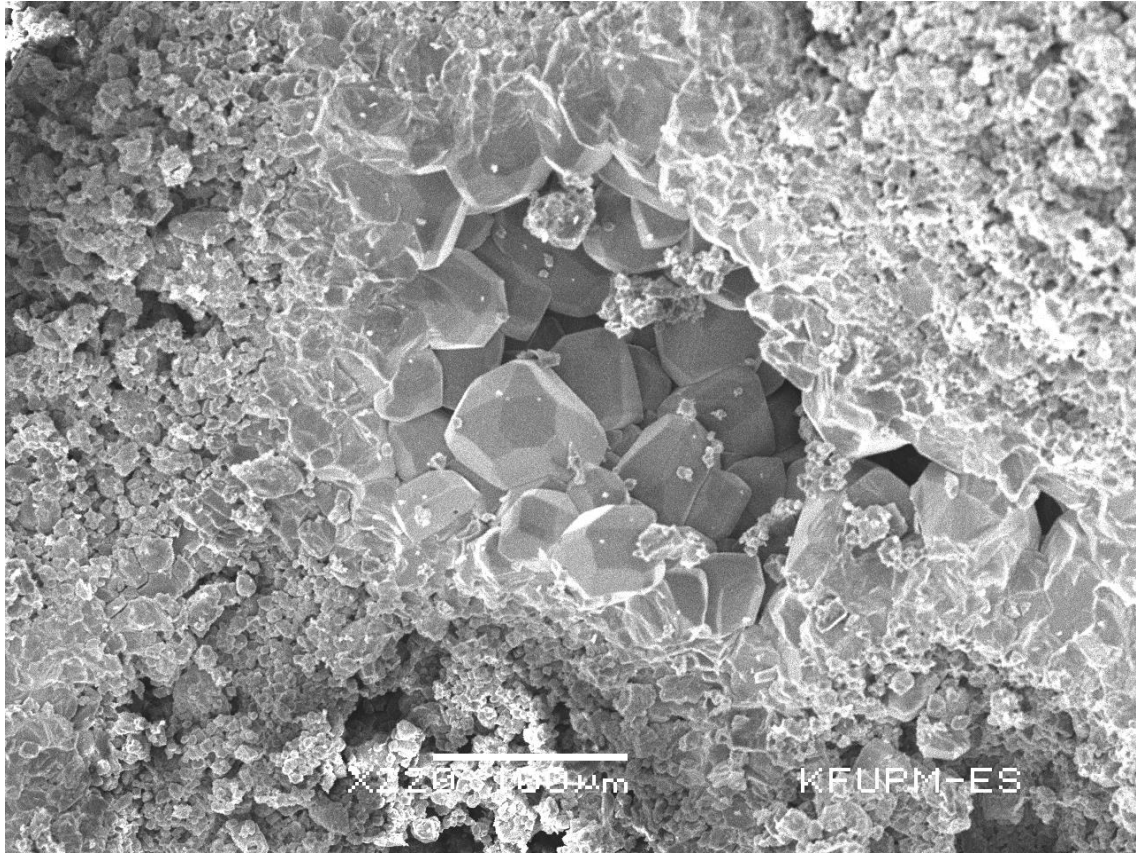
#### **4.2.13 Channelized Planar Cross-Bedded Skeletal Oolitic Grainstone (Gcp)**

**Description:** This facies is found only in outcrop 23. It has channel cross section morphology with a thickness of 70 cm and width of 230 cm, cutting through herringbone cross-bedded grainstones (Figure 4.14 (A)). It shows planar cross bedding with tangential bottom sets. This facies, in micro scale, is generally composed of coarse and moderately well sorted ooids with relatively thicker cortices and better preservation (Figure 4.14 (B)). Grapestones and abundant foraminifera and bivalves also characterized this facies. Many of the ooids grains have quartz grains and foraminifera in their nuclei. Samples of this facies are porous, showing inter- and intragranular types. Between the ooids, granular calcite cement was noticed in some samples (Figure 4.14 (C)).

**Interpretation:** The coarse grain size of the ooids with planar cross bedding structure in addition to the cut and fill morphology (channel) indicate a relatively high energy current cutting through intertidal zone represented in the planar cross-bedded grainstone and the siliciclastic heterolithic facies. On the basis of these observations, these planar cross-bedded coarse oolitic grainstone deposits are result of a tidal channel bars migration.



**Figure 4.14: Channelized grainstone facies: (A) Channel architecture cutting through other facies. (B) Thin section showing ooids and skeletal grains with moderately well sorting and intergranular and intragranular porosities**



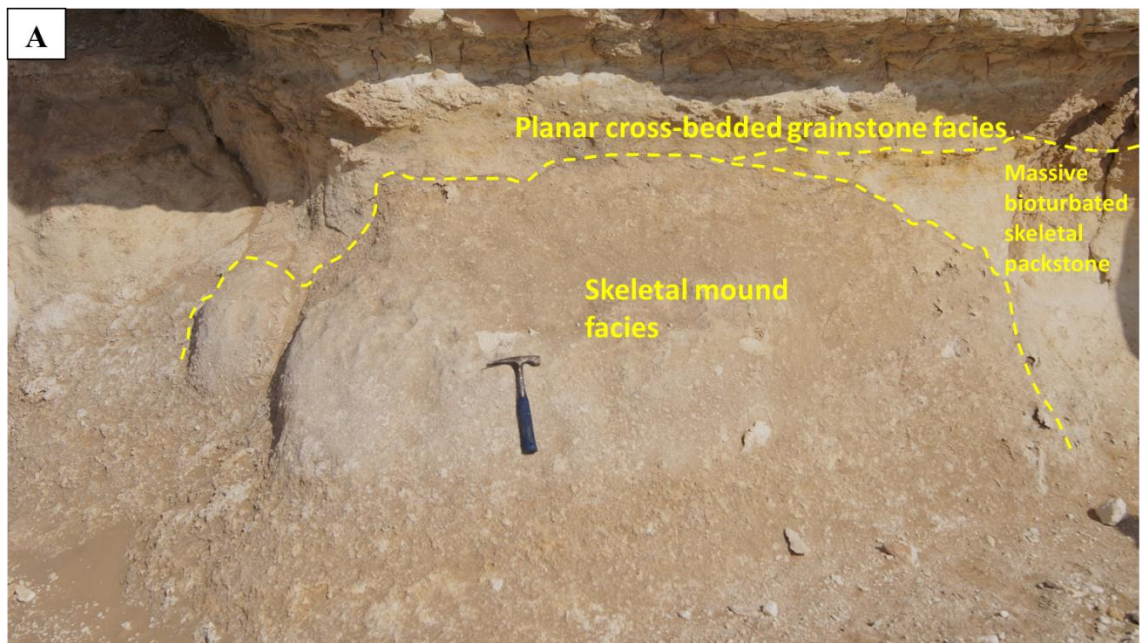
**Figure 4.14(continued): (C) SEM image of tidal channel grainstone facies showing granular calcite cement between ooids.**

#### **4.2.14 Massive Skeletal Wackstone (Wm)**

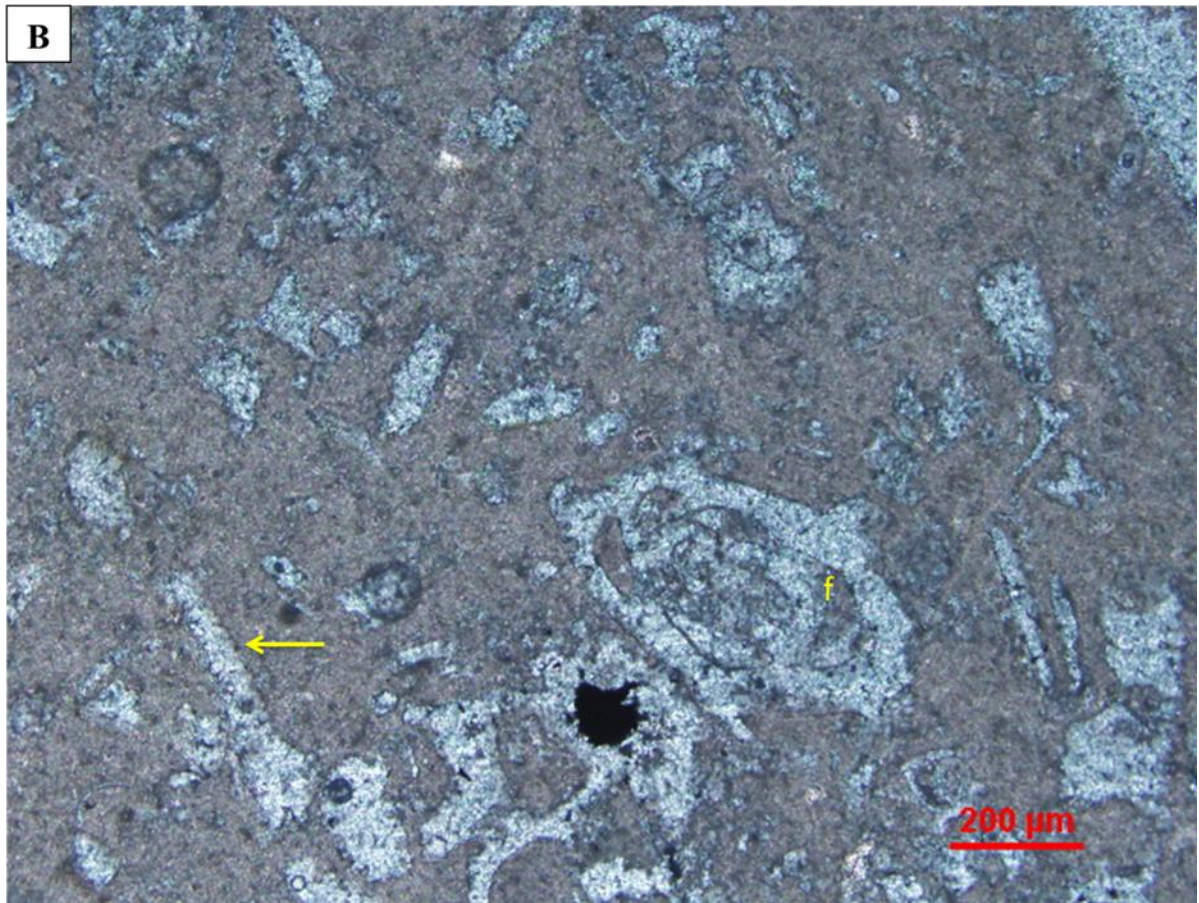
**Description:** It is represented by a dark gray colored massive carbonate body. This facies has domal shape and cut through massive skeletal packstone and planar cross-bedded grainstones facies (Figure 4.15 (A)). It, also, has sugar-like texture, relatively hard to be sampled and only found in outcrop 1. In thin sections, the samples of this facies show wackestone texture, with skeletal grains as only components. They are well abundant in the samples and are mainly of foraminifera, echinoids spines and bivalves (Figure 4.15 (B)). Most of these fossils were completely dissolved and formed moldic porosity.

**Interpretation:** The dark color of the mud in this facies could be attributed to the high percentage of organic materials within it. Both the absence of current physical structures, bioturbation and the pure skeletal components, indicate an insitu skeletal build up. The domal architecture, the environmental indications of adjacent facies, the cross cutting relationship with these facies in addition to previous observations lead to the interpretation that this facies is most probably an inner–mid ramp skeletal mound.





**Figure 4.15: (A) The domal shape of massive skeletal wackestone facies (dashed line follows the boundaries) and the associated facies**



**Figure 4.15 (continued) (B) Thin section of skeletal mound facies showing wackestone texture with dominance of skeletal grains; foraminifera (f) and echinoid spine (arrow). The only porosity type in this facies is through the skeletal grains (moldic porosity).**



#### **4.2.15 Dipping Planar-bedded Skeletal Oolitic Grainstone (G1)**

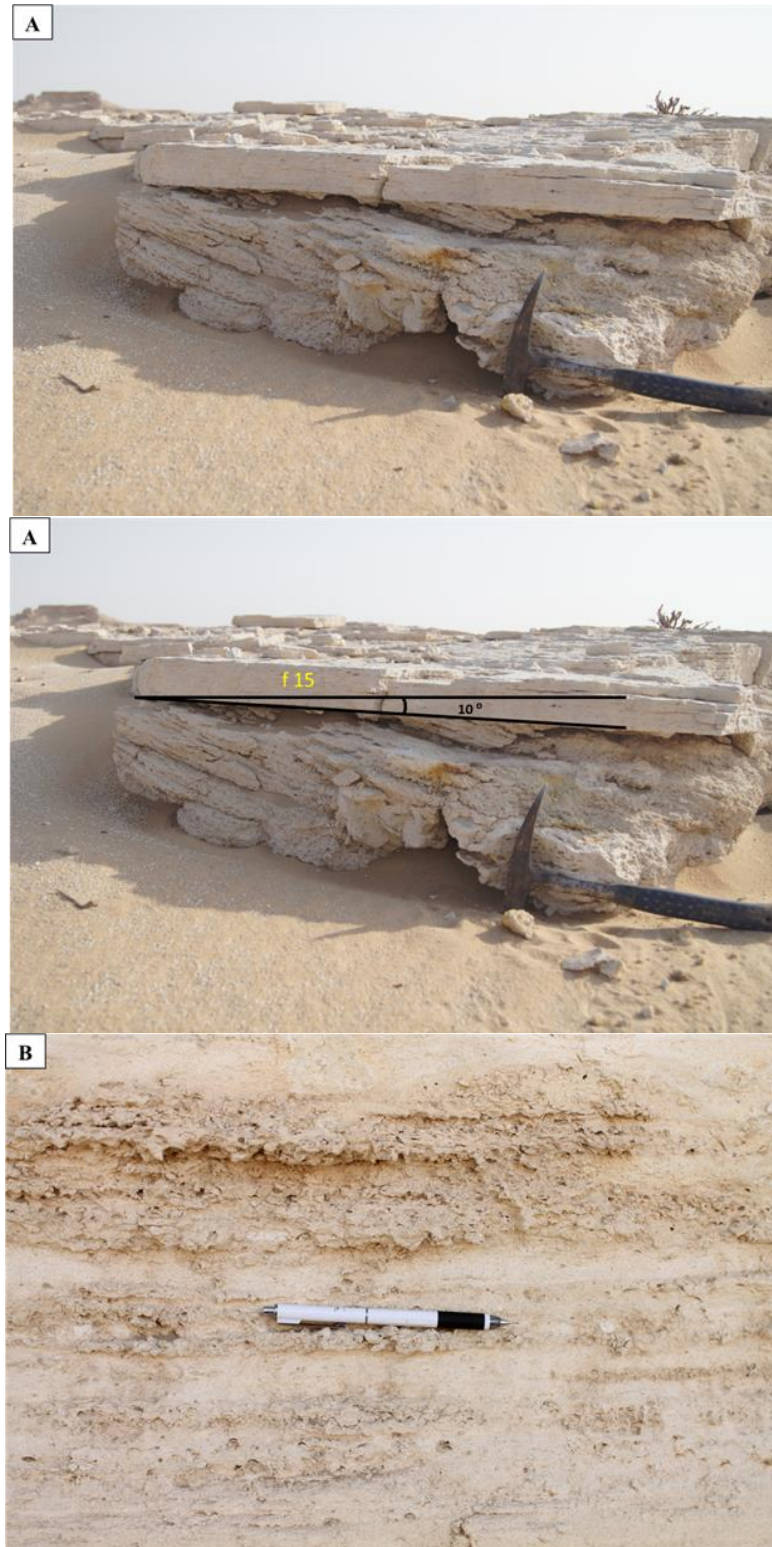
**Description:** This facies is found in outcrops 2, 8, 16 and 23. It has creamy to white color, an average thickness of 40 cm, and contains keystone vugs. The layers of this facies have gentle dip angle of about 10° S (Figure 4.16 (A)). They are internally laminated; alternating between oolitic- and skeletal- dominated laminae (coquina). This lamination gets thicker, in some locations, to form interbedding between the lamination end members (Figure 4.16 (B)).

The upper surfaces of this facies layers show rain drop impressions and current lineations in a general NNW–SSE trend (Figure 4.16 C). This facies is, always, adjacent to trough cross-bedded grainstones or herringbone cross-bedded grainstone.

Petrographic thin sections shows grainstone texture which is composed of peloids that are originally micritized ooids, ooids and bivalves. The macroscale lamination is, also, present in thin sections (Figure 4.16 (D)). The ooids are mainly fine, in term of grain size, ( $m = 2.65 \text{ } \phi$ ) and are very well sorted (Figure 4.16 (E & F)). Visual porosity estimation is about 25 %; mainly intergranular, moldic and shelter porosity (Figure 4.16 (E)). Blocky, miniscus, bladed and stalactitic within skeletal are the main cement types (Figure 4.16 (G)).

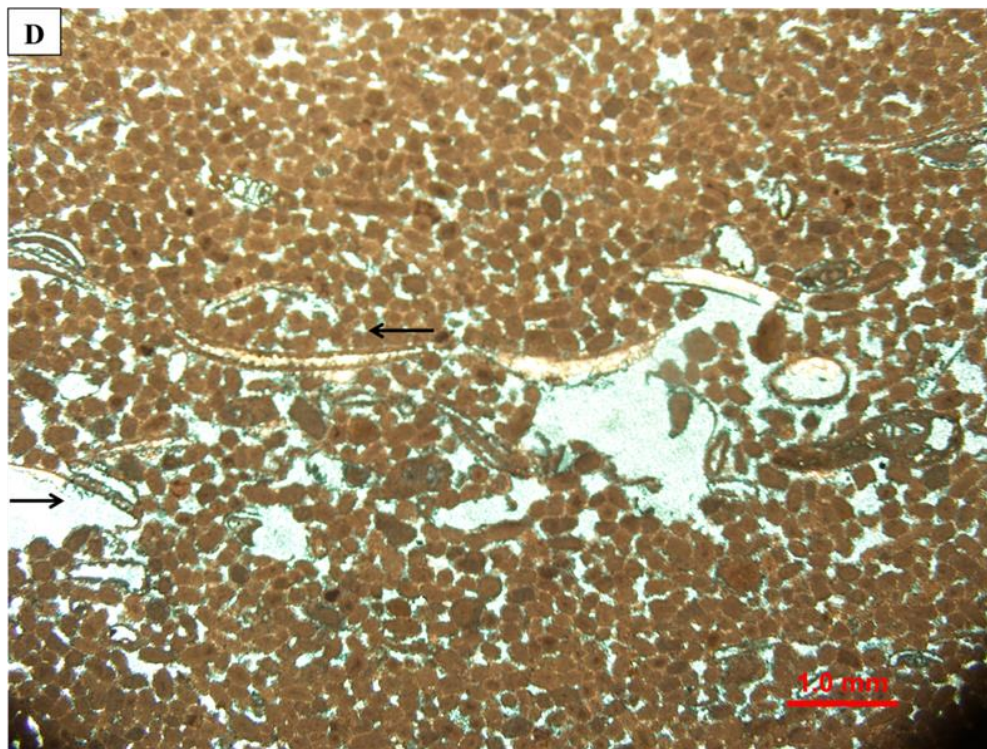
**Interpretation:** The dip of this facies layers is mainly a depositional dip, following the paleogeography of the depositional site, and not tectonic because all adjacent layers are approximately horizontal. The keystone vugs are most probably air bubbles trapped during deposition, are indicating the shallowness of this facies. The rain drops impressions confirm this suggestion and, furthermore, give evidence of exposure. The

parallel horizontal lamination, in addition to the fine grain size of this facies suggests a turbulent flow with high energy environment. Moreover, the existence of primary current lineations on the top of the layers indicates deposition in the upper flow regime, too. The early cementation, the adjacent facies, the very well sorting of ooids, the shells accumulations in addition to previous observations strongly signify a surf \ swash foreshore beach deposition (Tucker, 2001).

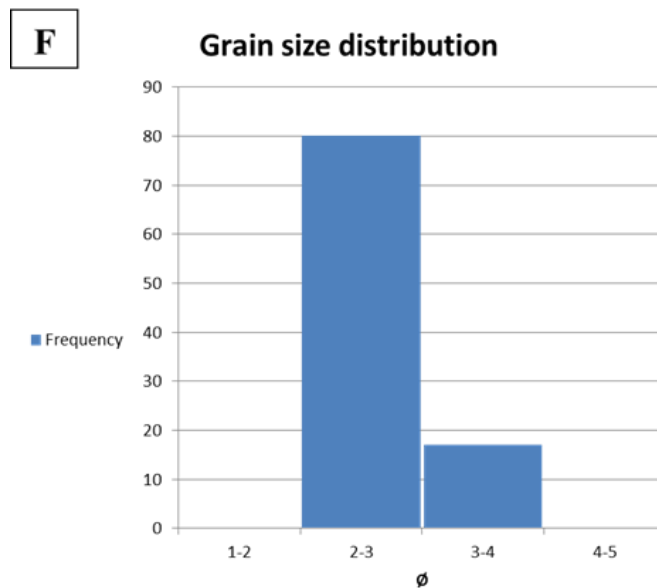
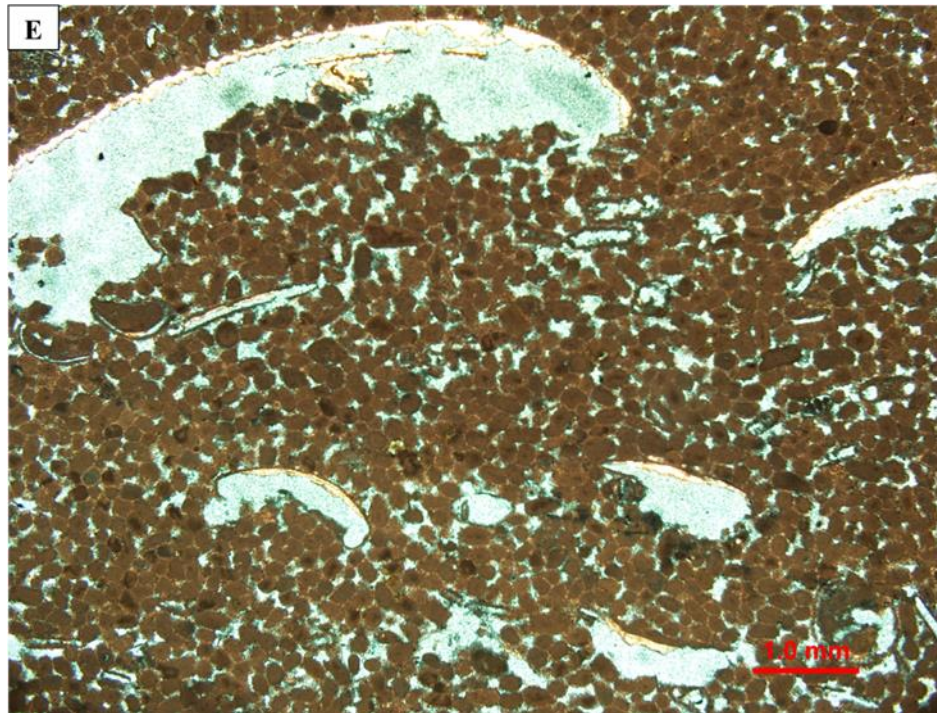


**Figure 4.16 (A) Dipping layers of beach facies. (B) Changing from lamination to bedding upward**



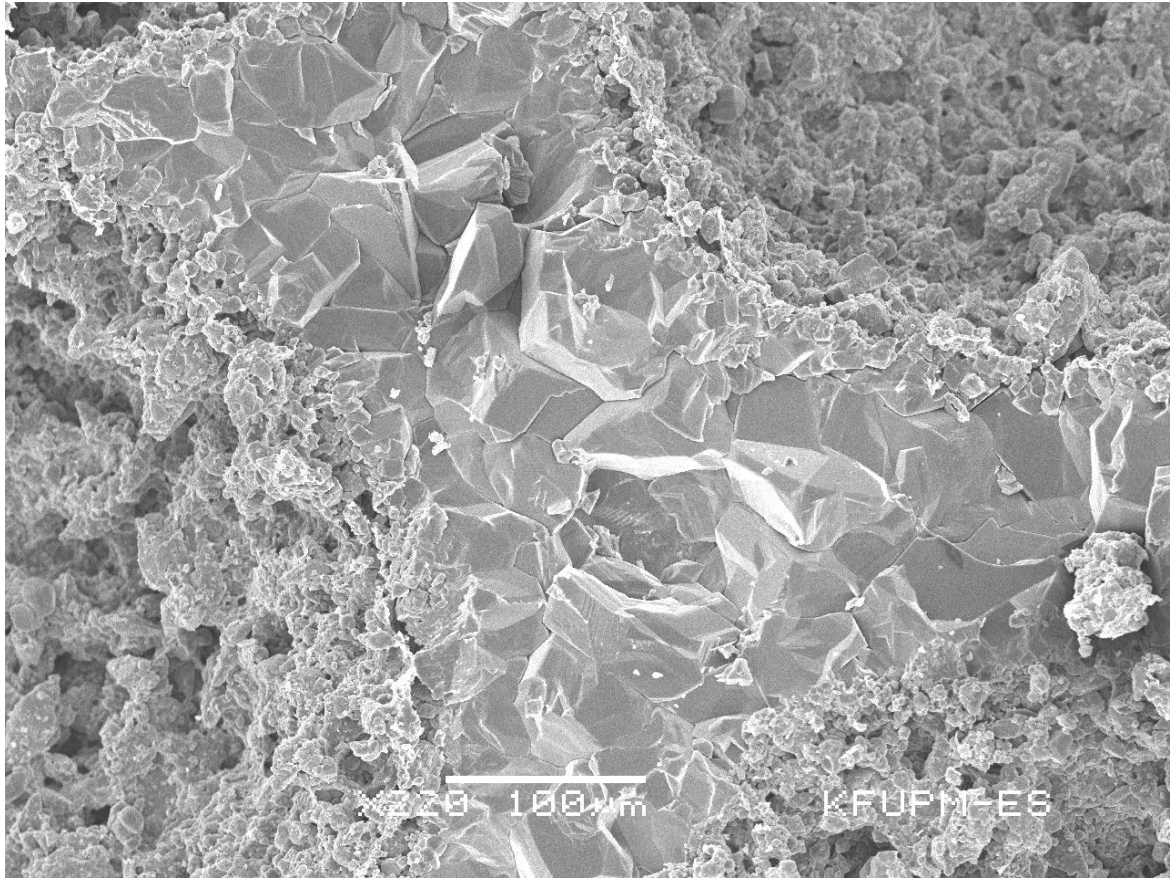


**Figure 4.16 (continued): (C) Plan view of beach grainstones showing rain drops (circles) and current lineation (arrow). (D) Lamination in thin section between skeletal and oolitic laminae. Shelter porosity below the bivalve shells sometimes increases and form vuggy porosity in addition to the intergranular.**



**Figure 4.16 (continued): (E) Thin section of beach facies showing the very well sorted ooids with intergranular porosity and the shelter porosity below bivalve fragments. (F) Histogram showing ooids grain size distribution; note the unimodal distribution.**





**Figure 4.16 (continued): (G) SEM image showing the blocky calcite cement within the oolitic grainstone of the beach deposits.**



## **4.3 Discussion**

### **4.3.1 Processes**

Depending on identified lithofacies in the Miocene Dam Formation in the Al Lidam area, more than one dominant physical process could be interpreted. The dominant shallow marine processes were waves and tidal currents with a minor role of storms. Deeper facies recorded storms, deposition out of suspension and biogenic processes. Shallow to subaerially exposed facies also show deposition out of suspension, biogenic activities in addition to evaporation.

The lower shoreface facies do not show any major current or wave influence. In addition to the benthic biota, they are mainly as a result of suspended load gravity settling. This lack of agitation signifies deposition away from the shoreline where only very fine sediments were transported as suspended load and deposited when the transportation energy is diminished. The transportation of the fine materials from proximal to distal areas could also be by the action of wind rather than hyperpycnal subaqueous flows. This might help in interpreting the existence of fine quartz grains in the relatively deep water wackestones. The absence of current structures such as the cross bedding and lamination could also be attributed to the predominance of biogenic processes.

Storms effect was noticed in both deep and shallow depositional environments. They reflect ancient unstable meteorological forces (Johnson and Baldwin, 1996).

The wavy bedding and planar lamination\bedding in the beach rocks show waves and currents dominance within their facies interval and position. There is general decrease of the beach rocks eastwards but still some wavy bedding could be found.

The abundance of herringbone cross bedding indicates bidirectional tidal current deposition. The tidal currents dominance is also indicated by the tidal bundles, reactivation surfaces and mud drapes. The trough and planar cross bedding could originally indicate wave's action but in some location in the study area they show flaser bedding with deposition of thin mud lamina which could be interpreted as mixed tidal-wave influence.



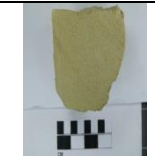



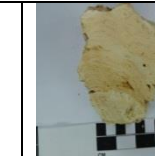

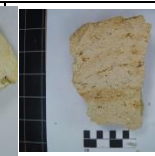
The existence of evaporites in adds another depositional process which is evaporation. This process is not dominant through studied facies, but it's important as arid to semiarid paleoclimate indicator.

#### **4.3.2 Depositional Environments**







From the studied outcrops (**Error! Reference source not found.**) it can concluded that the Dam Formation depositional history in the Al Lidam area represents a complex ancient mixed siliciclastic-carbonate shoreline facies (Table 4.1 and Table 4.2) (Figure 4.17). From east to west relatively deep/shallow marine carbonates pass up basin slope into shallow carbonate/siliciclastic succession deposited within intertidal and supratidal zones. These shallow water facies interfinger with backshore sabkha deposition. Locally, this ancient shoreline was interrupted by small estuaries that could be

the source of shallow intertidal siliciclastics deposits that were redistributed by marine currents and

Table 4.1: Summary of characteristics of lithofacies in the Dam Formation

	Sedimentary description								
Sample									
Facies name	Interbedded Dolomudstone and Evaporites (ME)	Interbedded Cross-bedded Sandstone and Mudstone (SM)	Channelized Medium Sandstone (Sc)	Trough Cross-Bedded Sandstone (St)	Interbedded Cross-bedded Coarse Limestone and Mudstone (GM)	Intra-formational Limestone Conglomerate (Gmm)	Stromatolites (BS)	Massive Quartz Skeletal Pelletal Wacke-Packstone (PWm)	Planar Cross-Bedded Skeletal Peloidal Grainstone (Gp)
Depositional Environment	Sabkha	Sand and mud tidal flats in intertidal zone	Estuarine Channel	Upper shoreface	Intertidal carbonate sand waves	Tempestites	upper shoreface, intertidal to supratidal flats	Outer ramp	Lower intertidal zone
Rock Type (Dunham 1962)	Mudstone & evaporites	Sandstone + Mudstone	Sandstone	Sandstone	Grainstone and mudstone	Grainstone	Boundstone	Wackestone-Packstone	Grainstone
Mineralogy	Dolomite + Anhydrite	Quartz + Calcite	Quartz + Calcite	Quartz	Calcite	Calcite	Calcite	Calcite	Calcite
Grain Type	—————	Quartz grains	Quartz + skeletal	Quartz grains	Ooids & skeletal	Mud clasts	—————	Quartz, skeletal & pellets	Skeletal and peloidal
Fossils	—————	—————	Bivalves	Ophiomorpha trace fossils	Bivalve & Foraminifera	—————	—————	Bivalve & Foraminifera	Bivalve and Foraminifera
Sedimentary Structure	Some lamination	Flaser bedding, tidal bundles and reactivation surfaces	Herringbone cross bedding	Trough cross bedding	Fenestrae vugs & tepee structure	—————	Lamination	—————	Planar cross bedding
Grain Size	Fine	Fine to silty	Fine	Medium to fine	Fine to medium	Gravels	—————	—————	Fine
Rock Color	Gray to red	Yellow-reddish	Yellow to Beige	Green to brown	Beige to white	Brown to gray	Beige	Beige to white	Yellow to Beige
Porosity types	Fracture	Intergranular	Intergranular + burrows	Intergranular + burrow	Intragranular + Moldic	—————	Intergranular	Moldic	Inter-Intragranular

**Table 4.2: Summary of characteristics of lithofacies in the Dam Formation**

	<b>Sedimentary description</b>					
<b>Sample</b>						
<b>Facies name</b>	Herringbone Cross-Bedded Skeletal Oolitic Grainstone (Gh)	Trough Cross-Bedded Aggregate Intraclast Oolitic Grainstones (Gt)	Massive Peloidal Skeletal Packstone (Pm)	Channelized Planar Cross-Bedded Skeletal Oolitic Grainstone (Gcp)	Massive Skeletal Wackestone (Wm)	Dipping Planar-bedded Skeletal Oolitic Grainstone (Gl)
<b>Depositional Environment</b>	Intertidal zone	Upper shoreface	Mid intertidal zone	Transgressive tidal channel	Inner-mid ramp skeletal mound	Foreshore
<b>Rock Type (Dunham 1962)</b>	Grainstone	Grainstone	Grainstone	Grainstone	Wackestone	Grainstone
<b>Mineralogy</b>	Calcite	Calcite	Calcite	Calcite	Calcite	Calcite
<b>Grain Type</b>	Ooids + skeletal	Aggregate, intraclasts & ooids	Peloids & skeletons	Ooids & skeletons & grapestones	Skeletons	Ooids & skeletons
<b>Fossils</b>	BV & Foraminifera	Bivalves	BV, Gastropods & Foraminifera	BV and Foraminifera	Foraminifera, echinoderm spine	Bivalves
<b>Sedimentary Structure</b>	Herringbone cross bedding & keystone vugs	Trough cross bedding	_____	Planar cross bedding	_____	Planar bedding and lamination
<b>Grain Size</b>	Medium	Medium	_____	Coarse	_____	Fine
<b>Rock Color</b>	Yellow to Beige	Yellow to white	Beige	Yellow-Beige	Dark green-gray	Yellow to white
<b>Porosity types</b>	Moldic + inter/intragranular	Moldic+ inter/intragranular	Moldic + Vugy	Intergranular	Moldic	Inter/intragranular + Moldic + Shelter



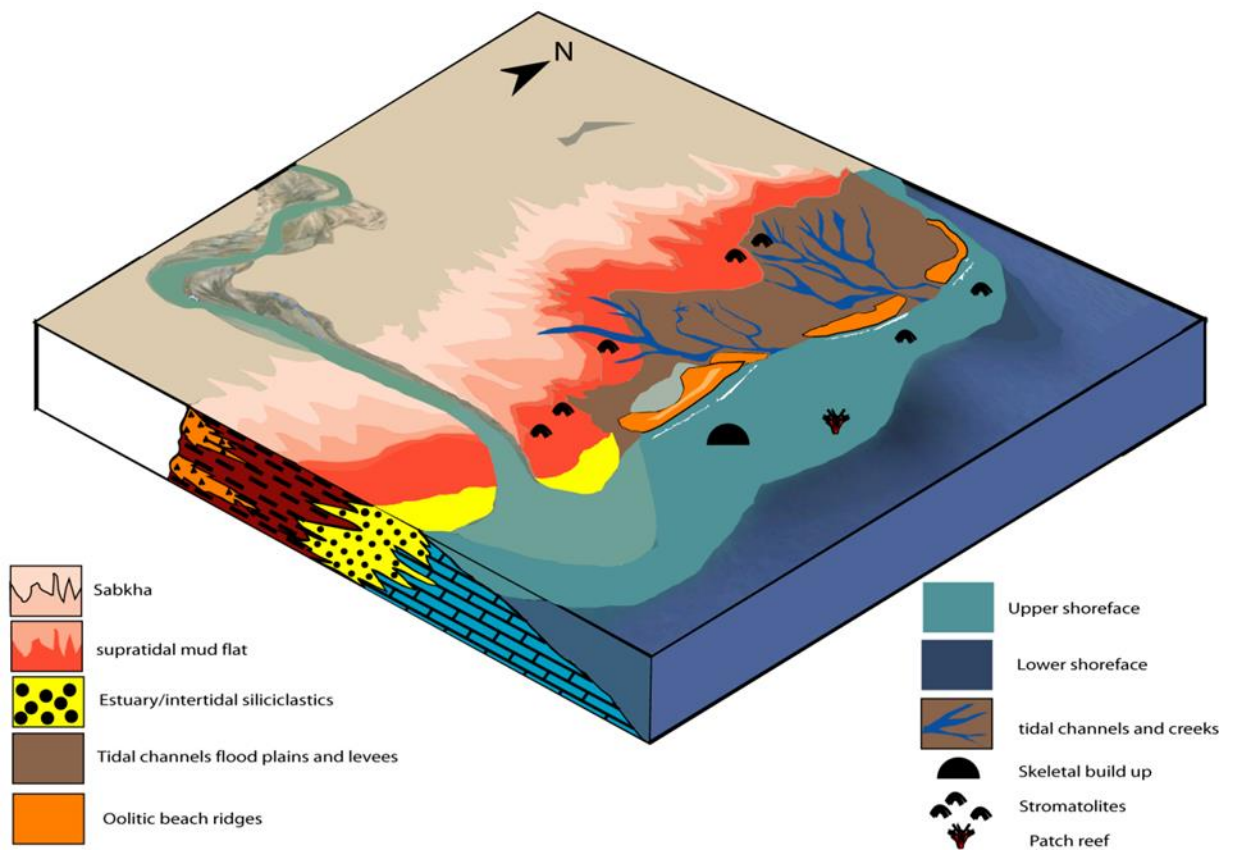
waves. The shoreline was, also, interrupted by tidal channels and creeks that were filled by cross bedded coarse carbonates. These creeks when been abandoned were the sites for shale and evaporites deposition.

The presence of coral reef fragments in the massive bioturbated packstone facies could be attributed to the existence of small reef patches in the shallow carbonate settings. The absence of huge reef build ups in the Dam Formation might be because of the existence of nearby source of siliciclastic deposits and their influx into the basin or the high energy of the waves and storms that deposited coarse carbonates and destroyed the reefs (Flügel, 2010).

The beach ridges formed small wave energy barriers which helped in the development of sabkha and mud tidal flats. When sabkha was flooded, mud was firstly deposited out of suspension and then followed by the deposition of the evaporites. The interbedding between the evaporites and the mudstone suggests that this process seems to have been repeated more than once.

The general fine grain size of the sand grains and the paucity of large estuary channels indicate low coarse siliciclastic sediment supply which could be attributed either to low precipitation rate and weak drainage system or the absence of nearby coarse-grained siliciclastic sources.

Stromatolites in the Dam Formation could be used as a powerful environmental indicators. They were found as different types and depending on their shapes they indicate different hydrodynamic systems. They associate the facies and extend from upper shoreface setting to supratidal environments.



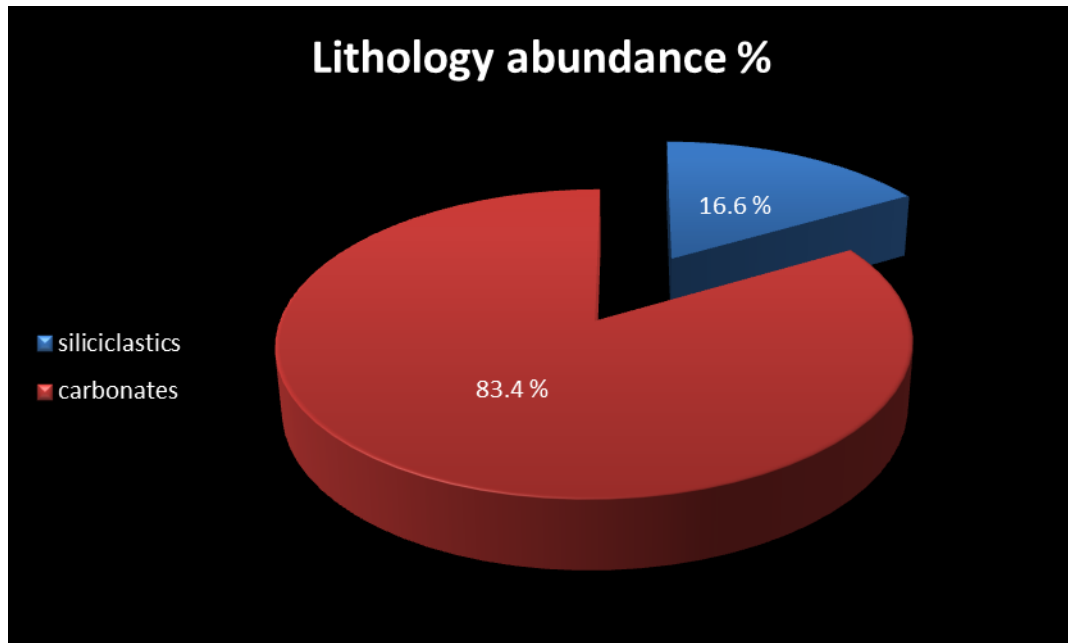
**Figure 4.17: Schematic 3D diagram for depositional model of the Dam Formation in the study area**

### **4.3.3 Relative Abundance of Facies**

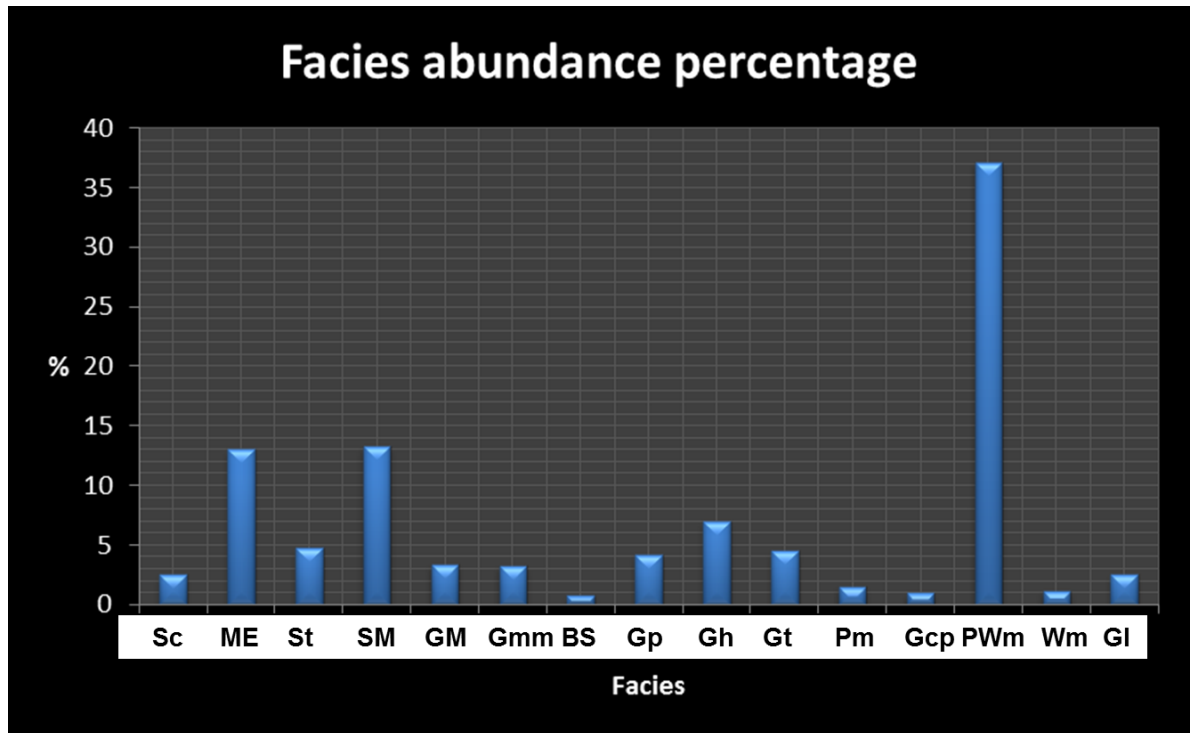
The study reveals obvious dominance of carbonate lithofacies over siliciclastics (Figure 4.18). The siliciclastics are almost absent in most eastern outcrops (1 & 2) and start to appear and increase in thickness from outcrop 23 to the west. Overall, the massive quartz skeletal peloidal wacke-packestone is the thickest and the most occurring in all the identified facies (Figure 4.19).

### **4.3.4 Palaeocurrent Analysis**

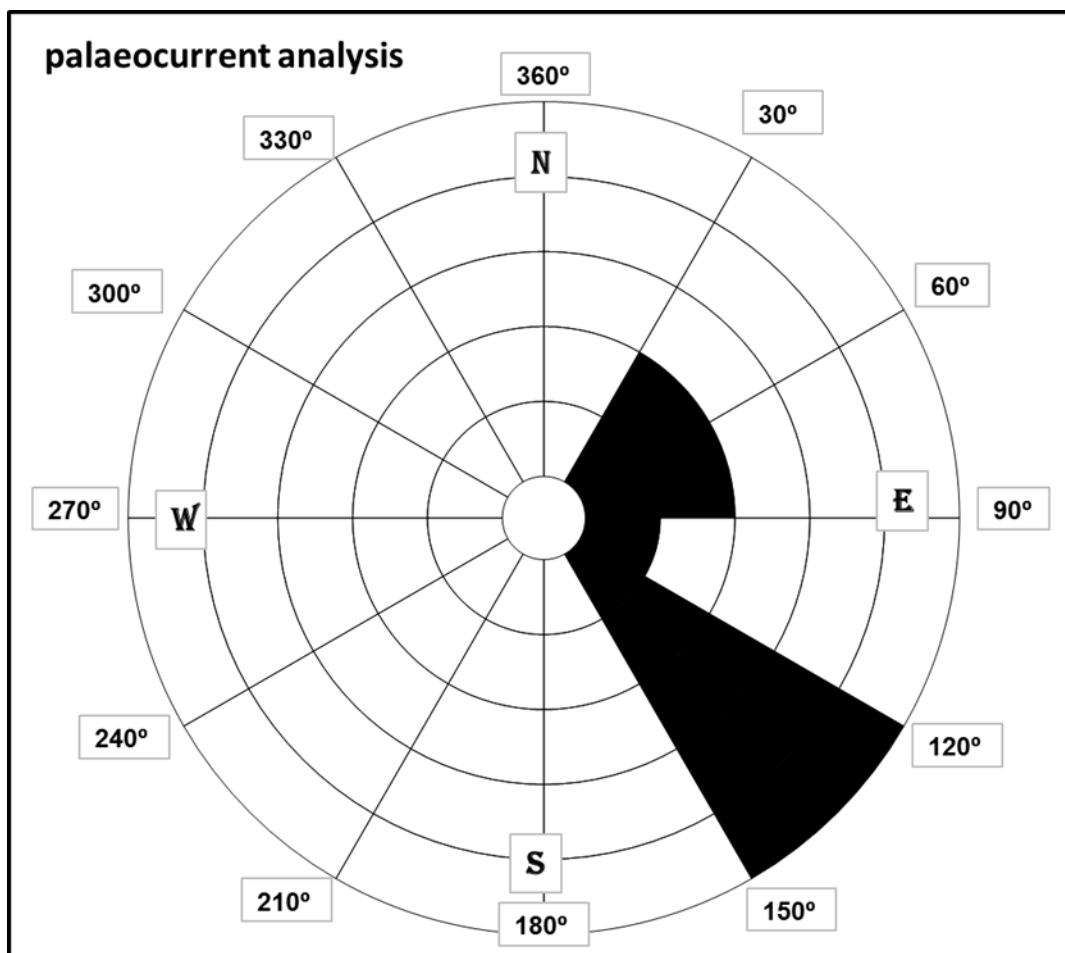
Paleocurrents were measured using the sedimentary structures; current lineation and planar cross bedding where a 3D view is available. The current lineation follows the depositing current and the dip direction of the planar cross bedding sets indicate their dune migration direction. The paleocurrent analysis shows general eastward deposition with major SE direction (Figure 4.20). This is consistent with the general setting of the basin (E-W) and the little deviation from the ideal orientation could be interpreted by an irregularity in the shoreline or the effect of the wind which could make shoreline currents.



**Figure 4.18: Lithology abundance percentage in the Dam Formation in the study area**



**Figure 4.19: Relative abundance of facies in the study area**



**Figure 4.20: Rose diagram for the paleocurrent measurements**



#### **4.3.5 Dolomite in the XRD Analysis**

The mud layers interbedded with evaporites were analyzed using X-Ray Diffraction technique. Most of the diffraction peaks in the diffractogram are attributed to dolomite with small peaks of quartz and calcite (Figure 4.21). The facies analysis could help interpreting this mineralogical dominance of Dolomite. The existence of evaporites (chicken wire anhydrite traces) means high water evaporation. This process consumes the  $\text{Ca}^{++}$  ions in the formation of anhydrite (calcium sulphate). The residual solution would be highly saturated with  $\text{Mg}^{++}$  and will act as dolomitizing fluid.

#### **Seismites**

Syn depositional deformational features were previously reported by old geologist. Many of them had attributed them to earthquakes shocks. One of the very first descriptions of these features was by Fuller (1912). He described the deformation in the sedimentary layers caused by three earthquakes in New Madrid in 1811 and 1812. They were first named "Seismites" by Seilacher (1969). They had never been studied in details until the end of the 1980's (Montenat et al. 2007).

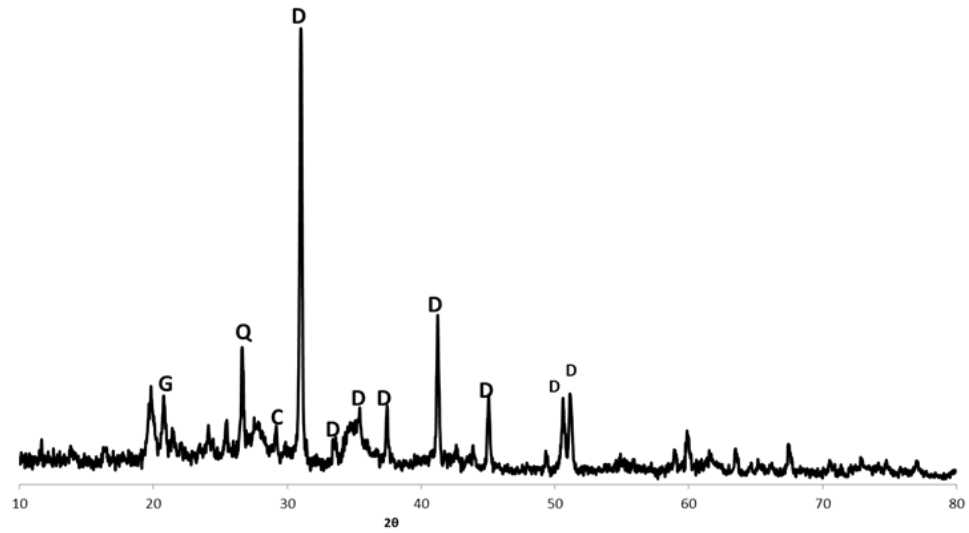
In the study area, the Dam Formation successions show some seismites features such as soft sediments deformational structures. Since the high sensitivity to seismic shock waves is in the fine sediments, especially when interbedded with different granulometric systems (Obermeier et al. 1993), the main seismites are represented in the interbedded fine sandstone and mudstone facies.

Small localized mud diapir structures were found within the undeformed succession or within completely chaotic beds of the interbedding sandstone-mudstone facies (Figure 4.22). They have straight lower bedding planes which suggest that they were not formed due tectonic anticline folding. It is most probably small mud diapir of ancient liquefied mud. The water-saturated mudstone was likely squeezed out into the overlying higher density fine sandstone layer.

Ball and pillow structures were also observed in more than one outcrops in the study area (Figure 4.23). They are formed by sandstone which occurs as partially to completely isolated bodies floating in the associated mudstone. They are interpreted to have been formed initially as load casts of the relatively higher density sandstone into the underlying lower density mud (Boggs, 2006).

Ball and pillow structures are attributed to segregation and breakup of semi-lithified sandstone due to partial liquification which occurred in the underlying muddy layers, which in turn, is attributed to seismic shocking (Boggs, 2006). This liquification process is also the main reason for mud to diapir by increasing its ductility.

Besides seismites, some minor faults were detected (Figure 4.24). These fault structures are mainly normal faults caused dragging and fracturing of the muddy and sandy layers, following their difference in ductility.



**Figure 4.21: Diffractogram showing the dolomite as main mineral content in the mudstone when interbedded with evaporites**



**Figure 4.22: Small mud diapir in mudstone-sandstone facies**



**Figure 4.23 Ball and pillow structures in the sandstone-mudstone facies**



**Figure 4.24 Minor normal fault with dragging and fracturing in its hanging wall**

## **CHAPTER 5**

### **SEQUENCE STRATIGRAPHY**

#### **5.1 Introduction**

Sequence stratigraphy is one of the, relatively, youngest branches of the science of stratigraphy. It is a methodology which builds a framework for a sedimentary succession using certain elements to reconstruct the paleogeography and to predict the lateral lithofacies variation. It helps in interpreting the evolution of the sedimentary successions in term of sediment availability, space and time (Catuneanu et al. 2011).

The stratal stacking patterns and the bounding surfaces, that subdivide the succession, are the main tools used in a sequence stratigraphic analysis. The building blocks of the analysis are sequences, system tracts and parasequences. Each one of these has its own distinctive strata stacking pattern and key bounding surfaces. Sequence stratigraphy depends on genetic analysis of sedimentary processes and basinal attitudes with time.

#### **5.2 Sequence Stratigraphic Units**

The sequence stratigraphic analysis is carried out by identifying previously mentioned units and organizing them temporally. They are defined and discussed below.



**Sequence:** It was defined initially by Sloss (1949, 1963) as stratigraphic unit that is bounded by unconformities. This definition was modified by Mitchum (1977) who defined the sequence as genetically related stratigraphic succession that is bounded by unconformities and their correlative conformities. Group of stratigraphers (e.g. Vail, 1987; Hunt and Tucker, 1992) added the condition of subaerial exposure to the definition of Mitchum and named it as "depositional sequence". Galloway (1989) identified the sequence as a genetic stratigraphic unit bounded by maximum flooding surfaces. "Transgressive-Regressive sequence" (T-R cycles) nomenclature was proposed by Johnson and Murphy (1984) and Johnson et al. (1985). It was redefined by Embry and Johannessen (1992) as a stratigraphic unit bounded by maximum regressive surfaces. Catuneanu et al. (2011) redefined the sequence as sedimentary succession that was deposited during a full cycle of change in terms of accommodation space and sediment supply.

**Systems Tract:** It is a depositional system formed at the same period and subdivides a sequence (Brown and Fisher 1977). The difference between it and the sequence is that the sequence could contain unconformities within it, while systems tract do not but instead unconformities could represent boundaries between the systems tracts (Catuneanu et al., 2011). Every systems tract is characterized by its strata stacking patterns and its position within the sequence and surfaces bounding it. Description of systems tracts is as follow:

**Lowstand systems tract (LST):** It is restricted between the lower sequence boundary (SB) and the transgressive surface (TS). Its sediments accumulate at as soon as the relative sea-level starts to drop till the onset of transgression.

***Transgressive systems tract (TST):*** It is bounded by transgressive surface (TS) and the maximum flooding surface (MFS), and its sediments accumulate from the onset of sea transgression till its maximum transgression; just before regression.

***Highstand system tract (HST):*** It represents the top of the sequence and bounded by the maximum flooding surface (MFS) at the bottom and capped by the sequence boundary (SB).

In this study, the Posamentier and Allen (1999) proposed subdivision of a sequence into system tracts is applied.

### **5.3 Terrigenous Siliciclastics vs Carbonate Sequence Stratigraphy**

These two lithologic end members show great differences during the formation of a sequence. In the lowstand system tract, the siliciclastics show more dominance. The currents erode the exposed areas and they bypass them as they are deposited in relatively deeper settings. On the other hand, the carbonate factory is approximately shut down except of the planktonic precipitation in deeper settings (Jacquin et al., 1991). This stage is also characterized by carbonate karstification. Evaporites have the greatest development during this stage. In transgressive systems tract, the siliciclastics are overcome and carbonate factory operates at the optimum rate. It is characterized by the accumulation of thick subtidal facies and the growth of reefs. Evaporites could be

deposited in small relative sea level falls in restricted areas. During the highstand system tract, both the siliciclastics and carbonate settings are almost the same. The creation rate of more accommodation space is lower and the carbonate formation decreases (James & Kendall, 1992).

## **5.4 The Dam Formation Sequence Stratigraphy Literature**

The Dam Formation lies within a big tectonostratigraphic mega sequence (TMS AP 11) (Sharland, et al., 2001). This TMS lies between two unconformities marking both the onset of the Red Sea opening and the collision initiation between Eurasia and the Arabian Plate as the lower boundary (Beydoun, 1993) and the present topographic surface as the top boundary. This TMS also includes major geologic events. The Neo-Tethys was completely closed in the Late Oligocene to Early Miocene (Hooper et al., 1995). Moreover, subsidence occurred in the eastern part of the plate due to the Zagros imbricated thrust sheets loading, while the western parts were uplifted thermally (Sharland, et al., 2001). This resulted in gradual change in the foredeep basin sedimentology from carbonates to subaerial continental clastics. While the accommodation space in the east was developing, it was terminated in the west by thermal uplifting and tectonic structural inversion.

Kuwait was stated to be located at 24° N during Burdigalian (Al-Fares et al., 1998). Presently, it lies at about 29° N, which means a northward latitude shift of about 5°. In

the same pattern, the study area is presently located at 26° N while wasit was mainly situated at 21° N during Burdigalian.

In the (TMS AP 11), Dam Formation contains carbonates of Middle Miocene that were sandwiched between two non-marine stratigraphic units. As a result, the Dam Formation represents regional early-mid Miocene transgressive event. The Dam Formation is interpreted as 3<sup>rd</sup> order sequence and carbonates near its base is correlated to MFS Ng20 (Sharland et al., 2001).

## **5.5 The study Area Sequence Stratigraphic Interpretation**

Alkhaldi, 2009 studied one of the best exposed outcrops in the study area in high detail (Outcrop 5). He concluded that Dam Formation as represented in that outcrop is composed of three composite sequences with higher number of high frequency sequences and cycles.

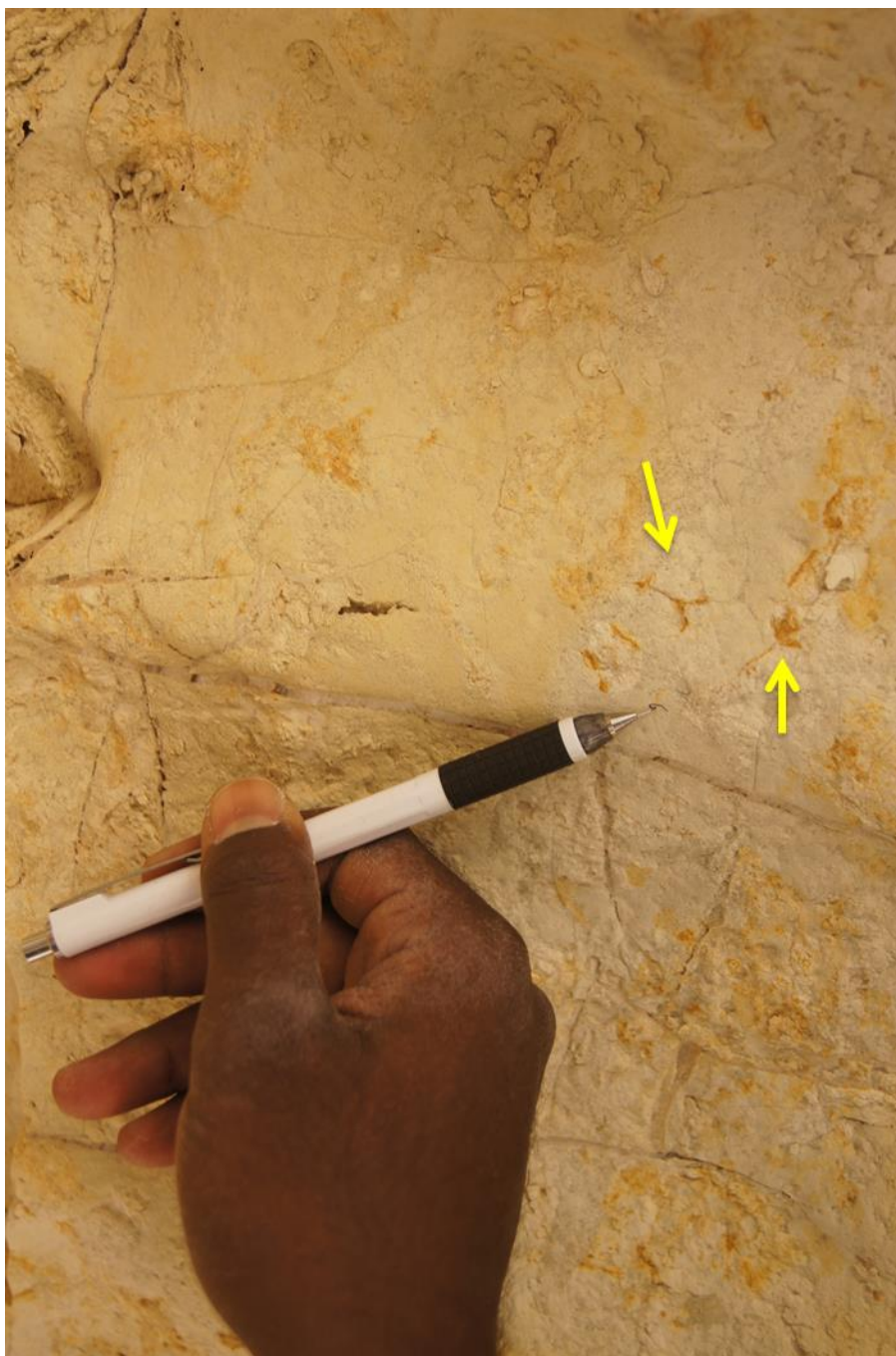
The studied outcrops, also, show that the Dam Formation was mainly deposited in three, most probably fourth order, depositional sequences. The lower and upper sequences are unbounded by lower and upper sequence boundaries, respectively, while the middle sequence is complete. Therefore, the interpretations presented herein, focus mainly on the complete sequence.

The two sequence boundaries (SB) recognized in the studied outcrops are associated with subaerial exposure indicators. The facies change demonstrates a great variation (drop) in the sea-level. In all the outcrop sections, the lower SB is associated with the deposition of

sabkha deposits (mud and evaporites) and the existence of Rhizolith (Figure 5.1). These facies were deposited over shallow marine coarse grained oolitic grainstones. Following Posamentier and Allan (1999), this continuous drop in the sea level associated with the exposure indicators mark the sequence boundary, and the facies deposited during this drop mainly represent the early LST.

With the deposition of intertidal siliciclastics, the late LST shows evidence of relative sea level rise. This stage reaches the subtidal upper shoreface sandstone facies conditions in outcrop 16. The interbedded intertidal mud-sandstone shows three thickening upward sequences, which are consistent with the proposed increase in the accommodation space, and is typical of the late LST (Catuneanu et al., 2011).





**Figure 5.1: Rhizolith (arrows) in the mud of mud-evaporite facies as indicator of exposure**

The grainstone tidal channels facies and the subtidal lower shoreface quartz skeletal peloidal wacke-packstone facies dominate over the estuarine channelized calcareous sandstone facies. The channels cut through the underlying facies and the wacke-packstone facies cover them all. The fine carbonate wacke-packstone has erosive sharp base, sometimes with intraformational pebbles, mainly of mud clasts and of Stromatolites (Figure 5.2). With this abrupt change from intertidal siliciclastic to estuarine sandstone, carbonate tidal channels and subtidal lower shoreface wacke-packstone, an increase in accommodation space is proposed. Consequently, these facies mainly represent transgressive system tracts (TST) and the erosive base is a transgressive surface (TS). Since the relatively older sediments in the same sequence are preserved, this TS could represent Diastemic Shoreline Ravinement surface (SR-D) (Embry, 2009).

The maximum flooding surface is represented in the middle of thickest layer of the wacke-packstone facies (which is regarded as the deepest facies in the whole succession). The thickest layer of this facies is always the first to appear; and it reaches 3.5 m thick. The highstand systems tract is dominated by shallowing upward carbonate parasequences. The sequence commences with the deposition of the wacke-packstone facies and followed by the deposition of different skeletal peloidal/oolitic grainstone shallower facies in the upper shoreface, foreshore and intertidal zones (the cross-bedded grainstone facies). These parasequences become thinner upwards indicating a relative decrease in the accommodation space which is consistent with the characteristics of the HST (Catuneanu et al., 2011). Thin supratidal mud flat facies (probably part of the interbedded mudstone-evaporites) containing mud desiccation cracks and Rhizoliths that indicate subaerial exposure occurs at the top of the HST.



**Figure 5.2: Transgressive ravinement surface with mud intraclasts (A) and Stromatolites (B) (arrow);**



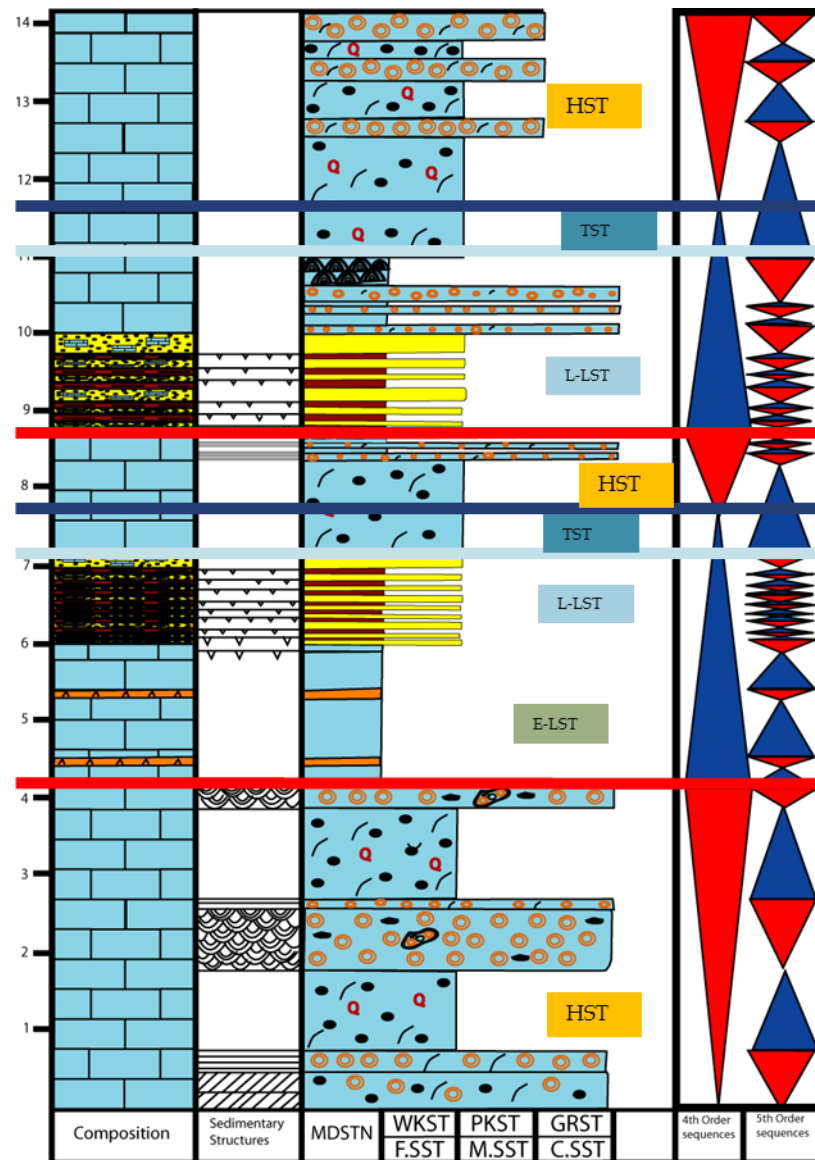


**Figure 5.2 (continued): (C) Transgressive sharp erosive base (arrows) without basal lag deposits.**

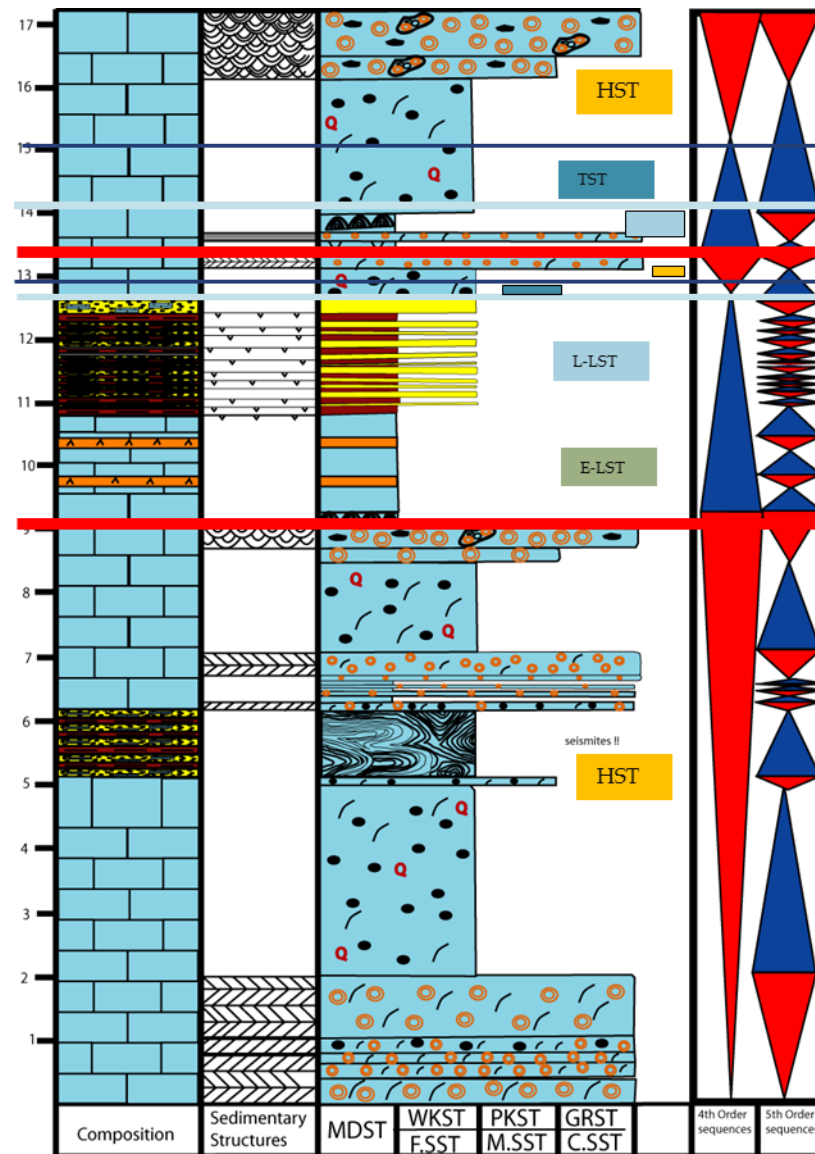
This point finishes the sequence and starts a new one with transgressive ravinement surface. This surface represents the (TS) of the new upper sequence while the small mud could be interpreted as the LST. Although this upper sequence is not complete and its upper boundary is missing, the MFS can be delineated because its parasequences show the gradual thinning upward character of the HST. The MFS could be likely present in the middle of the thick wacke-packstone facies at the beginning of the sequence. The lower sequence does not show any distinctive features other than thinning and shallowing upwards of the shallow carbonate parasequences similar to those representing the HST in the lower and the upper sequences.

Every outcrop has been subdivided, in detail, into 5<sup>th</sup> order sequences (parasequences) and bigger 4<sup>th</sup> order ones (Figure 5.3, Figure 5.4, Figure 5.5 and Figure 5.6). Between these outcrops a correlation has been made on the base of system tracts and sequence subdividing time surfaces (Figure 5.7). Depending on the analyzed facies and sequences, outcrops photomosaic had been interpreted (Figure 5.8, Figure 5.9 and Figure 5.10).

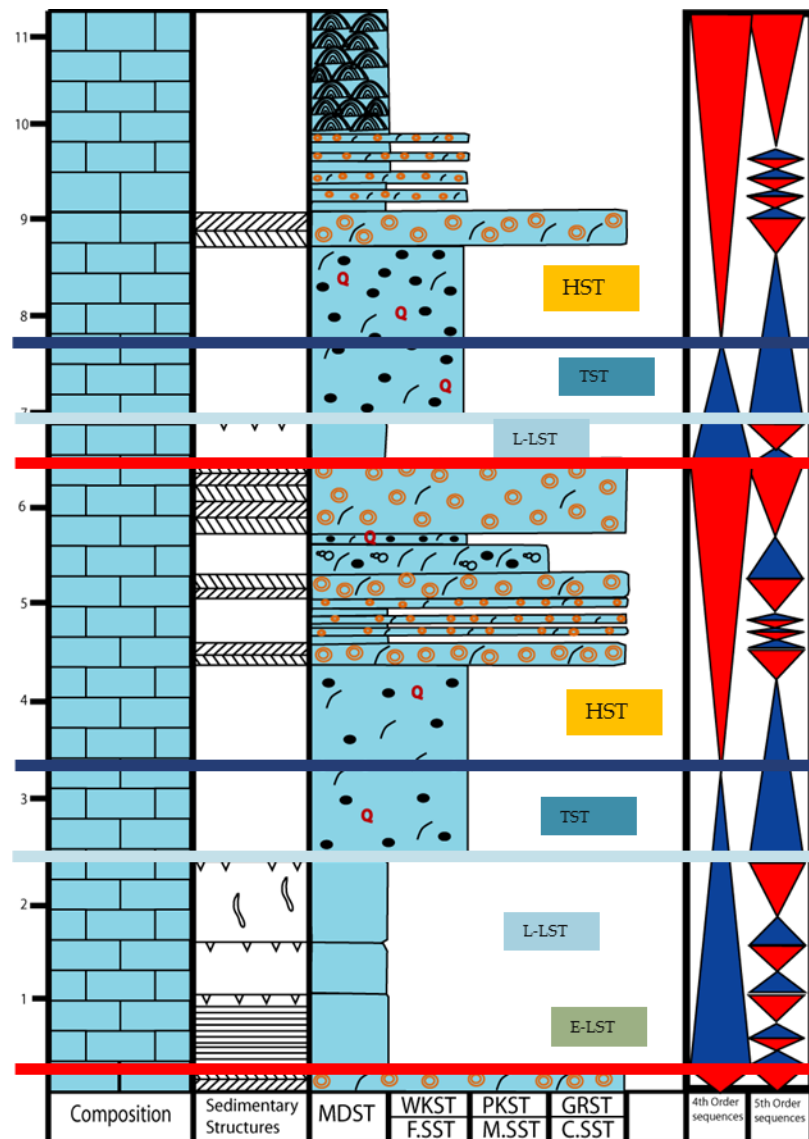




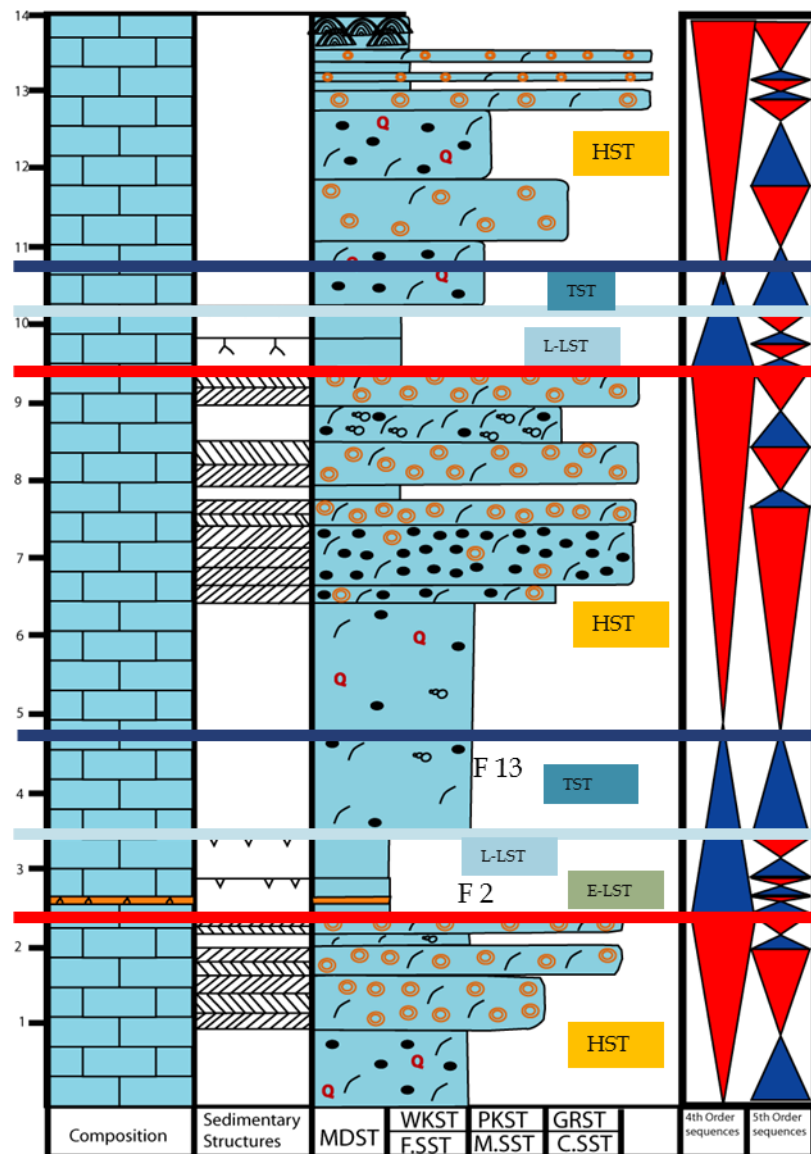
**Figure 5.3: Composite Stratigraphic Section of outcrop 8 showing fabric textures, structures and and sequence stratigraphic subdivisions**



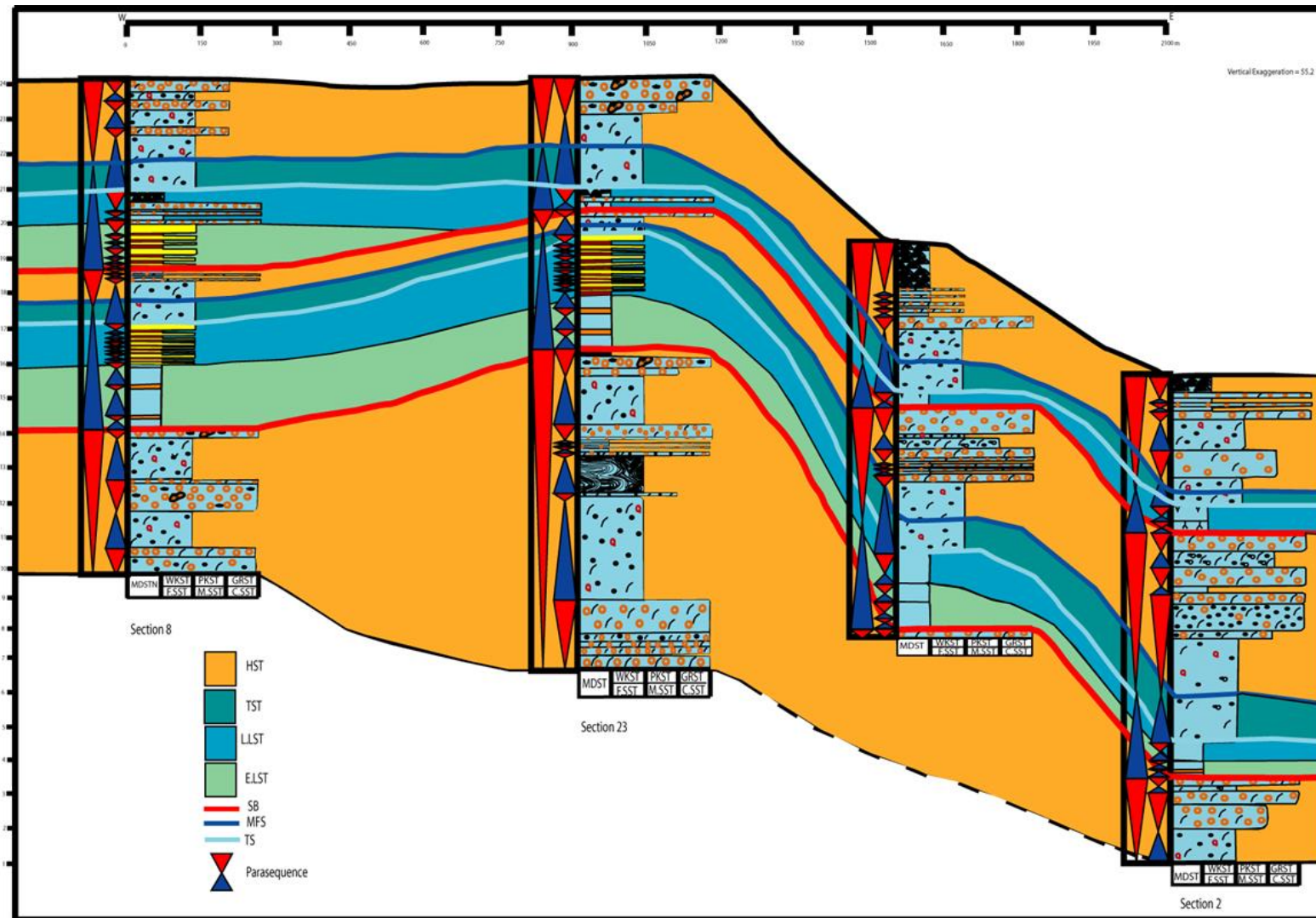
**Figure 5.4: Composite stratigraphic section of outcrop 23 showing fabric textures, structures, lithology and sequence stratigraphic subdivisions**



**Figure 5.5: Composite stratigraphic section of outcrop 1 showing fabric textures, structures and sequence stratigraphic subdivisions**

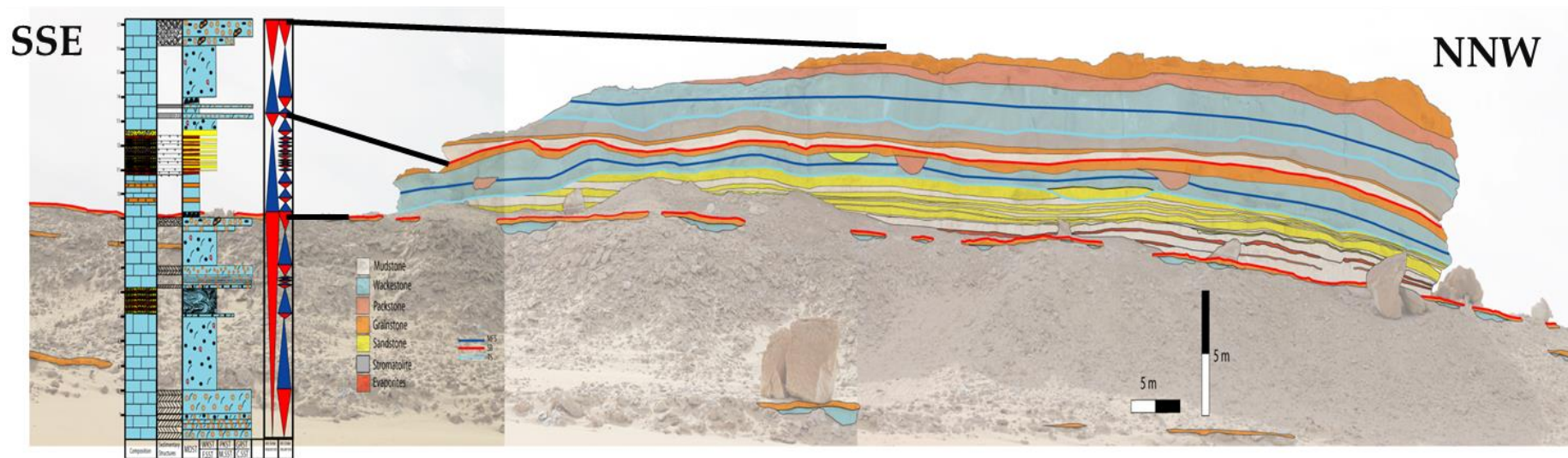


**Figure 5.6: Composite stratigraphic section of Outcrop 2 showing fabric textures, structures and sequence stratigraphic subdivisions**

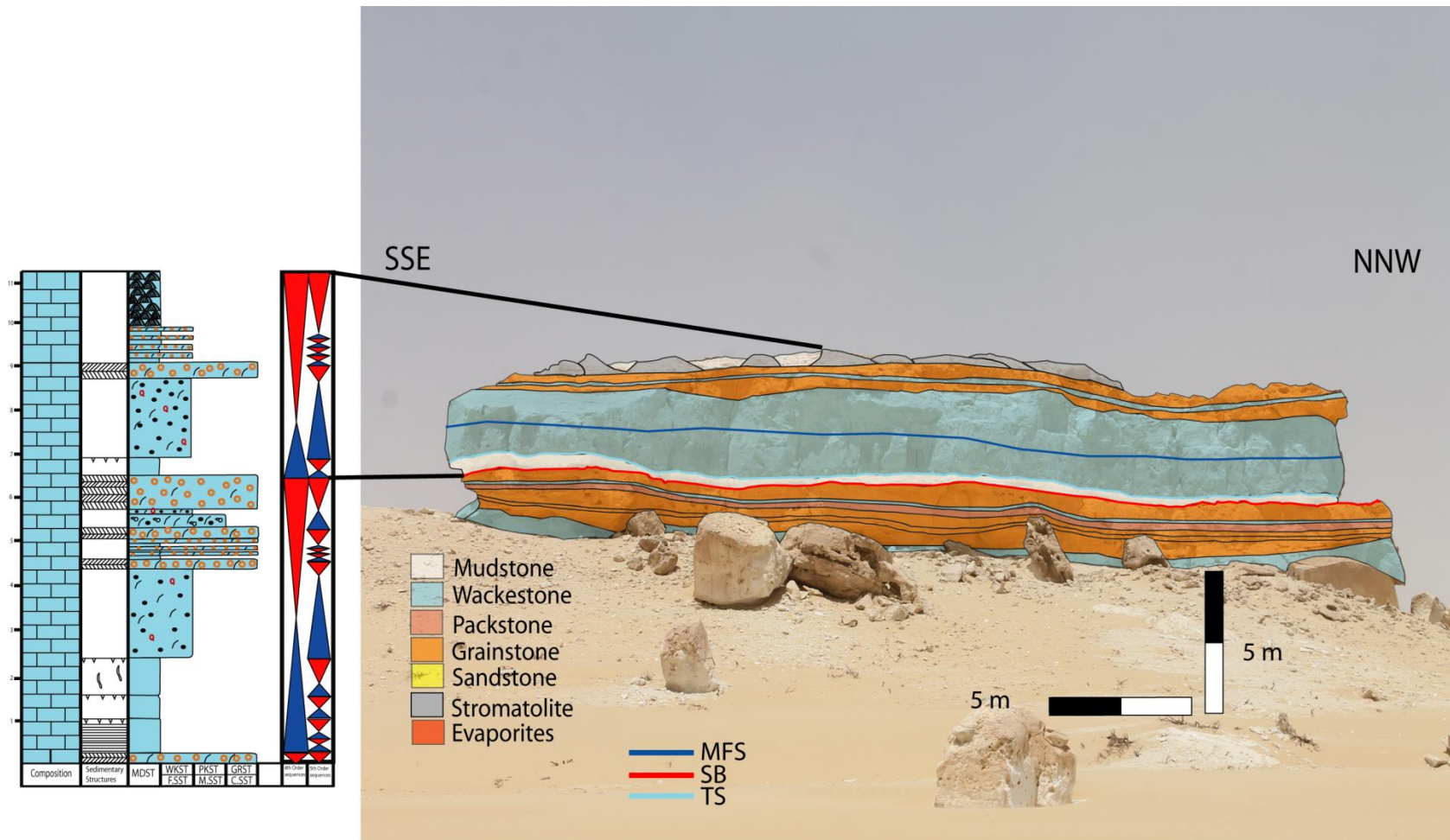


**Figure 5.7: Cross section through studied outcrops showing the sequence stratigraphy of the Dam Formation in the study area**

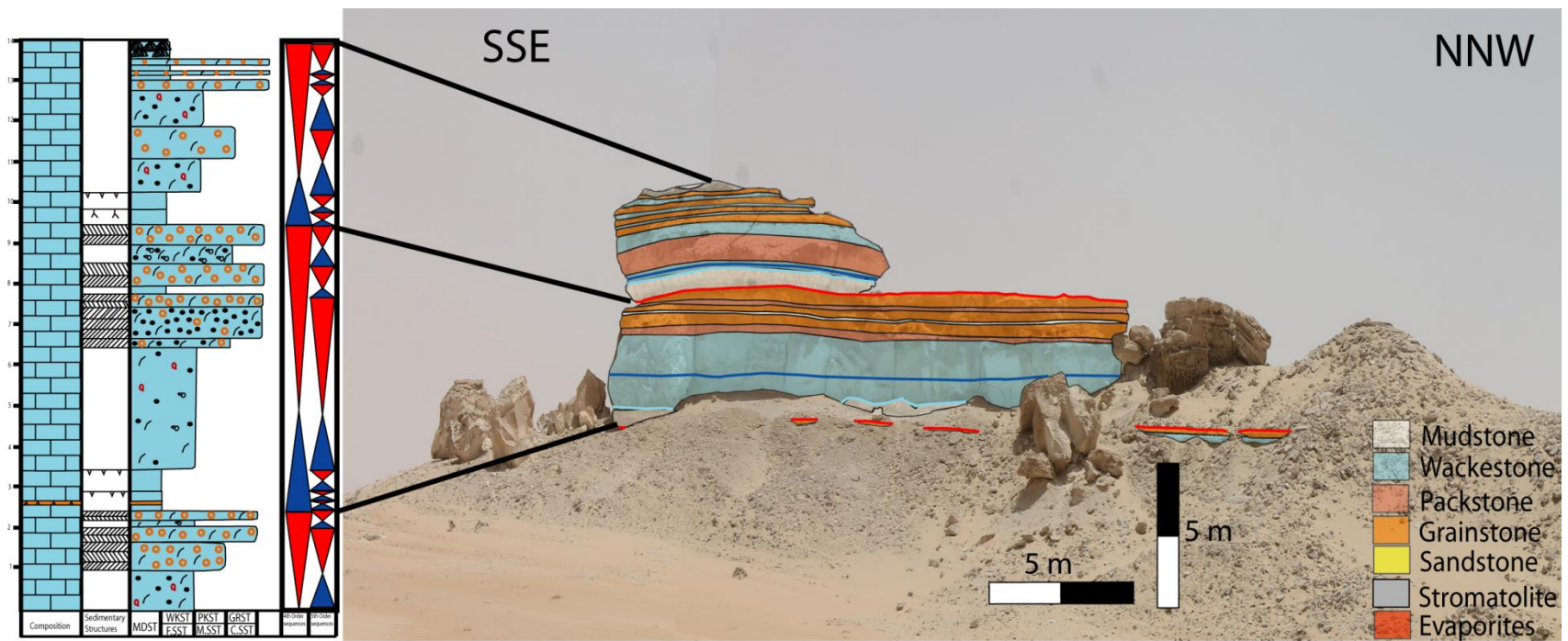




**Figure 5.8: Facies and sequence stratigraphy interpretation of outcrop No. 23**



**Figure 5.9: Facies and sequence stratigraphy interpretation of outcrop No. 1**



**Figure 5.10: Facies and sequence stratigraphy interpretation of outcrop No. 2**

## **CHAPTER 6**

### **CONCLUSIONS AND RECOMMENDATIONS**

#### **6.1 Conclusions**

The main findings of this study could be summarized as follows:

- 1) The Lower Miocene Dam Formation in Al-Lidam area is represented by a succession of mixed siliciclastic-carbonate deposits. This succession was accumulated on a shallow marine carbonate platform which is most probably a land-attached ramp.
- 2) Fifteen lithofacies were identified based on their lithology, sedimentary structures, fossils contents, paleocurrent patterns and their architectures and morphologies. These characteristics were helpful in interpreting their depositional environments.
- 3) The depositional environments show a gradual change between relative deep parts of the platform eastwards towards shallower conditions westwards throughout the studied outcrops. This variation is evidenced by the complete absence of siliciclastics in the eastern part of the studied traverse (outcrops 1 & 2 on the base map).
- 4) The carbonate facies comprising of more than 80 % are predominant over the siliciclastics. Their depositional subenvironments range from subtidal, intertidal, supratidal, shoreface, foreshore, backshore, skeletal mounds, patch reefs to tidal

channels. On the other hand, siliciclastics are restricted to intertidal to supratidal sand and mud flats, and estuarine channels.

- 5) The parasequences of the studied sections show a generally shallowing upward facies pattern. Within them, minor marine flooding surfaces were recognized. On a larger view, three 4<sup>th</sup> order sequences with two sequence boundaries were identified. Where both siliciclastics and carbonates are found, siliciclastics were interpreted to form the base level rising initiation phase (LST and the early TST) while carbonates most probably represent the whole rest of that phase (TST and HST) in addition to the base-level falling phase (accompanied with evaporites in early LST).

## **6.2 Recommendations**

The following points are highly recommended for further research:

- 1) To expand the study area to cover the Dam Formation outcrops in longer E-W traverse
- 2) To control the age of those sediments either by applying biostratigraphy or other chronostratigraphic techniques
- 3) To apply benthic foraminifera and bivalves biostratigraphy to make Burdigalian species distribution models for both of them because of their wide distribution through studied facies.
- 4) To apply the principles of elemental and isotopes chemostratigraphy on studied outcrops to delineate their sequences. This will be greatly useful because of the



high geochemical variation between facies (carbonates, siliciclastics and evaporites).

- 5) To correlate the findings in terms of facies and stratal stacking pattern with subsurface data.

## References

- Abdulsamad, E., and F. Bu-Argoub. 2006. "Sedimentary Facies and Foraminifera of The Miocene Carbonates of the Ar Rajmah Group In Cyrenaica, NE-Libya." *Petroleum Research Journal* 19(2006):49 – 60.
- Abdulsamad, E. O., F. M. Bu-Argoub, and a. F. a. Tmalla. 2009. "A Stratigraphic Review of the Eocene to Miocene Rock Units in the Al Jabal Al Akhdar, NE Libya." *Marine and Petroleum Geology* 26(7):1228–39.
- Aigner, Thomas. 1985. "An Ancient Storm Storm Depositional System: Dynamic Stratigraphy of Intracratonic Carbonates, Upper Muschelkalk (middle Triassic), South-German Basin." *Lecture Notes in Earth Sciences*.
- Al-husseini, Moujahed I. 2000. "Origin of the Arabian Plate Structures : Amar Collision and Najd Rift. *Precambrian Amar Collision* : 640-620 Ma." 5(4).
- Al-Jallal, I. A. 2010. " The Khuff Formation: Its Regional Reservoir Potential in Saudi Arabia and Other Gulf Countries; Depositional and Stratigraphic Approach. In M.I. Al-Huseini (Ed.), Middle East Petroleum Geosciences Conference, GEO'94. Gulf PetroLink," *GeoArabia, Journal of the Middle East Petroleum Geosciences*. Retrieved April 7, 2014
- Alkhaldi, F. 2009. "Controls on Hierarchy of Miocene Buildups within a High Resolution Cycle Stratigraphic Framework of Dam Formation, Lidam Area, Saudi Arabia." *MSc thesis* (June).

- Alkhaldi, F., Tawil, A. and F. Raed.N.D. 2010. “ABSTRACT Controls on Sequence Stratigraphy of Miocene Mixed-Carbonate-Siliciclastic Systems Early Miocene Dam Formation Eastern Saudi Arabia
- Al-saad, Hamad, and Mohamed I. Ibrahim. 2002. “Stratigraphy, Micropaleontology, and Paleocology of the Miocene Dam Formation, Qatar.” 7(1):9–28.
- Bakhtiar, A. 2006. “Geological Relations between Clastic, Evaporite and Limestone Layers of Fatha Formation in the High Folded Zone, NE-Iraq.”
- Beydoun, Z. R 1993. Evolution of the Northeastern Arabian Plate Margin and Shelf: Hydrocarbon Habitat and Conceptual Future Potential. *Revue de l'Institut Francais du Petrole*, v. 48, p. 311-345
- Blasband, B., S. White, P. Brooijmans, H. D. E. Boorder, and W. Visser. 2000. “Late Proterozoic Extensional Collapse in the Arabian – Nubian Shield.” 157(Table 2):615–28.
- Boggs, Jr. 2006. “Principles of Sedimentology and Stratigraphy.”
- Brew, Graham, Robert Litak, and Muawia Barazangi. 1999. “Tectonic Evolution of Northeast Syria : Regional Implications and Hydrocarbon Prospects.”
- Brown, L. F., Jr., Fisher, W. L., 1977. Seismic stratigraphic interpretation of depositional systems: examples from Brazilian rift and pull apart basins. In: Payton, C. E. (ed.), *Seismic Stratigraphy – Applications to Hydrocarbon Exploration*. American Association of Petroleum Geologists Memoir 26, 213–248.

- Catuneanu, O., Galloway, W. E., Kendall, C. G. S. C., Miall, A. D., Posamentier, H. W., Strasser, A., & Tucker, M. E. (2011). Sequence Stratigraphy: Methodology and Nomenclature. *Newsletters on Stratigraphy*, 44(3), 173–245. doi:10.1127/0078-0421/2011/0011
- Davis, R. A. (2012). Tidal signatures and their preservation potential in stratigraphic sequences. In: Davis, R.A., Dalrymple, R.W. (Eds.), *Principles of Tidal Sedimentology*. Springer, Heidelberg, pp. 35–55.
- Dill, H. G. et al. 2005. “Sedimentary Facies, Mineralogy, and Geochemistry of the Sulphate-Bearing Miocene Dam Formation in Qatar.” *Sedimentary Geology* 174(1-2):63–96. Retrieved April 6, 2014
- Dill, H.G., and Henjes-kunst, F.. 2007. “Strontium (  $^{87}\text{Sr}/^{86}\text{Sr}$  ) and Calcium Isotope Ratios (  $^{44}\text{Ca}/^{40}\text{Ca}$ -  $^{44}\text{Ca}/^{42}\text{Ca}$  ) of the Miocene Dam Formation in Qatar : Tools for Stratigraphic Correlation and Environment Analysis.”
- Dupraz, et al. 2009. “Processes of Carbonate Precipitation in Modern Microbial Mats.” *Earth-Science Reviews* 96(3): 141–62.
- Embry, A. (2009). Practical Sequence Stratigraphy. *Canadian Society of Petroleum Geologists*.
- Embry, A. F., Johannessen, E. P., 1992. T-R sequence stratigraphy, facies analysis and reservoir distribution in the uppermost Triassic-Lower Jurassic succession, western Sverdrup Basin, Arctic Canada. In: Vorren, T. O., Berg - sager, E., Dahl-Stamnes, O. A., Holter, E., Johansen, B., Lie, E., Lund, T. B. (Eds.), *Arctic*

- Geology and Petroleum Potential, vol. 2 (Special Publication). Norwegian Petroleum Society (NPF), pp. 121–146.
- Eriksson, K.A., Simpson, E.L., 2004. Precambrian tidalites: recognition and significance. In: Eriksson, P.G., Altermann, W., Nelson, D., Mueller, W., Cateneau, O., Strand, K. (Eds.), *Tempos and Events in Precambrian Time. Developments in Precambrian Geology* 12. Elsevier, Amsterdam, pp. 631– 642.
- Flügel, Erik. 2010. *Microfacies of Carbonate Rocks*. Springer, Berlin.
- Friedman, Gerald M. 1993. “CARBONATE STORM DEPOSITS(TEMPESTITES) OF MIDDLE TO UPPER CAMBRIAN AGE IN THE HELAN MOUNTAINS, NORTHWEST CHINA.” (2): 181–90.
- Galloway, W. E., 1989. Genetic stratigraphic sequences in basin analysis, I. Architecture and genesis of floodingsurface bounded depositional units. *American Association of Petroleum Geologists Bulletin* 73, 125–142.
- Ghebreab, W. 1998. “Tectonics of the Red Sea Region Reassessed.” *Earth-Science Reviews* 45(1-2):1–44.
- Hassan, S, M. 2013. “Sequence Stratigraphy of the Lower Miocene Moghra Formation in the Qattara Depression, North Western Desert, Egypt.” Retrieved April 8, 2014
- Howard, J.D., 1975. The sedimentological significance of trace fossils. In: Frey, R.W. (Ed.), *The Study of Trace Fossils*. Springer, New York, pp. 131–146.
- Hunt, D., Tucker, M. E., 1992. Stranded parasequences and the forced regressive wedge systems tract: deposition during base-level fall. *Sedimentary Geology* 81, 1–9.



- Husseini, M, I., and I. Husseini, S. 1990. "Origin of the Infracambrian Salt Basins of the Middle East." *Geological Society, London, Special Publications* 50(1):279–92.  
Retrieved April 8, 2014
- Irttem, O. 1987. "Miocene Tidal Flat Stromatolites of the Dam Formation, Saudi Arabia."
- Jacquini, T., Vail. P. R., Arnaud-Vanneau, A., Arnaud, H. and Ravenne, C., 1991, system tracts and depositional systems in a carbonate setting: a study of continuous outcrops from platform to basin on the scale of seismic lines: *Marine and Petroleum Geology*, v. 8, p. 122-139
- James, N. P. and Kendall, A. C., 1992 introduction to carbonate and evaporites facies models, in R. G. Walker, and N. P. James, eds., *Facies Models: St Johns*, Geological Association of Canada, p. 265-275
- Johnson, H. D, and C. T Baldwin. 1996. "Shallow Clastic Seas." *Sedimentary Environments: Processes, Facies and Stratigraphy*: 232–80.
- Johnson, J. G., Murphy, M. A., 1984. Time-rock model for Siluro-Devonian continental shelf, western United States. *Geological Society of America Bulletin* 95, 1349–1359.
- Johnson, J. G., Klapper, G., Sandberg, C. A., 1985. Devonian eustatic fluctuations in Euramerica. *Geological Society of America Bulletin* 96, 567–587.
- Kendall, Christopher G. St. C., and John Warren. 1987. "A Review of the Origin and Setting of Tepees and Their Associated Fabrics." *Sedimentology* 34(6): 1007–27.  
<http://doi.wiley.com/10.1111/j.1365-3091.1987.tb00590.x>.

- Lasemi, Y., Jahani, D., Amin-Rasouli, H., Lasemi, Z., 2012. Ancient carbonate tidalites. In: Davis, R.A., Dalrymple, R.W. (Eds.), *Principles of Tidal Sedimentology*. Springer, Heidelberg, pp. 567–607.
- Lee, H.S., Chough, S.K., 2006. Lithostratigraphy and depositional environments of the Pyeongan Super group (Carboniferous–Permian) in the Taebaek area mid-east Korea. *Journal of Asian Earth Sciences* 26, 339–352.
- Logan, B., R. Rezak, and R. Ginsburg. 1964. “Classification and Environmental Significance of Algal Stromatolites Author ( S ): B . W . Logan , R . Rezak and R . N . Ginsburg Published by : The University of Chicago Press.” *The Journal of Geology* 72(1): 68–83.
- Loosveld, Ramon J. H., Andy Bell, and Jos J. M. Terken. 1996. “The Tectonic Evolution of Interior Oman Unit I: Basement - Pan-African Accretion in the Arabian Peninsula.” L(1).
- Mitchum, R, Vail, P., and Thompson, S. 1977. Seismic stratigraphy and global changes in sea level, part 2: the depositional sequence as the basic unit for stratigraphic analysis. in: Payton, C. (ed.) *Seismic stratigraphy: application to hydrocarbon exploration*. AAPG Memoir 26, p. 53-62.
- Montenat, Christian, Pascal Barrier, Philippe Ott d’Estevou, and Christian Hibschi. 2007. “Seismites: An Attempt at Critical Analysis and Classification.” *Sedimentary Geology* 196(1-4): 5–30.

- Muttoni, Giovanni et al. 2009. "Opening of the Neo-Tethys Ocean and the Pangea B to Pangea A Transformation during the Permian." 14(4).
- Obermeier, S. F. 1993. 1536 US Geological Survey Professional Paper *Liquefaction Evidence for One or More Strong Holocene Earthquakes in the Wabash Valley of Southern Indiana and Illinois, with a Preliminary Estimate of Magnitude.*
- Palma, Ricardo M., José López-Gómez, and Ricardo D. Piethé. 2007. "Oxfordian Ramp System (La Manga Formation) in the Bardas Blancas Area (Mendoza Province) Neuquén Basin, Argentina: Facies and Depositional Sequences." *Sedimentary Geology* 195(3-4): 113–34.
- Pemberton, S.G., Flach, P.D., Mossop, G.D., 1982. Trace fossils from the Athabasca Oil Sands, Alberta, Canada. *Science* 217, 825–827.
- Pemberton, S. G., Macheachern, J. A., Dashtgard, S. E., Bann, K. L., Gingras, M. K., & Zonneveld, J. 2012. *Trace Fossils as Indicators of Sedimentary Environments (shorefaces)*. (Vol 64) Elsevier.
- Posamentier, H.W., Allen, G. P., 1999. Siliciclastic sequence stratigraphy: concepts and applications. *SEPM Concepts in Sedimentology and Paleontology* no. 7, 210 pp.
- Powers, R., L. Ramirez, C. Redmond, and E. Elberg. 1966. "Geology of the Arabian Peninsula Sedimentary Geology of Saudi Arabia." *U.S. GEOLOGICAL SURVEY PROFESSIONAL PAPERS*.

- Rankey, E. C., Berkeley, A., 2012. Holocene Carbonate Tidal Flats. In: Davis, R.A., Dalrymple, R.W. (Eds.), *Principles of Tidal Sedimentology*. Springer, Heidelberg, pp. 507–540.
- Reineck, H., & Singh, I. (1980). *Depositional Sedimentary Environments*. Zhurnal Eksperimental'noi I Teoreticheskoi Fiziki. Retrieved from <http://scholar.google.com/scholar?hl=en&btnG=Search&q=intitle:No+Title#0>
- Roy, P.S., Thom, B.G., Wright, L.D., 1980. Holocene sequences on an embayed high-energy coast: an evolutionary model. *Sediment. Geol.* 26, 1–19.
- De Ruiter, R. S. .. 1995. “The Euphrates Graben of Eastern Syria: A New Petroleum Province in the Northern Middle East. In, M.I. Al-Husseini (Ed.), *Middle East Petroleum Geosciences, GEO'94*. Gulf PetroLink, Bahrain, v. 1, P. 357-368. - Geoarabian.net - Geoarabian.net © 2014.” Retrieved April 8, 2014 (<http://geoarabian.net/index.php/geoarabia-online/22-geoarabia-publication/9796-the-euphrates-graben-of-eastern-syria-a-new-petroleum-province-in-the-northern-middle-east-in-m-i-al-husseini-ed-middle-east-petroleum-geosciences-geo-94-gulf-petrolink-bahrain-v-1-p-357-368>).
- Saylor, B. Z. 2003. “Sequence Stratigraphy and Carbonate-Siliciclastic Mixing in a Terminal Proterozoic Foreland Basin, Urusis Formation, Nama Group, Namibia.” *Journal of Sedimentary Research* 73(2):264–79. Retrieved April 7, 2014
- Seilacher, ADOLF. 1969. “Fault-graded beds interpreted as Seismites.” *Sedimentology* 13(1-2): 155–59

- Sharafi, M., Mahboubi, A., Moussavi-harami, R., Mosaddegh, H., & Gharaie, M. H. M. (2014). Trace fossils analysis of fluvial to open marine transitional sediments : Example from the Upper Devonian ( Geirud Formation ), Central Alborz , Iran. *Palaeoworld*, 23(1), 50–68. doi:10.1016/j.palwor.2013.10.004
- Sharland, R. P., Archer, R., Casey, D. M., Davies, R. B., Hall, S. H., Heward, A. P., ... Simmons, M. D. (2001). *Arabian Plate Sequence Stratigraphy* (Paleo.blogfa.com).pdf.
- Sloss, L. 1963. Sequences in the cratonic interior of North America. *GSA Bulletin*, v. 74, p. 93-113.
- Sloss, L., Krumbein, W., and Dapples, E. 1949. Integrated facies analysis. in: Longwell, C. (ed.). *Sedimentary facies in geologic history*. Geological Society America, Memoir 39, p. 91-124.
- Stamp, G. M., and G. D. Borel. 2002. "A Plate Tectonic Model for the Paleozoic and Mesozoic Constrained by Dynamic Plate Boundaries and Restored Synthetic Oceanic Isochrons." 196:17–33.
- Steineke, Max, Bramkamp, R. A., and Sander, N. J., 1958, Stratigraphic relations of Arabian Jurassic oil *in* Habitat of oil: Am. Assoc. Petroleum Geologists Symposium, p. 1294-1329.
- Thom, B.G., Roy, P.S., Short, A.D., Hudson, J., Davis Jr., R.A., 1986. Modern coastal and estuarine environments of deposition in southeastern Australia. In: Guide for Excursion 4A, 12th International Sedimentological Congress, Canberra, 279 pp.



- Tucker, Maurice E. 2001. "SEDIMENTARY An Introduction to the Origin of Sedimentary Rocks." *Blackwell sciences Ltd.*
- Vail, P. R., 1987. Seismic stratigraphy interpretation procedure. In: Bally, A.W. (Ed.), Atlas of Seismic Stratigraphy, vol. 27. American Association of Petroleum Geologists Studies in Geology, p. 1–10.
- Weijermars, Ruud. 1999. "Surface Geology , Lithostratigraphy and Tertiary Growth of the Dammam Dome , Saudi Arabia : A New Field Guide." 4(2):199–226.
- Ziegler, Martin A. 2001. "Late Permian to Holocene Paleofacies Evolution of the Arabian Plate and Its Hydrocarbon Occurrences." 6(3):445–504.

## **Vitae**

**MAZIN ABDELGADIR ABDELRAZIG BASHRI**

**Dhahran – Saudi Arabia**

**Mobile: +966534434563**

**E-mail: [mazinbashari@yahoo.com](mailto:mazinbashari@yahoo.com)**

---

### **Personal Data:**

- ❖ **Date of Birth:** 21<sup>st</sup> July, 1986
- ❖ **Religion:** Muslim
- ❖ **Nationality:** Sudanese
- ❖ **Present Address:** Dhahran, Saudi Arabia
- ❖ **Permanent Address:** Khartoum, Sudan

### **Academic Qualifications:**

- ❖ Master in Geology (expect to be graduated in **March, 2015**) in Earth Sciences Department, King Fahd University of Petroleum & Minerals (CGPA: 3.69).
- ❖ **September, 2009**: Awarded a B. Sc.; degree (honours with first class) in Geology, specializing in Petroleum Geology in University of Khartoum, Faculty of Sciences, Department of Geology (CGPA: 7.77).

#### **Awarded Prizes:**

- ❖ **2005 & 2006**: Schlumberger prizes for academic innovation.
- ❖ **2009**: University of Khartoum prize for the best academic performance in the Department of Geology.

#### **Volunteer work:**

- Active member of geologic community in University of Khartoum during studying years & teaching assistance interval.
- Assistance in students' field trips for lower classes and labs preparations. Also volunteer in post graduated students' field trips and lab works.

#### **Training & Work Experience:**

- **November 2011- July 2012**: Exploration sedimentologist, Geological Research Authority of Sudan (GRAS)

- **February, 2012 – July 2012:** Part-timer teaching assistant, Faculty of Earth Sciences, Red Sea University.
- **September, 2009 – August 2012:** Part-timer teaching assistant in the Geology Department of Khartoum University.
- **September 2010 – October 2010:** Training period in Geological Research Authority of Sudan (GRAS)/ Ministry of Minerals

#### **Field Trips, Dissertation & Research Work:**

**March, 2014:** Field trip to Texas & New Mexico states, USA dealing with different stratigraphical units. The trip targeted Cambrian-Ordovician Bliss Sandstone Formation, Different associated Cambrian Carbonate successions, Volcanoclastic Sediments, carbonates caving in Carlsbad Caverns and the great Permian Capitan Reef in Guadalupe Mountains. The field was under the supervision of Stanford University staff (Prof. Donald Lowe, Prof. Stephan Graham and Doc. Jonathan Payne).

**2014** Facies Analysis and Paleoenvironmental Interpretation of Mixed Clastic-Carbonate Deposits of the Miocene Dam Formation Outcrops, Nebak and Al-Lidam areas, Eastern Province of Saudi Arabia (paper in process).

**2013** Upper Khartam Member, Khuff Formation reservoir characterization using lithostratigraphy and elemental chemostratigraphy, Qasim area (paper in process).

**2011** Exploration of gold in Volcanogenic Massive Sulphides (VMS) belts in the Nubian Shield, Sudan, for Ariab Gold Mining Company.

**2009** Assisted Dr. M.Shadad, chief of astronomy field in Department of Physics, University of Khartoum, in his widely published TC3 meteorite trip, as a member of his exploration team at train station 6 (200 km South of Halfa city) in the Nubian Desert, Sudan. That trip was attended by No of professional astronomers and geologists from all over the world (17 professors), and more than 600 pieces of TC3 meteorite were collected.

**2007, 2008** Detail Mapping for the Sabaloka Area, central Sudan, with application of Gravity and Resistivity Geophysical methods.

**BSc Dissertation Title:** Facies analysis and sedimentological characteristics of Upper Cretaceous Shendi Formation, Musawarat area, Atbara rift basin, Sudan.

**MSc Thesis Title:** High Resolution Facies Analysis and Sequence Stratigraphy of Mixed Siliciclastic-Carbonate Deposits of Miocene Dam Formation in Al Lidam Area, Eastern Province, Saudi Arabia

#### **Conference Papers:**

- (M. Osman, O. Abdullatif, M. Al-Farhan, H. Eltom & **M. Bashri**, **2014**) "High Resolution Stratigraphy and Reservoir Heterogeneity of Khartam Member of Khuff Formation from Outcrop, Saudi Arabia". EAGE 76th EAGE Conference & Exhibition 2014.
- (M. Osman, **M. Bashri**, O. Abdullatif, M. Abdulrazig. A, H. Eltoum, **April 2013**): "Sedimentology and Stratigraphy of the Late Triassic

Minjur and Early Jurassic Marrat Formations: Implication to Sequence Development and Reservoir Architecture, Central Saudi Arabia.

- **(M. Bashri, 2011):** "Sedimentological characteristics of Upper part of Shendi Formation, Musawarat area, Central Sudan". Sudanese Association of Petroleum Geoscientists 3<sup>rd</sup> conference, Khartoum 2011.

**Publications:**

- High Resolution Sedimentology and Facies Analysis of Mixed Siliciclastic-Carbonate Deposits of the Miocene Dam Formation, Al Lidam Area, eastern Province, Saudi Arabia (under preparation to be submitted to Sedimentary Geology in November 2015)